

ABSTRACT

Title of thesis HETEROGENEOUS POLYMERIZATION OF METHYL
METHACRYLATE AT LOW TEMPERATURE IN
DISPERSED SYSTEMS

Laleh Emdadi, Master of Science, 2011

Directed by: Professor, Dr. Kyu Yong Choi, Chemical and
Biomolecular Engineering Department

Dispersion polymerization is a unique method to prepare monodisperse polymer particles of 1-10 μm in a single step process. This process is usually carried out at high temperatures that are not cost effective and suitable for special applications such as encapsulation of bio materials. Production of uniform polymer particles at low temperatures via dispersion polymerization has not been studied widely yet.

In this research, dispersion polymerization of methyl methacrylate (MMA) in a nonpolar solvent, n-hexane, using N,N-dimethylaniline (DMA) and lauroyl peroxide (LPO) as redox initiators at low temperature has been studied. The evolutions of monomer conversion, polymer molecular weight distribution (MWD), and particle morphology were determined. Under specific reaction conditions, monodisperse micron-sized polymer particles were produced. The same technique was applied in the confined reaction space of a monomer droplet. Using this new process, called micro dispersive suspension polymerization, polymer particles with different internal morphologies produced with various potential applications.

HETEROGENEOUS POLYMERIZATION OF METHYL METHACRYLATE AT
LOW TEMPERATURE IN DISPERSED SYSTEMS

by

Laleh Emdadi

Thesis submitted to the Faculty of the Graduate School of the
University of Maryland, College Park, in partial fulfillment
of the requirements for the degree of
Master of Science
2011

Advisory Committee:
Professor Kyu Yong Choi, Chair
Professor Nam Sun Wang
Professor Chunsheng Wang

© Copyright by
Laleh Emdadi
2011

Dedication

This work is dedicated to my parents, Shohreh Emdadi and Mahmood Emdadi.

They began my education. They motivated me to continue it.

They will always contribute to it.

I love you.

Acknowledgements

I wish to thank, first and foremost, my advisor Prof. Kyu Yong Choi, for his guidance, help, and support. His sage advice, insightful criticisms, and patient encouragement aided the writing of this thesis in innumerable ways. I thank him also for providing me an opportunity to grow as a student and engineer in the unique research environment he creates. One simply could not wish for a better or friendlier supervisor.

Special thanks and appreciation to Dr. Carla Vanessa Luciani who worked with me as a post-doctorate when I started. I thank her for sound advice, arduous and diligent editing, and stringent standards. Without her, I would not have achieved my goals for this thesis.

I would like to thank fellow graduate students Sang Yool Lee and In hak Baick for sharing all of their technical knowledge and expertise with me and their assistance in using scanning electron microscopy and gel permeation chromatography techniques.

Last, but not least, I would like to thank my family members, especially my parents Shohreh Emdadi and Mahmood Emdadi, my sister Golsa, my uncle Ali Niak, and my aunt Shideh Emdadi. Without them I would have never made it this far in life. They have been there for me every step of the way, have always loved me unconditionally, and have supported me through all of my tough decisions.

Table of Contents

List of Tables	vii
List of Figures	viii
Chapter 1: Introduction	1
1.1 Background	1
1.2 Objectives and Motivations	2
1.3 Literature survey	7
1.3.1 Polymerization techniques for the production of polymer particles	8
1.3.1.1 Suspension Polymerization	8
1.3.1.2 Emulsion Polymerization	12
1.3.1.3 Miniemulsion Polymerization	14
1.3.1.4 Precipitation Polymerization	16
1.3.1.5 Dispersion Polymerization	17
1.3.2 Effect of recipe and reaction conditions on dispersion polymerization	25
1.3.2.1 The effect of stabilizer type and concentration	25
1.3.2.2 The effect of reaction temperature	28
1.3.2.3 The effect of initiator type and concentration	30
1.3.2.4 The effect of solvent type and concentration	32
1.3.2.5 The effect of monomer type and concentration	34
1.3.2.6 The effect of rate and type of agitation	35
1.3.2.7 The effect of purging nitrogen	36
1.3.3 Micro dispersive suspension polymerization	37
1.3.4 Dispersion polymerization at low temperature	40

Chapter 2: Macroscopic dispersion polymerization of methyl methacrylate at low temperature	43
2.1 Theory of free radical dispersion polymerization using a redox pair	43
of initiators	43
2.2 Materials and Methods.....	49
2.2.1 Determination of conversion.....	51
2.2.2 Characterization of polymer particle morphology	51
2.2.3 Polymer molecular weight distribution.....	53
2.2.4 Determination of partition coefficients of redox pair	54
2.3 Results and Discussion	56
A. Preliminary Experiments.....	57
B. Main Experiments	66
B-1) Determination of LPO and DMA Partition Coefficients.....	66
B-2) Dispersion Polymerizations (Low Conversion Experiments)	67
B-3) Dispersion Polymerizations (High Conversion Experiments).....	69
B-4) Study of the stability of the polymer particles and phase inversion.....	81
phenomenon	81
Chapter 3: Micro dispersive suspension polymerization of methyl methacrylate at low temperature.....	91
3.1 Materials and Methods.....	91
- Micro dispersive suspension polymerization	91
- Determination of PMMA/MMA/n-hexane cloud points	94
3.2 Results and Discussion	95
Chapter 4: Conclusion and future work considerations	109

Nomenclature	112
References	114

List of Tables

Table 1. 1 Comparison of properties of heterogeneous polymerization systems	20
Table 2. 1 Properties of monomer, redox system, solvent, and stabilizer	50
Table 2. 2 Reaction conditions for dispersion polymerizations of MMA in <i>n</i> -hexane at 30°C	58
Table 2. 3 Reaction conditions for dispersion polymerizations of MMA in <i>n</i> -hexane at 30°C	62
Table 2. 4 Reaction conditions for dispersion polymerizations of MMA in <i>n</i> -hexane at 30°C	64
Table 2. 5 Determination of the LPO partition coefficients	66
Table 2. 6 Determination of the DMA partition coefficients	66
Table 2. 7 Reaction conditions for dispersion polymerizations of MMA in <i>n</i> -hexane at 30°C (low conversion experiments)	67
Table 2. 8 Results of dispersion polymerizations of MMA in <i>n</i> -hexane at 30°C (low conversion experiments)	68
Table 2. 9 Reaction conditions for dispersion polymerizations of MMA in <i>n</i> -hexane at 30°C (high conversion experiments)	70
Table 2. 10 Results of dispersion polymerizations of MMA in <i>n</i> -hexane at 30°C (high conversion experiments)	70
Table 2. 11 Reaction conditions for dispersion polymerizations of MMA in <i>n</i> -hexane at 30°C	82
Table 3. 1 Reaction conditions for micro dispersive suspension polymerization of MMA at 30°C	96
Table 3. 2 Reaction conditions for micro dispersive suspension polymerization of MMA at 30°C	97
Table 3. 3 Reaction conditions for micro dispersive suspension polymerization of MMA at 30°C	100
Table 3. 4 Reaction conditions for micro dispersive suspension polymerization of MMA at 30°C	102

List of Figures

Figure 1. 1 PMMA particles as light diffraction path lengtheners.	6
Figure 1. 2 Schematic representation of suspension polymerization.....	9
Figure 1. 3 Schematic representation of emulsion polymerization.....	13
Figure 1. 4 Schematic representation of miniemulsion polymerization	15
Figure 1. 5 Schematic of particle growth in dispersion polymerization	19
Figure 1. 6 Schematic representation of a ternary phase diagram for dispersion polymerization.	24
Figure 1. 7 Schematic representation of micro-dispersive polymerization in a confined reaction space (MDPCRS).....	39
Figure 1. 8 Micron-sized polymer particles with complex internal structure produced using micro-dispersive polymerization in a confined reaction space (MDPCRS)	40
Figure 1. 9 Reaction between LPO and DMA to initiate free-radical polymerizations.....	41
Figure 2. 1 Schematic representation of a ternary phase diagram for dispersion polymerization.	47
Figure 2. 2 Scanning electron microscopy (SEM) (Hitachi SU-70 and AMRAY)	52
Figure 2. 3 Schematic diagram of Gel-Permeation Chromatography.....	53
Figure 2. 4 PMMA particles obtained by dispersion polymerization of MMA in <i>n</i> -hexane at 30°C.	60
Figure 2. 5 Comparison of SEM micrographs using 2 different preparation techniques for Exp. A3.....	61
Figure 2. 6 PMMA obtained by dispersion polymerization of MMA in <i>n</i> -hexane at 30 °C after 10 hours.	63
Figure 2. 7 PMMA obtained by dispersion polymerization of MMA in <i>n</i> -hexane at 30 °C after 5 hours using different agitation speeds.	65
Figure 2. 8 Particle size histograms for samples in Fig. 2.7	65
Figure 2. 9 Polymer particles obtained at early stages of dispersion polymerizations of MMA in <i>n</i> -hexane at 30°C.....	68
Figure 2. 10 Evolution of the monomer conversion for experiments B8 and B9.....	71

Figure 2. 11 Evolution of the polymer molecular weight with the monomer conversion for Exp. B8.	73
Figure 2. 12 Molecular weight distributions (MWDs) for Exp. B8 at different conversions where x shows conversion	75
Figure 2. 13 PMMA particles obtained by dispersion polymerization of MMA in <i>n</i> -hexane at 30°C.	76
Figure 2. 14 Particle size histograms for samples in Fig. 3.10.	78
Figure 2. 15 Evolution of the poly(methyl methacrylate) (PMMA) morphology with time for Exp. B8.....	79
Figure 2. 16 Evolution of particle morphology for Exp. B6.	80
Figure 2. 17 Evolution of the poly(methyl methacrylate) (PMMA) morphology with time for Exp. B11.....	83
Figure 2. 18 Evolution of the PMMA morphology with time for Exp. B12.	84
Figure 2. 19 Evolution of the poly(methyl methacrylate) (PMMA) morphology with time for Exp. B13.....	85
Figure 2. 20 Evolution of the poly(methyl methacrylate) (PMMA) morphology with time for Exp. B14.....	86
Figure 2. 21 Evolution of the poly(methyl methacrylate) (PMMA) morphology with time for Exp. B15.....	88
Figure 2. 22 Evolution of the poly(methyl methacrylate) (PMMA) morphology with time for Exp. B16.....	89
 Figure 3. 1 Schematic diagram of the apparatus used for MDSP experiments	93
Figure 3. 2 Morphology of the poly(methyl methacrylate) (PMMA) particles obtained by micro dispersive suspension polymerization of MMA in water at 30°C for Exp. C4.....	97
Figure 3. 3 Morphology of the poly(methyl methacrylate) (PMMA) particles obtained by micro dispersive suspension polymerization of MMA in water at 30°C for Exp. C7.....	98
Figure 3. 4 Ternary phase diagram for dispersion polymerization of MMA in <i>n</i> -hexane calculated at 30°C.....	99
Figure 3. 5 Evolution of the PMMA morphology with time for Exp. C8.	101

Figure 3. 6 Evolution of the PMMA morphology with time for Exp. C9.	103
Figure 3. 7 Morphology of the poly(methyl methacrylate) (PMMA) particles obtained by micro dispersive suspension polymerization of MMA at 30°C after 5 hours.....	104
Figure 3. 8 Morphology of the poly(methyl methacrylate) (PMMA) particles obtained for Exp. C15 using different methods of drying.....	106
Figure 3. 9 Morphology of the poly(methyl methacrylate) (PMMA) particles obtained for Exp. C15 using different methods of drying.....	107

Chapter 1: Introduction

1.1 Background

There has been substantial interest in monodisperse polymer particles ever since J. W. Vanderhoff and E. B. Bradford announced their preparation of polystyrene particles with highly uniform particle size in 1955 (Vanderhoff et al. 1971). Preparation of uniform polymer particles in the micron-size range has recently received a great attention among others due to their special properties such as higher specific surface area, the ability of promoting surface reaction, and stronger adsorption. These particles have widespread applications in fields such as biomedical, drug delivery, diagnostics, information industry, microelectronics, toners, painting technology, chromatography, etc (Ho et al. 1997, Horak et al. 2000, Yang et al. 2001, Guven et al. 2004, and Bai et al. 2006). Their applications are usually determined by the particle size distribution and the molecular weight of the polymer (Yang et al. 2004). Therefore, the control of particle size and particle uniformity needs to be studied. The morphology of the particles and the surface characteristics also have strong effect on these successful applications (Qiang et al. 2002).

Traditionally, micron size polymer particles have been prepared by suspension polymerization. In suspension polymerization, mechanical stirring can produce small micron sized monomer droplets suspended in the polymerization medium, and each monomer droplet then becomes a miniature reaction vessel. The initiator used must be monomer soluble to effectively initiate the polymerization. Water is a common suspension medium in this type of polymerization process. There are difficulties involving coalescence of particles, however, so a variety of additives are used to stabilize the monomer droplets. A broad particle size distribution is usually observed

in suspension polymerization process as a result of non uniformity of shear rate in the reaction vessel. Therefore, this technique is usually used to produce spherical polymer particles in the size range of 50-1000 μm (Yang et al. 2001).

Submicron polymeric particles in the size range of 0.1-1 μm are produced by emulsion polymerization. Surfactant (soap) is used to form an emulsion. Surfactant molecules consist of a polar head and a non-polar tail and they form numerous micelles in the polymerization medium (usually water). Unlike suspension polymerization, where a water insoluble initiator is used, in emulsion polymerization, a water soluble initiator is added. The polymerization for the most part, occurs in the swollen micelles, which can be thought of as a meeting place for the water soluble initiator and the (largely) water insoluble monomer.

1.2 Objectives and Motivations

Dispersion polymerization by free radical mechanism is a well-known technique to produce fairly monodisperse micron-sized polymer particles in a single step process. Polymer particles are usually produced at very high polymerization rates and relatively high purity. In a typical dispersion polymerization process, a monomer, a dispersive medium (solvent), and a steric stabilizer are mixed together with an initiator. The dispersive agent is a poor solvent for the polymer, and hence, growing polymer chains become insoluble in the reaction medium and precipitate in the form of unstable primary particles. In the presence of a steric stabilizer, these primary particles agglomerate to produce larger but stable monomer-swollen micron-sized polymer particles.

Extensive investigations have been conducted on dispersion polymerization of oil-soluble monomers such as methyl methacrylate in nonpolar hydrocarbon solvents at high temperature in the past years since it allows producing well-defined micron-sized polymer particles of relatively narrow distributions (Barret et al. 1969, Dawkins et al. 1979, Antl et al. 1986, Pathmamanoharan et al. 1989, Pelton et al. 1990, Stejskal et al. 1991, Kargupta et al. 1993, Srinivasan et al. 1998, and Klein et al. 2003). However, dispersion polymerization at low temperature (i.e., 20-40°C) has not been studied extensively. Most of the dispersion polymerizations are carried out at high temperatures (>70°C) to promote a fast decomposition of initiator and to increase the solubility of monomers and stabilizer in the solvent. Although special low-temperature initiators are currently available, their decomposition kinetics is mostly too slow. For example, the azo-initiator 2,2'-azobis-[2-(2-dimidazolin-2-yl)propane] dihydrochloride has a half life of 10 h at 44°C. For this reason, little information is available on the dispersion polymerization at low temperature using commercial oil-soluble initiators. However, there is a need to develop a dispersion polymerization technique at low temperature for special applications such as encapsulation of biologically-active materials. A few articles are available regarding low temperature dispersion polymerization. All of them involve some types of radiation-initiating systems (UV or Gamma-rays) (Ye et al. 2002 (b), Chen et al. 2008).

There is also a growing interest in micron-sized polymer particles with complex internal morphologies for a variety of novel applications in electronics and bio-technology. Core-shell, single-hollow, multi-hollow, and cage type morphologies are just a few examples of these complex morphologies of polymer particles. Different techniques such as emulsion polymerization are used to produce these types

of polymer particles. However, the existing methods have many disadvantages. They have multiple steps and they are time consuming and expensive. They cannot produce polymer particles larger than 1 μm ; therefore, they are not suitable for some special applications such as encapsulation of materials larger than 1 μm or for industrial uses as light diffraction path lengtheners. Scale up and mass production using these techniques are very difficult. Moreover, they are typically carried out at high temperatures ($>70^{\circ}\text{C}$) which is not proper for some special applications such as encapsulation of biologically active materials. Thus, it is necessary to develop a new polymerization technique to overcome all these disadvantages. A single step polymerization method which is easy to run should be developed at low temperature. Also, it is crucial to understand how the internal morphology is developed. In order to achieve these goals, there are several scientific and technical challenges that should be considered. First of all, is it possible to develop a non-emulsion polymerization technique? Secondly, what are the fundamental thermodynamic and kinetic principles that govern the morphological evolution of the polymer particles along this novel polymerization technique? Finally, is it possible to control the particle structure using the knowledge of the phenomena that take place?

In this research work, the dispersion polymerization of MMA in n-hexane was investigated at 30°C using lauroyl peroxide (LPO) and dimethyl aniline (DMA) as redox pair of initiators. Methacryloxypropyl-terminated polydimethylsiloxane (PDMS) was used as steric stabilizer. Special attention was paid to the locus of the polymerization and its effect on the evolution of monomer conversion, particle morphology, and polymer molecular weight distribution (MWD). The final goal was to develop and improve a well-documented dispersion polymerization technique to

produce stable and uniform polymer particles in conventional batch reactors. The knowledge of this study is then used to carry out the dispersion polymerization in micron-sized monomer droplets suspended in an aqueous medium at room temperature. In this set of experiments, water was used as suspension medium and polyvinyl alcohol (PVA) was used as water-soluble stabilizer. In this method, each suspended droplet contains monomer, redox pair of initiators, oil-soluble stabilizer, and a poor solvent for the polymer. It is interesting to emphasize that each polymer particle acts as a micro-reactor, where conventional dispersion polymerization takes place. This proposed technique, called micro-dispersive suspension polymerization in a confined reaction space, offers several unique advantages. It is a very versatile and easy method to generate a wide variety of micron-sized polymer particles with complex internal morphologies in a single step polymerization process.

One of the most important potential applications of these particles is that the multi-hollow polymer particles can be used in the back light unit (BLU) of a liquid crystal display (LCD) device to increase the diffraction of the light. In a conventional BLU, a light diffusion film is made of a polyester coated with several layers of “solid” polymer particles of poly(methyl methacrylate) (PMMA). Micron-sized polymer particles with internal cavities are more effective than these conventional solid particles because they offer an increased light diffraction path length for the same or even smaller particle layer thickness. With minimal particle population, these novel particles can reduce the power requirement for the BLU, and make the display brighter. In Figure 1.1 (a-b) a simple representation of the effect of the internal morphology on the scattered laser light is presented. Figure 1.1 (a) shows the light diffraction path for solid polymer particles and Figure 1.1 (b) shows the light

diffraction path for multi-hollow polymer particles. It is obvious that multi-hollow polymer particles are more efficient to increase the diffraction of light in comparison to solid polymer particles. Figures 1.1 (c-d) show two crude experiments of light dispersion carried out in our lab when a laser beam (wavelength=670/650 nm) is irradiated on a thin film of either solid or multi-hollow PMMA particles of 50-70 μm diameter coated on a glass slide. In spite of the simplicity of this experiment using a coated glass slide, a much more efficient and uniform light diffraction can be observed for multi-hollow polymer particles.

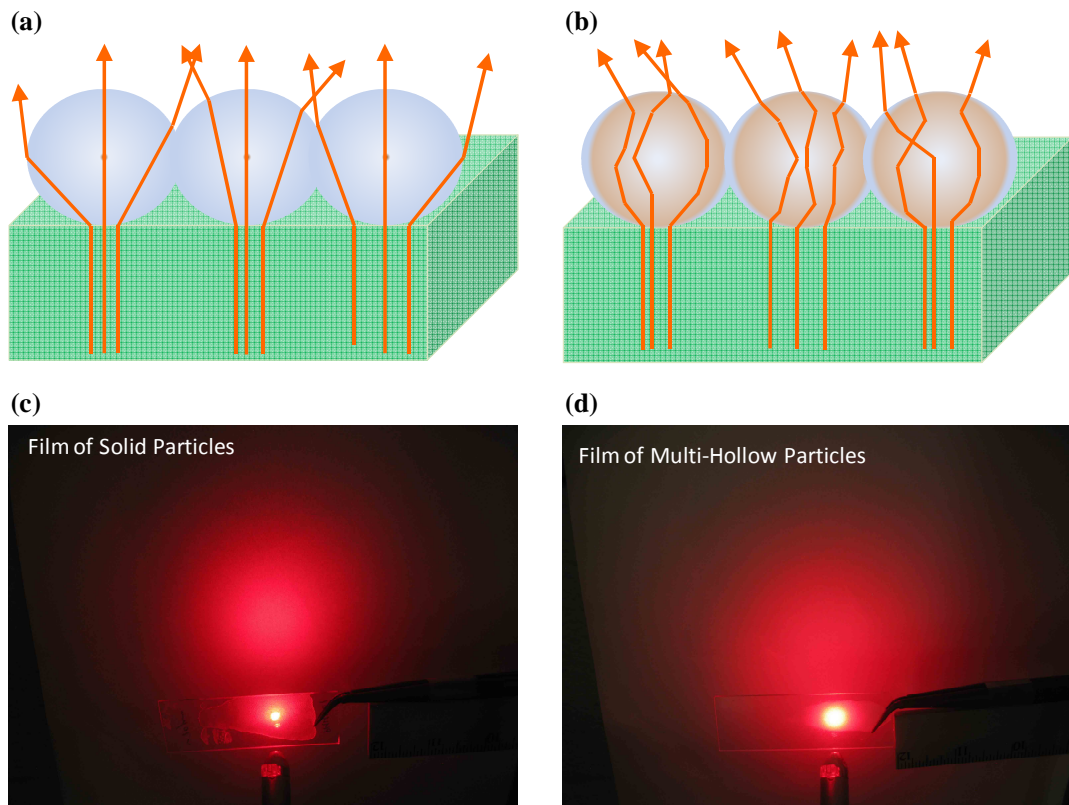


Figure 1. 1 PMMA particles as light diffraction path lengtheners. (a, c) show solid polymer particles and (b, d) show multi-hollow polymer particles (adopted from Dr. Luciani et al. proposal with her permission).

In the next section of this chapter, a literature survey on the polymerization techniques, in particular dispersion polymerizations, and the parameters that affect the process kinetics is presented. In chapter 2, first materials and the experimental methods used in macroscopic dispersion polymerization of MMA at low temperature are described. Then, the experimental results will be presented and the effect of initiator concentration, monomer to solvent ratio, and stabilizer concentration on the conversion and rate of polymerization will be discussed. In addition, characterization of the polymer particles through the use of scanning electron microscopy and gel permeation chromatography is presented. Experimental results and theoretical background is used to discuss the main findings of this work. In chapter 3, micro-dispersive suspension polymerization of MMA at low temperature is discussed. Finally, chapter 4 includes the main conclusions of this research work and some proposed work that should be done in the future to extend the impact of this research.

1.3 Literature survey

Various methods of producing polymer beads have been developed, such as suspension polymerization, emulsion polymerization, and dispersion polymerization. Among these techniques, dispersion polymerization is a very attractive method due to its inherent simplicity of the single-step process, which was first set up by ICI Corporation in the 1970s (Barret, 1987). In fact, monodisperse particles in the micron-size range (2-20 μm) are difficult to obtain because this size is just between the diameter range of particles produced by conventional emulsion polymerization (0.1-0.7 μm) and suspension polymerization (50-1000 μm). Thus, different techniques such as two-stage swelling method have been used to produce such

particles, but dispersion polymerization is an efficient alternative to other multi-stages polymerization methods which are complex, time-consuming, and difficult to implement in large scale (Ugelstad et al. 1980 and 1982).

1.3.1 Polymerization techniques for the production of polymer particles

1.3.1.1 Suspension Polymerization

Suspension polymerization is a polymerization process in which monomer, or a mixture of monomers, and monomer-soluble initiator are dispersed by mechanical agitation in a liquid phase (usually water) in the presence of a suitable suspending agent (e.g., stabilizer), in which suspended monomer droplets are polymerized. Monomer and the initiator are insoluble in the polymerization medium (Arshady et al. 1983). The monomer droplets themselves are gradually converted into insoluble polymer particles but no new particles are formed in the aqueous phase. This polymerization technique is also known as pearl polymerization, bead polymerization, and granular polymerization. Figure 1.2 shows a schematic diagram of suspension polymerization.

Size of the droplet/particle in suspension polymerization is usually larger than $1\text{ }\mu\text{m}$ and smaller than 2 mm. The major aim in suspension polymerization is the formation of an as uniform as possible dispersion of monomer droplets in the aqueous phase with controlled coalescence of these droplets during the polymerization process.

The interfacial tension, the agitation rate, and the design of the stirrer/reactor system govern the dispersion of monomer droplets. The presence of stabilizers prevents the coalescence of monomer droplets during the polymerization process.

Stabilizers are polymeric or oligomeric molecules such as polyvinyl alcohol (PVA) that are adsorbed on the surface and provide steric stabilization against coalescence. Usually, suspension stabilizers cannot form micelles due to their molecular weight distribution and emulsion polymerization in the micelles can be neglected.

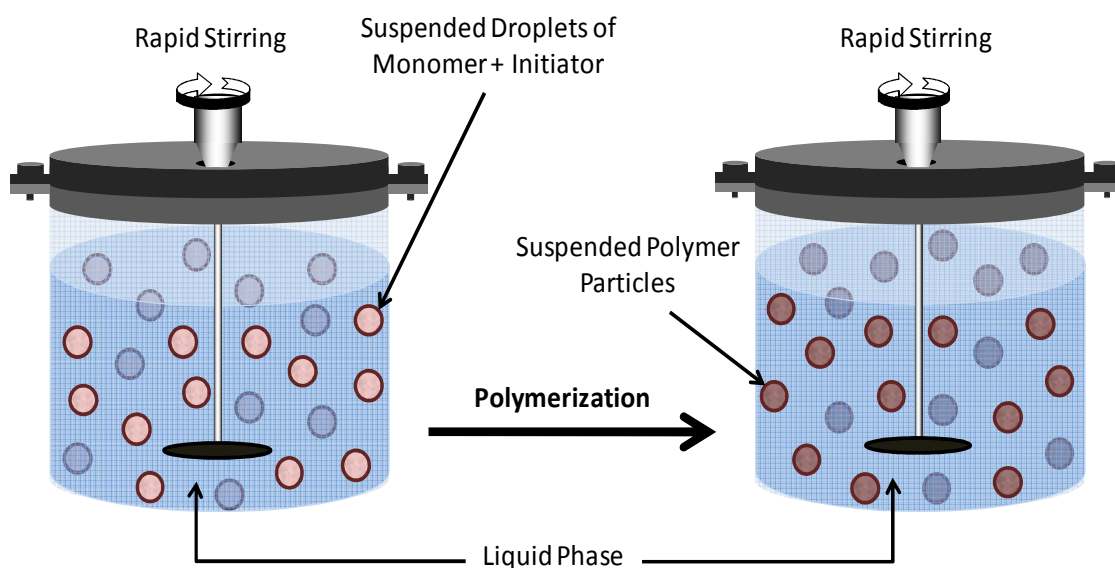


Figure 1. 2 Schematic representation of suspension polymerization.

In regular suspension polymerization, an oil-soluble monomer such as methyl methacrylate is polymerized in aqueous media (usually water). This process is called oil-in-water (O/W) suspension polymerization. Examples of industrially important polymers produced by oil-in-water (O/W) suspension polymerization include polystyrene, poly(vinyl chloride) (PVC), polyacrylates and poly(vinyl acetate). The initiator for this type of suspension polymerization is usually an azo compound (e.g., azo-bis-2-methylpropionitrile, AIBN), or an organic peroxide (e.g. benzoyl peroxide), and the polymerization is performed at a temperature of about 50-100°C.

Polyvinylpyrrolidone (PVP) is a typical droplet stabilizer which is used for O/W suspension polymerization.

Kinetics in suspension polymerization is similar to that of bulk or solution polymerization, depending on the absence or presence of a diluent inside the monomer droplets. Therefore, suspension polymerization may be considered as a “microbulk” or “microsolution” polymerization, because each monomer droplet acts as reactor for bulk or solution polymerization process. The suspension medium housing the microreactors acts as an efficient heat transfer agent. As a result, high rates of polymerization can be maintained to achieve complete conversion during relatively short periods of time.

Suspension polymerization has the following advantages compared with the other polymerization processes: easy heat removal and temperature control; low dispersion viscosity; low levels of impurities in the polymer product (compared with emulsion); low separation costs (compared with emulsion); and final product in particle form. However, this process has some disadvantages, such as wastewater treatment problems, polymer build-up on the reactor wall, baffles, agitators, and other surfaces, and difficulty in commercial semibatch and continuous operation with suspension versus emulsion polymerization because of the lower interfacial area (particle/water).

The most important issue in the practical operation of suspension polymerization is the control of the final particle size distribution. The size of the particles will depend on the monomer type, volume ratio of the monomer to suspension medium, the viscosity change of the dispersed phase with time, the type and concentration of stabilizer, and the agitation conditions in the reactor. Among all

these parameters, stirrer speed is the most convenient means of controlling the particle size distribution and hence the properties of the polymer suspension.

A number of important commercial resins are manufactured by suspension polymerization, including poly(vinyl chloride) (PVC) and its copolymers, styrene resins (general purpose polystyrene), expandable polystyrene (EPS), high-impact polystyrene (HIPS), poly(acrylonitrile-butadiene-styrene) (ABS), poly(methyl methacrylate) (PMMA) and its copolymers, and poly(vinyl acetate) (Yuan et al., 1991).

The morphology of the polymer particles in suspension polymerization is basically related to the degree by which the polymer dissolves, swells or precipitates in the monomer phase. When the polymer is soluble in its monomer mixture (such as polystyrene and poly(methyl methacrylate)), the resulting polymer particles have a smooth surface and a relatively homogeneous (nonporous) texture. On the other hand, when the polymer is not soluble in its monomer mixture (such as poly(vinyl chloride) and polyacrylonitrile), the final particles have a rough surface and a porous morphology. The degree of polymer particle porosity and the details of pore structure and particle morphology can be strongly influenced by the use of suitable monomer diluents. In fact, the monomer can be diluted by an inert liquid which may be a good or poor solvent, or a precipitant for the resulting polymer particles. In this way, polymer particles with a wide range of porosities can be produced, depending on the nature and the percentage of the monomer diluent (Jacobelli et al. 1979, Moore 1969).

1.3.1.2 Emulsion Polymerization

In emulsion polymerization, the main components are the monomer, dispersant, emulsifier, and an initiator. The initiator is, unlike in suspension polymerization, soluble in the medium, and not in the monomer. The dispersant is a liquid (usually water) in which the monomer is insoluble (or scarcely soluble) and is emulsified by means of a surfactant. The action of the surfactant (also referred to as emulsifier or soap) is due to its molecules having both hydrophilic and hydrophobic segments. When the concentration of emulsifier exceeds the critical micellar concentration (CMC), emulsifier molecules with their nonpolar tails in the interior and their hydrophilic ends oriented towards the aqueous medium aggregate to form micelles. The term latex is used to denote the end product of emulsion polymerization. Polymer particles which are produced using this method are in the size range of 0.01 to 0.5 μm . The polymerization usually is carried out at 40-80°C.

In early stages of emulsion polymerization, the monomer is present in the form of droplets with size range of 1 to 10 μm or larger. A very small fraction of monomer dissolves and goes into solution and a larger but still small portion of the monomer enters the interior hydrocarbon part of the micelles. The initiator is present in the medium and this is where the initiating radicals are produced. Monomer droplets are not the main locus of polymerization since the initiators employed are insoluble in the organic monomer. Polymerization takes place almost exclusively in the interior of the micelles. The micelles also favored as the reaction site because of their high monomer concentration compared to the monomer in solution and their high surface-to-volume ratio compared to the monomer droplets. As polymerization proceeds, the micelles grow by the addition of monomer from the aqueous solution.

The polymerization process continues as the nuclei grow gradually until the monomer is completely exhausted. The size of the latex particles which are produced is usually in the range of 50 to 500 nm (Song et al. 1988). Figure 1.3 shows a schematic diagram of emulsion polymerization.

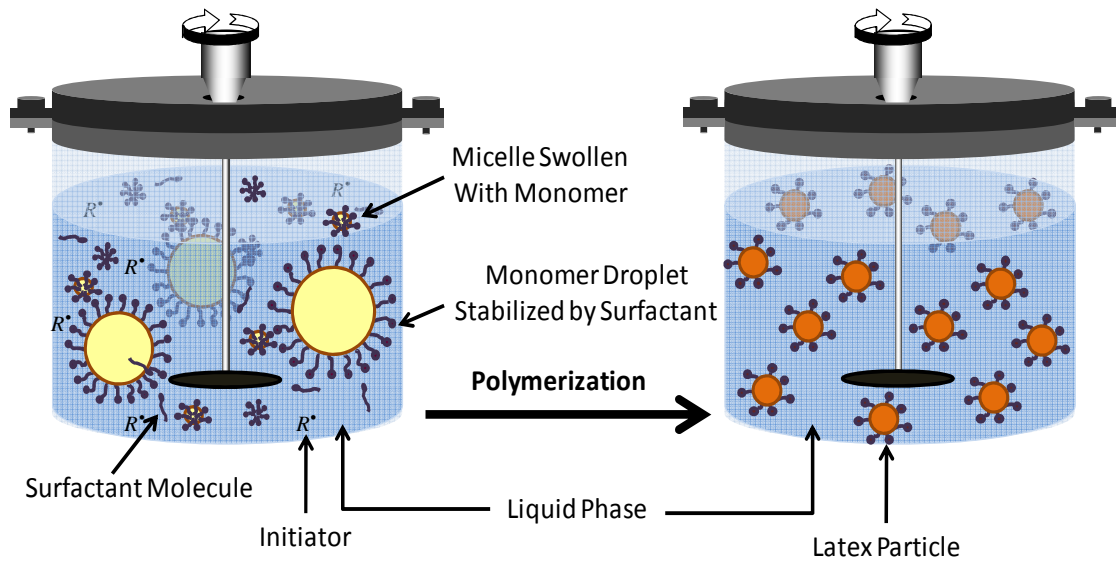


Figure 1. 3 Schematic representation of emulsion polymerization.

The size of the latex particles in emulsion polymerization has no direct relationship with the size of the initially formed monomer droplets or micelles since these do not contain any initiator and, hence, are not directly converted to the corresponding polymer particles. Instead, the fraction of the monomer molecularly dissolved in the medium, emulsifier concentration, and temperature affect the size of the latex particles.

The main kinetic difference of emulsion polymerization from other techniques of polymerization such as suspension polymerization, is that the propagating macro-radicals in emulsion reactions are isolated from each other. Encounters between

macro-radicals are hindered as a consequence, and termination reactions are less frequent than in comparable systems in which the reaction mixture is not subdivided. Emulsion polymerization thus often yield high-molecular-weight products at fast rates when suspension or bulk reactions of the same monomers are inefficient.

The emulsion polymerization process has several advantages. The physical state of the emulsion system makes it easy to control the process. Reaction heat can be easily dissipated. The polymer is low viscosity latex. High molecular weight polymer particles can be obtained at high polymerization rate compared to the other polymerization processes. On the other hand, this method has some disadvantages. For example, stabilizers and other additives may impair the product quality, separation of the polymer by coagulation or dewatering techniques is expensive, and polymerization kinetics and mechanisms of emulsion polymerization are more complex than other polymerization processes.

1.3.1.3 Miniemulsion Polymerization

In a conventional emulsion polymerization, the monomer droplets become the loci of polymerization if the monomer droplet size is reduced sufficiently (0.01-0.5 μm); this system is then referred to as a miniemulsion polymerization process. In this process, the polymer particle size range is from 50 to 500 nm. In miniemulsion polymerization, the droplet surface area is very large, and most of the surfactant is adsorbed at the droplet surface. Particle nucleation is primarily through radical entry into monomer droplets, given that little surfactant is present in the form of micelles, or as free surfactant available to stabilize particles formed in the continuous phase. Two phenomena occur in the miniemulsion polymerization process as a result of the

small size of the monomer droplets (below 0.5 μm). In the first phenomenon, the droplets are able to compete successfully for free radicals with any remaining micelles. In the second, the interfacial area increases in comparison to conventional emulsion polymerization as a result of the reduction of the droplet size. The surfactant necessary to stabilize this large interfacial area originates from the break-up of the surfactant micelles. In a properly formulated miniemulsion, all micelles are sacrificed in order to support the droplet interfacial area. Miniemulsions are produced by the combination of a high shear and a surfactant/costabilizer system (such as cetyl alcohol (CA) and hexadecane (HD)); the high shear breaks up the emulsion into submicron monomer droplets and the surfactant/costabilizer system, retards the monomer diffusion from the submicron monomer droplets. High shear is provided by a sonicator or a mechanical homogenizer (Schork et al. 2005). Figure 1.4 shows a schematic diagram of the miniemulsion polymerization process.

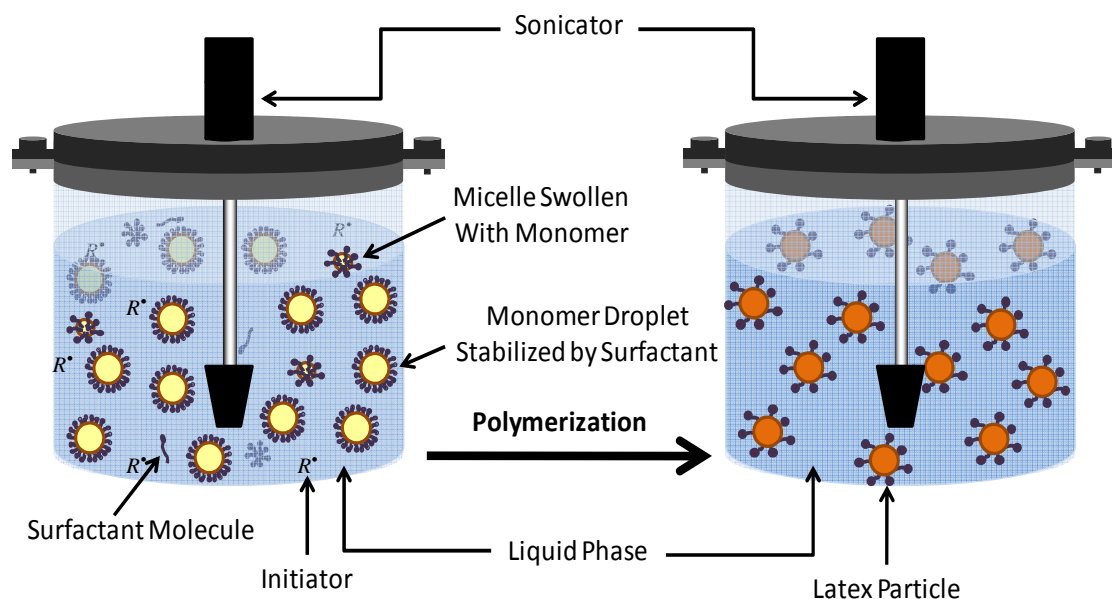


Figure 1. 4 Schematic representation of miniemulsion polymerization.

1.3.1.4 Precipitation Polymerization

In precipitation polymerization, the monomer and the initiator are dissolved in the polymerization medium and form a homogeneous system, but the monomer acts as a non-solvent (precipitant) to the polymer which is formed. Polymer precipitates out as it is formed. Poly(vinyl chloride) (PVC) and Poly(acrylonitrile) (PAN) are two examples of precipitation polymerization in the absence of any solvent. Water-based polymerization of acrylonitrile and polymerization of styrene in hexane or ethanol are two examples of precipitation polymerization where a solvent is added to induce the polymer precipitation. The resulting particles of precipitation polymerization technique are usually in the size range of 0.1 to 1000 μm .

The uniqueness of the precipitation polymerization lies in the absence of any stabilizing agent such as surfactants or steric stabilizers for obtaining stable particles. In fact, in this process, the formation of stable spheres is achieved by means of a self-stabilizing mechanism. Upon the discovery of precipitation polymerization in organic media, a variety of monomers including methacrylate, maleic anhydride, and chloromethylstyrene were copolymerized using this technique (Li et al. 1998, Frank et al. 1998). In this polymerization technique, primary particles do not swell in the medium, and both of the initiation and polymerization take place largely in the homogeneous medium. This leads to continuous nucleation and the coagulation of the resulting nuclei to form larger and larger particles. Thus, this method produces irregularly shaped and polydisperse particles. The uncontrolled aggregation of particles restricts the access of monomer to the polymer radicals and also prevents the even dissipation of the heat of polymerization, leading to runaway reactions and generally erratic behavior (Sowa et al. 1979).

1.3.1.5 Dispersion Polymerization

Dispersion polymerization has been known as an exceptional method to prepare monodisperse polymer particles of 1 to 15 μm in a single step process (Barret, 1969; Lok et al. 1985; Williamson et al. 1987; Stejskal et al. 1991; Bourgeat-Lami et al. 1997). This process is very similar to precipitation polymerization, except for the fact that a stabilizer is required to prevent the polymer particle agglomeration. These particles have a wide variety of applications in areas such as column packing materials for chromatography, standard particles for calibrating instruments, spacers of liquid-crystal panels, support materials for biochemicals, catalyst carriers, information storage materials, biomedical diagnostics, protein recovery, drug delivery, and coatings (Lovelace et al. 1981; Kulin et al. 1990; Urban et al. 2002). Other techniques of polymerization such as emulsion polymerization also can be used to produce polymer particles in this size range. However, these processes are complex and can be difficult to reproduce since they are very tedious multiple step processes.

In a dispersion polymerization, several stages can be identified during a reaction. First, the initiation takes place in an initially homogeneous solution which contains a monomer, a dispersive agent (solvent), and a steric stabilizer which are mixed together with an initiator that usually decomposes at relatively high temperatures to generate free radicals and initiate the reaction. Second, because the reaction medium is chosen to be a poor solvent for the polymer produced, the polymer chains will precipitate from the medium once they exceed a critical chain length. As the polymerization progresses, nucleation of the primary particles through the precipitation of oligomeric chains from the solvents takes place due to their incompatibility with the solvent, and the nuclei grow fast via agglomeration and

polymerization to form mature particles with subsequent adsorption of the stabilizer. There are different types of stabilization which will be discussed later in this chapter (section 1.2.2.1). The number of mature particles becomes constant after a low conversion in systems that produce a narrow particle size distribution. Thereafter, no further nucleation occurs, and the particle size increases until the monomer is consumed (Tseng et al. 1986; Sudol 1997). There are at least two significant polymerization loci, namely, the continuous phase and the polymer particle phase. The continuous solvent phase can be polar, nonpolar, or supercritical carbon dioxide. Polymer chains shorter than the critical chain length and unstable nuclei formed in the continuous phase can be captured by particles, contributing to particle growth, or can grow themselves to become new particles. Furthermore, as the monomer is consumed by reaction, the composition of the continuous phase changes, as well as the ratio between the two phases, and this can affect the partitioning of the components between two phases. Under suitable conditions, very narrow or even monodisperse particles can be obtained using dispersion polymerization techniques. It should be noticed that the primary particles which are formed in dispersion polymerization are swollen by the polymerization medium and/or the monomer. As a result, polymerization proceeds largely within the individual particles, leading to the formation of spherical particles. Figure 1.5 shows a schematic of particle formation and growth in dispersion polymerization.

Dispersion polymerization may be regarded as a form of precipitation polymerization modified by the presence of a polymeric stabilizer to prevent flocculation and aggregation of the precipitated particles. Since aggregation is prevented in dispersion

polymerization, both heat and mass transfer can take place without restriction resulting in a highly reproducible and controllable process.

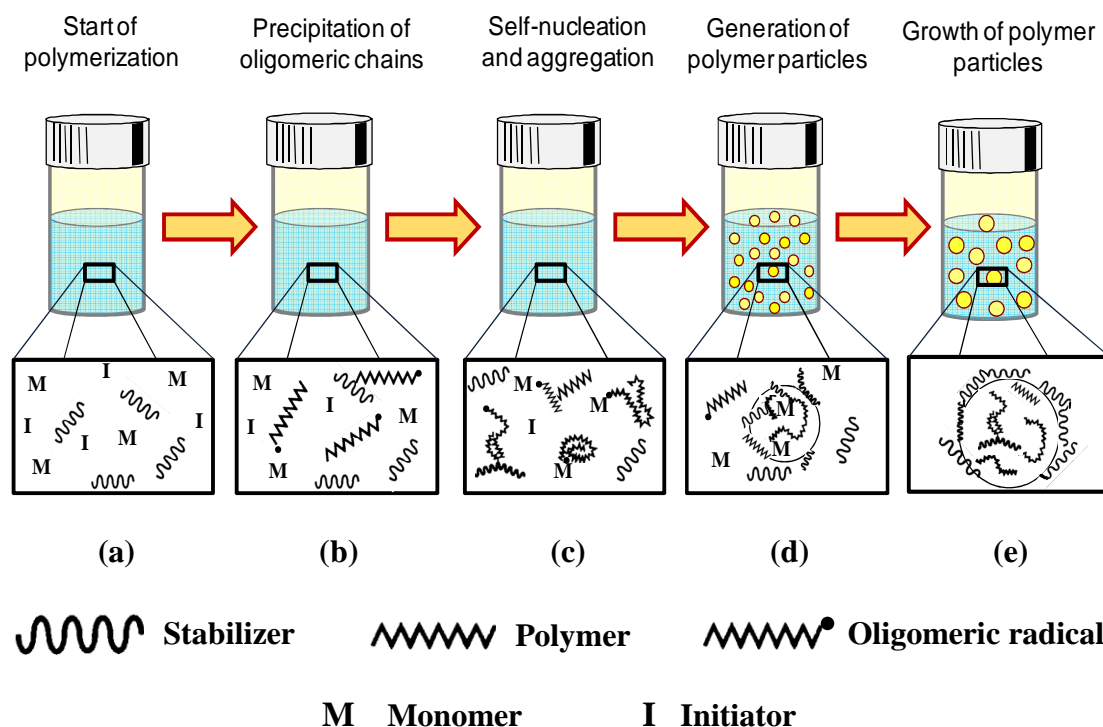


Figure 1. 5 Schematic of particle growth in dispersion polymerization. (a) Homogeneous solution of monomer, initiator and stabilizer. Initiator decomposes to give free radicals that attack the monomer to produce free oligomeric radicals (b) Oligomeric radicals which begin to precipitate once they reach the critical chain length, and particle stabilization begins. (c) Self-nucleation and aggregation of primary polymer species. (d) Particle growth by monomer swelling and further polymerization within particles; stabilization via grafted and/or adsorbed stabilizer. (e) Continued growth to produce final particles.

The first studies of dispersion polymerization technique were carried out in nonpolar organic solvents. Later, this method was studied in polar solvents such as C1-C5 alcohols to form monodisperse polymeric microspheres. The similarities and differences between dispersion polymerization and the other types of heterogeneous polymerization described before are summarized in Table 1 (Barret, 1987).

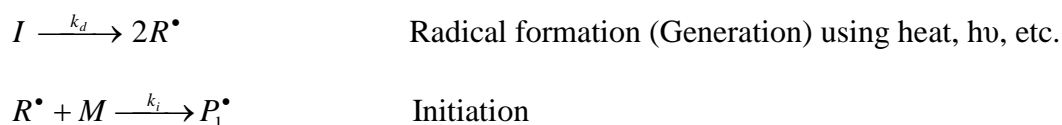
Most of the dispersion polymerizations are carried out using free radical polymerization techniques and thermal initiators. These initiators are activated at relatively high temperatures to produce free radicals which then can react with monomer to produce polymer chains. Free radical polymerizations involve initiation, propagation, chain transfer, and termination.

Table1. 1 Comparison of properties of heterogeneous polymerization systems.
(adopted from Barret, 1987)

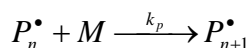
Condition	Dispersion	Precipitation	Suspension	Emulsion
Separate monomer phase	No	No	Yes	Yes
Initiator dissolved in diluent	Yes	Yes	No	Yes
Particles formed in diluent phase	Yes	Yes	No	Yes
Particles stabilized	Yes	No	Yes	Yes
Particle number dependent on stabilizer concentration	Yes	No	Yes	Yes
Polymerization rate dependent on particle number	No	No	No	Yes

The following scheme is a kinetic mechanism for a typical free radical polymerization initiated by thermal initiators. In heterogeneous polymerizations, these reactions can take place in each of the phases present in the system.

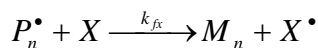
Initiation:



Propagation (for $n \geq 1$):



Chain Transfer:



Chain Termination:



where I = initiator, R^\bullet = initiator radical, M = monomer, P_n^\bullet = live polymer radical with n monomer units, X = monomer, chain transfer agent, solvent, polymer, impurity, and etc. M_n = dead polymer chain with n monomer units ($n \geq 2$).

According to this scheme, the polymer chains are initiated by free radicals generated by the attack of initiator radicals to monomer molecules. Initiator radicals can be produced using heat, irradiation, redox systems, etc. Then, the free radicals which are generated from decomposition of initiator, adds to the double bond of the monomer and another radical is produced by the resultant unpaired electron (primary radical). This new radical is then free to react with another monomer unit. The procedure of chain growth continues in this way until the radical is terminated by recombination or disproportionation when it is transferred to another chain.

In termination by combination, two chains join together and their unshared electrons coupled to form a single bond between them. In termination by disproportionation, there is an abstraction of proton from the penultimate carbon of one chain to the others. The relative proportion of each termination type depends on the reaction temperature and on the particular polymer. For instance, termination

reaction for styrene polymerization over 70°C is combination, but in case of methyl methacrylate termination reaction is almost exclusively via disproportionation.

An extra complexity in dispersion polymerizations is the transfer of species between phases. The knowledge of heterogeneous polymerization kinetics and thermodynamics of multicomponent phase separation phenomena is crucial in dispersion polymerization systems. The system evolution in dispersion polymerization depends on the composition and the molecular characteristics of the coexisting phases. Phase diagrams provide a better understanding of the equilibrium compositions of these coexisting phases and the relative amounts of these phases for a given composition. For example, if dispersion polymerization of a monomer in a non-solvent is considered to produce a polymer, a ternary phase diagram is explained (Fig. 1.6). The boundary between homogeneous and heterogeneous (unstable) regions is called a binodal curve. The well-known Flory-Huggins (FH) theory of polymer solutions is used to construct a ternary phase diagram for the monomer/polymer/non-solvent system. For a ternary system at equilibrium, the Gibbs free energy of mixing (ΔG_m) can be expressed as follows (Jung et al. 2010):

$$\frac{\Delta G_m}{RT} = \sum_{i=M,P,S} n_i \ln(\phi_i) + \chi_{S,P} n_S \phi_P + \chi_{M,P} n_M \phi_P + \chi_{S,M} n_S \phi_M \quad (1.1)$$

where n_i and ϕ_i are the number of moles and the volume fractions of species (with $i = M$ (monomer), P (polymer), and S (non-solvent) respectively), $\chi_{i,j}$ is the interaction parameter between species i and j , R is the gas constant, and T is the absolute temperature. The definition of the chemical potential of species i in the mixture is:

$$\left. \frac{\partial(\Delta G)}{\partial n_i} \right|_{T,P,n_j} = \mu_i \quad (1.2)$$

From Eq. (1.1) and Eq. (1.2), the chemical potential for each species referred to the standard state ($\Delta\mu_{i,k}$) can be written as follows (Jung et al. 2010):

$$\frac{\Delta\mu_{S,k}}{RT} = \ln(\phi_{S,k}) + 1 - \phi_{S,k} - s\phi_{M,k} - r\phi_{P,k} + (\chi_{S,M}\phi_{M,k} + \chi_{S,P}\phi_{P,k})(\phi_{M,k} + \phi_{P,k}) - s\chi_{M,P}\phi_{M,k}\phi_{P,k} \quad (1.3)$$

$$s\frac{\Delta\mu_{M,k}}{RT} = s\ln(\phi_{M,k}) + s - \phi_{S,k} - s\phi_{M,k} - r\phi_{P,k} + (\chi_{S,M}\phi_{S,k} + s\chi_{M,P}\phi_{P,k})(\phi_{S,k} + \phi_{P,k}) - \chi_{S,P}\phi_{S,k}\phi_{P,k} \quad (1.4)$$

$$r\frac{\Delta\mu_{P,k}}{RT} = r\ln(\phi_{P,k}) + r - \phi_{S,k} - s\phi_{M,k} - r\phi_{P,k} + (\chi_{S,P}\phi_{S,k} + s\chi_{M,P}\phi_{M,k})(\phi_{S,k} + \phi_{M,k}) - \chi_{S,M}\phi_{S,k}\phi_{M,k} \quad (1.5)$$

where subscript k indicates the phase (1 = non-solvent-rich phase, 2 = polymer-rich phase); s and r are the molar volume ratios of non-solvent/monomer and non-solvent/polymer, respectively. Equations (1.3) to (1.5) can be used to find the binodal curve. A schematical reaction path corresponding to a dispersion polymerization is also indicated in Fig. 1.6. Note that the non-solvent is inert and the reaction path is simply represented by a straight line parallel to monomer/polymer axis. Mixtures in the area inside the binodal curve are heterogeneous while those outside this curve are homogeneous. The initial monomer/nonsolvent mixture is a single homogeneous phase (Point A in Fig. 1.6). The reaction proceeds homogeneously until the amount of polymer in the system is high enough to induce the system phase separation (point B in Fig. 1.6). At this point, the mixture turns turbid and such turbidity can be detected to construct the ternary phase diagram (Jung et al. 2010).

There are many reports on dispersion polymerization that deal with the polymerization mechanism, effect of polymerization parameters, kinetics, modification with functional groups, cross-linking, polymerization processing, and other topics. The physical processes which are involved in dispersion polymerization are difficult to measure by conventional measurement methods, such as electron microscopy, light scattering, hydrodynamic, or capillary chromatography.

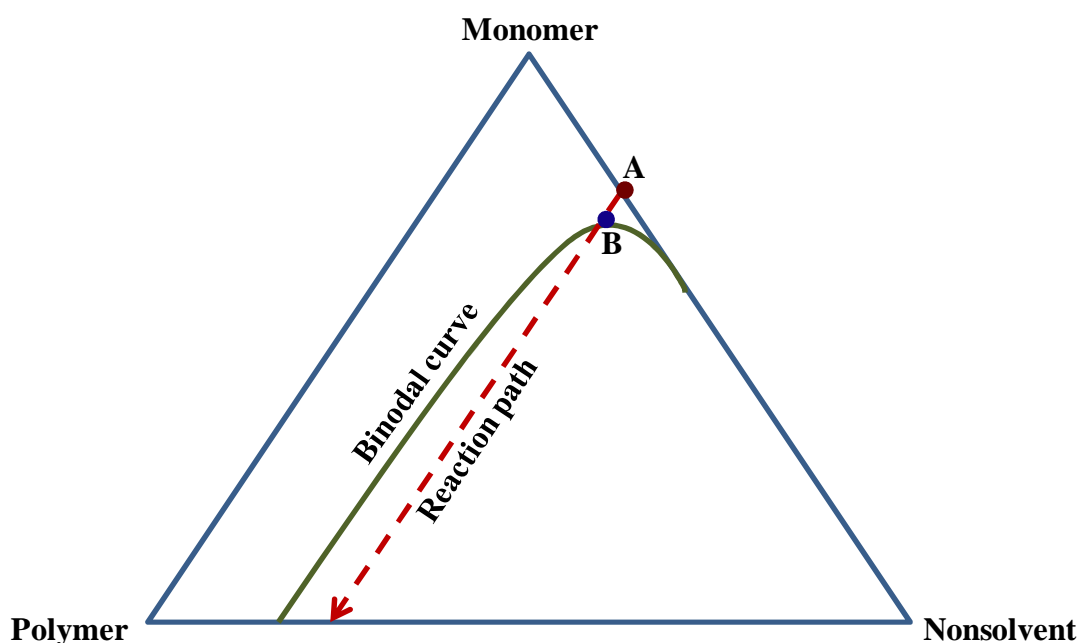


Figure 1. 6 Schematic representation of a ternary phase diagram for dispersion polymerization. Binodal curve and reaction path have been shown (adopted from Jung et al. 2010).

Although, the dynamic light scattering (DLS) can provide direct evidence for the proposed particle formation mechanism, the actual particle formation is open to variety of interpretations and theoretical models (Shen et al. 1994). In fact, the kinetics and the mechanisms involved in dispersion polymerization are still poorly

understood, because size and molecular weight of the polymer particles in dispersion polymerization depend on numerous reaction parameters such as type and concentration of stabilizer, initiator, solvent, and monomer. Reaction temperature and agitation also affect the dispersion polymerization mechanism. Dispersion polymerization process is highly sensitive to small changes in these parameters. These factors make the control of particle properties in terms of size and size distribution rather empirical. The effect of all these parameters on particle size, particle size distribution, and molecular weight of the formed particles are discussed in the following sections.

1.3.2 Effect of recipe and reaction conditions on dispersion polymerization

1.3.2.1 The effect of stabilizer type and concentration

The steric stabilizers play a critical role in the nucleation stage of dispersion polymerization. Selecting an appropriate stabilizer is crucial to produce stable and monodisperse polymer particles. In dispersion polymerization, produced particles are not sufficiently stable without using a stabilizer and there is a high probability of agglomeration of polymer particles during the course of particle formation. Coagulation of unstabilized polymer particles during dispersion polymerization is due to the effect of Van Der Waals attractive forces between individual particles. The stabilizer can form a barrier on the particle surface and weaken these forces and thus prevent the coagulation. The stabilization in a dispersion polymerization could result from strong interactions, either chemical method (grafting reaction) or physical

means (adsorption), between the stabilizer molecules and the polymer molecules to be prepared. Particle stabilization in dispersion polymerization is usually referred to as “steric stabilization”, as compared with emulsifier or charge stabilization in emulsion polymerization. The steric stabilizers have been shown to be located on the surface layers of the particles formed (Paine et al. 1990 (a)). For dispersion polymerization in polar media such as water and methanol, a common characteristic of the steric stabilizers which are used is that they all contain labile hydrogen atoms. During a reaction, the hydrogen atoms are readily abstracted, which allows grafting of the monomer to form an amphipathic copolymer (Croucher et al. 1987). This *in-situ* graft polymer may act as the real stabilizer by anchoring on the particle surface, providing steric stabilization. The existence of these *in-situ* graft polymer have been studied using infra-red (IR) spectroscopy, NMR, and electron microscopy (Hattori et al. 1993; Wang et al. 2001; Paine et al. 1990 (a)). For dispersion polymerization in non-polar media, usually a block or graft copolymer which contains both soluble and insoluble polymer segments is used as the stabilizer. Insoluble part of the stabilizer anchors strongly on the surface of the polymer particle while the soluble fraction of the steric stabilizer forms a barrier around the particle to hinder the aggregation. In fact, polymer and oligomer compounds with lower solubility in the medium and higher affinity for the polymer particles are the best stabilizers for dispersion polymerizations (Winnik et al. 1987, Barret 1987).

Various types of steric stabilizers have been used in dispersion polymerization processes. For example, poly12-hydroxystearic-acid-g-methyl methacrylate has been used as a stabilizer in non-aqueous media. Block copolymers of poly(styrene-b-methyl methacrylate), poly(styrene-b-dimethyl siloxane), and poly(styrene-b-

(ethylene-co-propylene)) have been used as stabilizers in cyclohexane (Bourgeat et al. 1997). Poly(N-vinyl pyrrolidone) (PVP) (Almog et al. 1982), hydroxypropyl cellulose (HPC) (Lee et al. 2002) , poly(acrylic acid) (PAA) (Ober 1987), poly(styrene-co-methacrylic acid), poly(vinyl alcohol) (PVA) (Kim et al. 2006), and poly(dimethyl siloxane) (PDMS) (Pelton et al. 1990 and 1991) are the other examples of steric stabilizers which have been used widely in dispersion polymerization processes.

The selection of an effective steric stabilizer depends on the monomer and the dispersion medium. A good stabilizer should be soluble in the system and be able to provide sufficient coverage for the polymer particle simultaneously. The effect of stabilizer concentration on particle size in dispersion polymerization has been investigated by many researchers. Increasing the stabilizer concentration generally decreases the polymer particle size because an increase in the concentration of stabilizer increases the viscosity of the medium and the rate of physical adsorption of the stabilizer. Thus, the extent of aggregation of particles decreases and consequently the particle size is reduced. Moreover, during the nucleation period in dispersion polymerization, the stabilizer chains form a structure that acts as a skeleton for particle growth. Thus, when the stabilizer concentration increases, the number of nuclei increases that leads to formation of more polymer particles with smaller size (Wang et al. 2001; Tseng et al. 1986; Shen et al. 1994).

Increasing the molecular weight of the stabilizer usually decreases the particle size since the viscosity of the medium increases. However, there are a few studies that have suggested that the molecular weight of the stabilizer has little or no effect on the particle size (Almog et al. 1982; Corner 1981). In some cases also polymer particle size has increased by increasing the molecular weight of the stabilizer (Klein et al.

2003). A change in molecular weight of stabilizer has two opposite effects. Higher molecular weight of the stabilizer increases the viscosity of the medium and amount of the adsorbed stabilizer. As a result, the extent of nuclei aggregation reduces and smaller polymer particles are formed. On the other hand, higher molecular weight of the stabilizer increases its solubility in the medium and thus reduces the rate of anchoring adsorption of the stabilizer.

The effect of co-stabilizer on particle size in dispersion polymerization has been also investigated by some researchers. For example, Tseng (1986) has reported that the co-stabilizer is necessary for monodisperse particles to be formed in dispersion polymerization of styrene in ethanol with azo-type initiators and PVP as stabilizer. On the other hand, Lu et al. have shown that co-stabilizers such as Aerosol OT and Triton N-57 have no effect on the size, size distribution, and molecular weight of the polystyrene particles which were formed using the same method (Tseng 1986, Lu et al. 1988).

1.3.2.2 The effect of reaction temperature

The reaction temperature plays an important role in determining the polymerization rate and thermodynamic properties of the polymerization system. The partitioning of the monomer between polymer particles phase and continuous solvent phase also is severely affected by reaction temperature. It also affects the particle size, particle size distribution, and the molecular weight distribution of polymer.

Usually as the polymerization temperature increases, the size and polydispersity of the polymer particles increases (Shen et al. 1994; Ober et al. 1986). Reaction temperature affects the rate of initiator decomposition, rate of propagation,

solubility of the oligomers/polymer molecules which are formed, viscosity of the system, and solubility of the steric stabilizer. The high rates of free-radical initiation due to the high polymerization temperatures lead to high monomer conversion. Increasing the polymerization temperature would also causes an increase in the critical chain length due to the increase in the solvency of the dispersion medium. Moreover, as the reaction temperature increases, the rate of adsorption of stabilizer (i.e. the solubility of the stabilizer in the medium increases with temperature) and the viscosity of the continuous phase decrease. Thus, the concentration of precipitated oligomer chains increases due to the increase in the decomposition rate of the initiator, propagation rate, and due to the decrease in the adsorption rate of the steric stabilizer. In other words, a few large polymer chains are produced at higher temperatures due to greater chain termination by initiator, then, fewer nuclei are produced. Furthermore, the concentration of the precipitated chains and the growth rate of existing particles increases. All of these factors can contribute to increase in particle size when the reaction temperature increases.

The average molecular weight of polymer particles usually decreases with increasing the temperature. At lower temperatures more monomer is converted to polymer per initiator fragment than at higher temperatures. As a result, the initiator becomes exhausted more quickly at the higher temperatures and the polymerization slows down and average molecular weight of polymer particles decreases. Additionally, increasing the temperature will increase the solubility of oligomer chains, and thus the locus of the polymerization shifts to the continuous phase before they are captured by the existing particles, resulting in a lower molecular weight. Moreover, at high temperatures, the acceleration of the polymerization rate due to gel

effect is smaller than that at low temperature because the high temperature reduces the viscosity of the polymerization medium with a consequent increase in polymerization rate and termination rate, so that a low molecular weight of polymer is produced.

1.3.2.3 The effect of initiator type and concentration

The initiation rate is critical in obtaining monodisperse polymer particles during dispersion polymerization process. The type of initiator and its concentration has a significant effect on the number of initiating species (free radicals). As a result, particle size, particle size distribution, and average molecular weight of the polymer are affected.

Selection of a suitable initiator for a system is a crucial factor for a successful dispersion polymerization. Most of the initiators such as benzoyl peroxide (BPO), lauroyl peroxide (LPO), and azobisisobutyronitrile (AIBN) decompose at temperatures well above 50°C. If the polymerization should be carry out at lower temperatures, redox pairs, photoinitiators or irradiation should be used to initiate the reaction. Also, if the decomposition rate of an initiator is very fast which leads to a large depletion or complete consumption of the initiator before maximum conversion of monomer to polymer is accomplished, it is quite likely to observe a limiting conversion which is less than the maximum possible conversion. This is known as the dead-end effect and should be prevented by choosing a good initiator or a combination of initiators for the polymerization system. Low conversion and a broad particle size distribution will be the result of using an initiator that decomposes prematurely at the initial stage of polymerization. Initiators with a shorter half-life

produce larger particle than initiators with longer half-lives since the former initiators produce free radicals faster and thus the rate of polymerization and precipitation of polymers would be faster than the rate of stabilizer adsorption.

Studies have shown that in a polar medium at low conversion, the rate of polymerization increases with the concentration of the initiator (Lu et al. 1988). This result may be explained, if it is considered that in the early stages, the polymerization is taking place primarily in continuous phase. The rate of polymerization depends on the concentration of free radicals. At low conversion, the concentration of free radicals is directly related to the initiator concentration. Thus, the rate of polymerization increases when the initiator concentration increases. However, at conversions exceeding 40-50%, the rate of the polymerization reaction becomes independent of the initiator concentration. This result can be rationalized by considering that at these conversion levels, the reaction primarily proceeds through a heterogeneous mechanism in the particle phase. Such a process does not involve the formation of any new polymer chains and would be therefore, expected to be independent of the solution phase initiator concentration.

The average molecular weight of the polymer particles usually decreases with increasing the initiator concentration (Ye et al. 2002 (a), Chen et al. 1992). This is consistent with the anticipated high initial rate of free radical formation at high initiator concentrations that leads to a larger number of oligomeric radicals, a higher degree of termination, and hence the lower average molecular weight.

Studies have shown that in polar media increasing the initiator concentration increases the particle size (Lee et al. 2002, Paine et al. 1990 (b), Chen et al. 1992). The reason is that by increasing the initiator concentration, the rate of radical

formation increases, which brings about the more frequent occurrence of chain transfer involving the initiator. Therefore, the number of particle nuclei formed decreases. Furthermore, lower molecular weight polymer particles are formed, making the grafted stabilizer-polymer more soluble in the media and the stabilizer less effective. As a result, larger polymer particles are produced.

1.3.2.4 The effect of solvent type and concentration

Among all the requirements for the solvent to be suitable for dispersion polymerization, the two most important involve its ability to dissolve the monomer, stabilizer, and initiator and, at the same time, to precipitate the polymer. The type, polarity, and solubility power of the solvent or combination of solvents and their concentration affect the polymerization rate and the particle size distribution in dispersion polymerization processes since the solubility of the monomer and initiator in the solvent is changed. The two major effects of solvent on dispersion polymerization process appear to be: (a) the partitioning of monomer and initiator between solution and particle phases (which affects the locus of polymerization and, therefore, the molecular weight); and (b) the solubility of the stabilizer (which affects the initial particle count and, therefore, the molecular weight). The rate of nucleation, the number of nuclei, and the diffusion rate of oligomer radicals are also affected by the solvent. The solubility of oil-soluble monomer and initiator in dispersion medium decreases with increasing the polarity of the medium. More monomer and initiator molecules may transfer to the forming particles when the polarity of the medium is high. Therefore, relatively high polymerization rates are observed.

The particle size usually decreases by increasing the polarity of the medium. Three component Hansen solubility parameters have been shown to be useful for rationalizing, analysis, and predicting particle sizes in dispersion polymerizations of monomers in polar solvents. For oil-soluble monomers, with increasing the polarity of the solvent, the critical chain length of the polymer would decrease and the adsorption of stabilizer would increase, and thus the rate of nuclei formation, the number of nuclei, and the rate of adsorption of the stabilizer would increase, resulting in smaller uniform particles (Seo et al. 1998, Uyama et al. 1994).

For oil-soluble monomers, the molecular weight of the polymer particles increases when the polarity of the medium increases. The polymerization mainly takes place within the particles with increase of medium polarity and delayed radical termination within the particles due to increased viscosity could be the reason of increasing the molecular weight of the particles.

The first studies of dispersion polymerization technique were carried out in nonpolar organic solvents. Later, this technique was used in polar solvents as a method for the formation of monodisperse polymeric microspheres. Many researchers have studied this technique in order to control particle size and achieve narrow particle size distribution. For example, Paine and his coworkers have examined the effect of alcoholic solvents on particle size of polystyrene. They have found that the effect of solvent is significant in series of solvents varying from 80% ethanol/water to ethanol and from methanol to decanol. Polymer particles with the size of 4 μm obtained in butanol and pentanol, 1.2 μm particles in 80% ethanol/water, and 1.6 μm particles in decanol (Paine et al. 1990 (b)).

1.3.2.5 The effect of monomer type and concentration

Micron-sized polymer particles have been prepared from a variety of monomers, such as styrene (Paine et al. 1990 (b), (c), Xu 2000, Nakashima et al. 2008), chloromethylstyrene (Bahar et al. 2004), vinyl acetate (Okaya et al. 2004), n-butyl acrylate (BuA) (Lee et al. 2009), methylmethacrylate (MMA) (Kim et al. 2006, Klein et al. 2003, Jiang et al. 2007), acrylamide (Ye et al. 2002 (a), Lee et al. 2002), and etc. Among all of these monomers, the dispersion polymerization of styrene in polar media and the dispersion polymerization of methyl methacrylate in non-polar media have been extensively studied. Dispersion copolymerization of MMA and BuA has also been studied, and it has been shown that particles with different morphologies can be obtained by changing the ratio of MMA to BuA (Jiang et al. 2007). Moreover, dispersion copolymerization of styrene and other monomers has been investigated (Li et al. 1998, Ober et al. 1987, Yang et al. 2001)

The monomer concentration in dispersion polymerization plays an important role in determining the final particle size, particle size distribution, molecular weight of the particle, and rate of polymerization. The average particle size and the polydispersity of the size distribution usually increase with increase in monomer concentration because increasing the monomer concentration would increase the solvency of the medium for the formed polymer, resulting in an increased critical chain length of the growing oligomer molecules and decrease in the adsorption rate of stabilizer at the same time. Also, the swelling of the particles by the monomer increases and the oligomeric radicals in solution can continue to aggregate (nucleate) and to generate new particles. These would lead to formation of large particles with broad size distributions.

Increasing the monomer concentration also increases the molecular weight of polymer particles and its distribution because using the same amount of initiator produces similar amounts of radicals and higher monomer concentrations result in faster propagation rates and thus more monomer units are added to each free radical prior to termination resulting in higher molecular weights. This result is quite coincident with the kinetics of radical polymerization in which the number average molecular weight is proportional to monomer concentration (O'dian 1981).

Bamnolker et al. (1996) showed that by increasing the styrene concentration from 16 to 48% (w/v) in a mixture of ethanol and 2-methoxy ethanol, the particles diameter consistently increased from 2.3 μm up to 5 μm . They found that the surface polarity of the polystyrene particles becomes lower at higher monomer concentrations. This decrease in surface polarity can be a major reason for the increase in particle size, since it affects all the mechanisms through which small particles grow to their final size. For example, lower surface polarity will increase the swelling of the polystyrene particles by styrene and the agglomeration of polystyrene nuclei.

1.3.2.6 The effect of rate and type of agitation

The stirring speed has an important effect on the particle formation in dispersion polymerization. Usually when the stirring speed is high, the rate of the particle aggregation due to the shear stress of the fluid is high. Also, by increasing the agitation, the rate of polymerization increases. To clarify why the polymerization rate at a high stirring speed is higher than that at a low stirring speed, the effect of the stirring speed on the mass transfer rates of radicals and monomer should be

considered. At higher stirring speed, the polymerization mainly takes place in continues phase (medium) because radical absorption rate from the medium to particles decreases and the monomer concentration in the medium increases. The particle size usually decreases as the agitation rate increases. Increasing the rate of agitation corresponds to increasing the shear force, which causes the particle size to decrease (Kiatkamjornwong et al. 2000). The average molecular weight usually decreases when the agitation speed increases. This might be because, at a high rate of agitation, the shearing force can overcome the solution viscosity to induce faster chain diffusion in the polymer solution. As a result, the rate of the chain termination is higher, thus yielding polymers with the lower molecular weights. The high stirring speed also results in the high rate of particle aggregation due to the shear stress of the fluid and the low surface area which has to be stabilized by the stabilizer molecules (Yasuda et al. 2001).

The type of agitation (for example using a shaker bath or a tumbler) has a weak influence on the monodispersity according to the results reported by Paine et al. and Tseng et al. (Paine et al. 1990 (b), Tseng et al. 1986).

1.3.2.7 The effect of purging nitrogen

Studies have shown that purging the reaction media with nitrogen decreases the polydispersity of polymer particles in dispersion polymerization. A possible explanation for the effect of the purging with nitrogen is based on the nucleation stage. Initially, the system is a homogeneous solution where radicals are produced by decomposition of the initiator. These radicals react with monomer to form polymer chains. The oxygen acts as an inhibitor because it reacts rapidly with free radicals and

reduces the concentration of free radicals and, hence, the nucleation rate will decrease. This will make the nucleation period longer, resulting in a broad particle size distribution. It should be noted that oxygen is not completely dissolved in the medium so the diffusion of the oxygen from the headspace of the polymerization container to the reaction mixture during the polymerization process leads to a continuous partial inhibition that makes polydisperse polymer particles (Nomura et al. 1972, Lopez de Arriba et al. 1994).

Hattori et al. (1993) found that the presence of oxygen affects the colloidal stability during the dispersion polymerization of divinylbenzene in methanol. They considered likely that the oxygen promotes the grafting of poly(divinylbenzene) to the poly(vinylpyrrolidone) stabilizer molecules because the particle size decreased when the presence of oxygen was increased (Hattori et al. 1993).

1.3.3 Micro dispersive suspension polymerization

Polymer particles having complex internal morphologies have been the subject of active research in recent years because of their significant and industrial importance. Core-shell, single hollow, and multi-hollow are just a few examples of these complex particles used for many applications that include encapsulation of drugs and functional cosmetic compounds (Emmerich et al. 1999, Langer 1998, Bergbreiter 1999, and Kim et al. 2002), protection of biologically active materials (e.g., enzymes, proteins, and DNA) (Im et al. 2005 and Ruiters et al. 2006), thermal insulation (Wu et al. 1998), hiding agents for coatings (Itou et al. 1999), floating materials for absorbing organic oils (Gross et al. 1995), electromagnetic wave absorbing materials for stealth applications (Mu et al. 2006), separation and

purification of enzymes and cells (Okubo et al. 2003), temperature-responsive microspheres (Li et al. 2008), phase change material for thermal energy storage (Boh et al. 2005), and thermally expandable polymer microspheres (Soane et al. 2003).

Most of the methods that are used to produce particles with complex internal structure are multi-step emulsion-based polymerization techniques. Dynamic swelling method (Okubo et al. 2001 and 2002), interfacial cross-linking polymerization and precipitation in an oil-in-water emulsion system (Jiang et al. 2006), colloidosome technique (Dinsmore et al. 2002), polymerization with functionalized silica-template and post-reaction etching method (Xu et al. 2004), atom transfer radical polymerization (ATRP) (Fu et al. 2005), and multi-stage water-in-oil-in-water emulsion technique (Kim et al. 1999, 2000, and 2003) are just some examples of these methods. All these emulsion-based processes yield submicron-sized polymer particles (diameter of the particle $< 1 \mu\text{m}$) with a single type of internal morphology. They require long process times and multiple steps, and they are nearly impossible to apply to produce larger, micron-sized particles with various types of internal morphologies. Moreover, scale up and mass production is very difficult using these techniques and they are not cost effective. These methods are usually used at relatively high temperature (70°C or more) which is not suitable for some special applications such as encapsulation of biologically active materials.

Jung et al. (2010) proposed a new technique to produce micron-sized polymer particles with a variety of internal morphologies. This technique is a single-step non-emulsion technique of polymerization which is called micro-dispersive polymerization in a confined reaction space (MDPCRS).

Figure 1.7 shows a schematic diagram of MDPCRS. Using this technique, different complex morphologies are developed after inducing a controlled micro-phase separation in the confined reaction space of a suspended droplet that contains monomer, initiator, stabilizer, and a poor solvent for the polymer. Inside the droplets, a micro-dispersion polymerization takes place after the system phase separation due to the presence of the nonsolvent. This method is very versatile and facile to generate a wide variety of micron-sized polymer particles with complex morphologies in a single step process, but it is still carried out at high temperature (70°C).

Figure 1.8 shows some examples of the polymer particles that Jung et al. (2010) produced using MDPCRS.

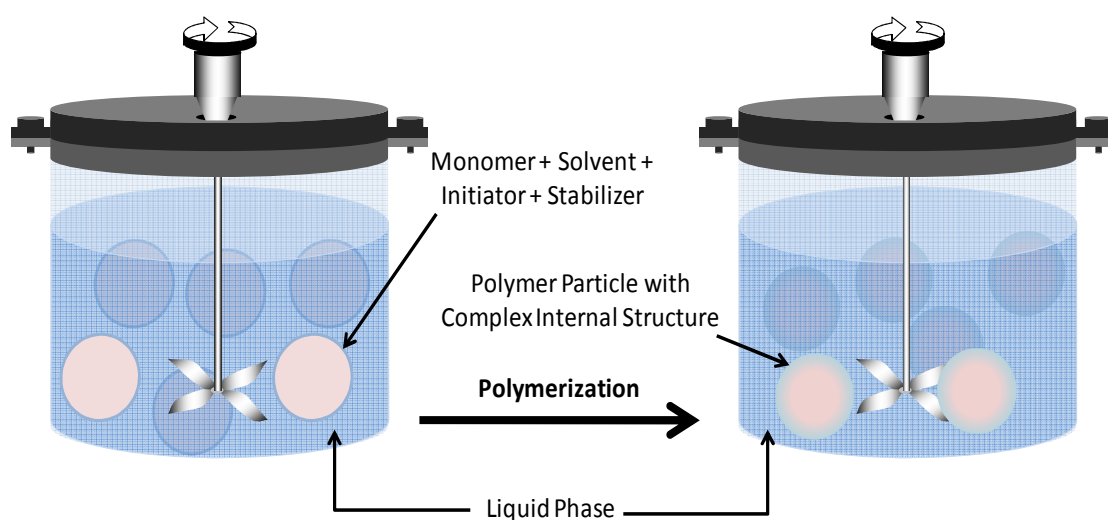


Figure 1. 7 Schematic representation of micro-dispersive polymerization in a confined reaction space (MDPCRS).

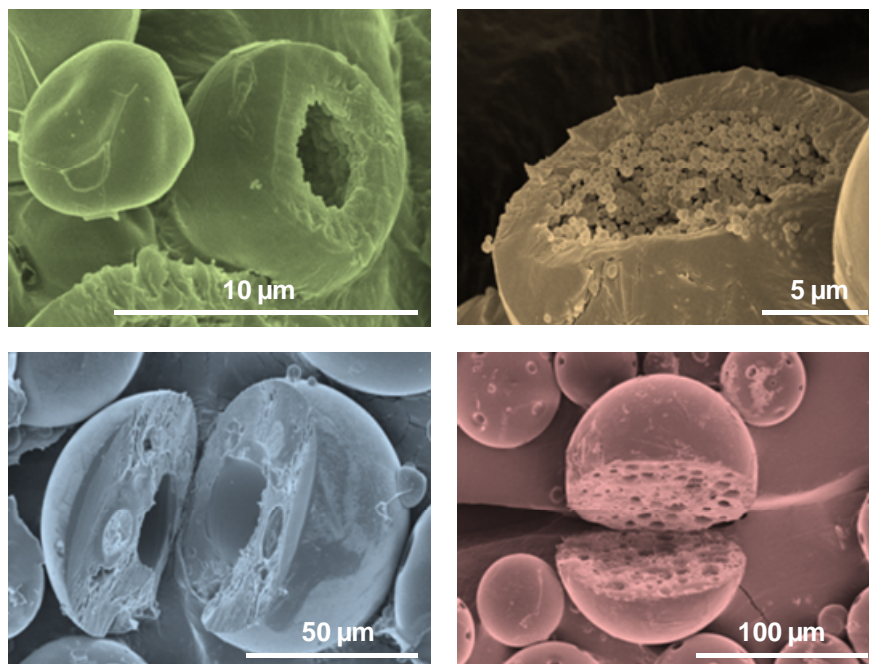


Figure 1. 8 Micron-sized polymer particles with complex internal structure produced using micro-dispersive polymerization in a confined reaction space (MDPCRS) (adopted from Jung et al. 2010).

1.3.4 Dispersion polymerization at low temperature

Polymerizations under “mild” reaction conditions have received great attention because of their applications in encapsulation and *in vivo* delivery of DNA, cells, proteins, and a variety of biologically active materials (Jeong et al. 2002, Delgado et al. 2002, Johnson et al. 2009). As it was mentioned before dispersion polymerization is a unique method to produce highly monodisperse micron-sized polymer particles in a single step in comparison to the other polymerization techniques which are multi-stages and difficult to carry out for this purpose. In spite of that, dispersion polymerizations at relatively low temperatures have been scarcely investigated. Ye et al. (2002 (b)) studied the dispersion polymerization of MMA at room temperature. They used a polar medium of water/alcohol and poly(N-vinylpyrrolidone) (PVP) as steric stabilizer. In their study, the reaction was initiated

by irradiation with gamma-rays (Ye et al. 2002 (b)). Dai et al. (2003) used the same technique with n-hexane/ethanol as medium and vinyl-terminated polysiloxane (PDMS) as stabilizer (Dai et al. 2003). Other researchers also have studied the dispersion polymerization of different monomers such as styrene, methyl acrylate, and acrylamide using the same technique (Chang et al. 2004, Zhang et al. 2007). Recently, dispersion polymerization of MMA in ethanol/water medium at room temperature using a UV photoinitiator has been investigated (Chen et al. 2008).

Redox systems are known as the best choice to initiate free radical polymerizations under mild reaction conditions. For instance, the polymerization of vinyl monomers in organic phase can be carried out at relatively low temperatures using diacyl peroxides and tertiary amines as redox pairs (Sato et al. 1975, Turovskii et al. 2003). Another example is the bulk polymerization of MMA at 45°C using lauroyl peroxide (LPO) and N.N-dimethylaniline (DMA) as a redox system (Qiu et al. 1984). According to the mechanism that was proposed by Sato et al. (1975) the

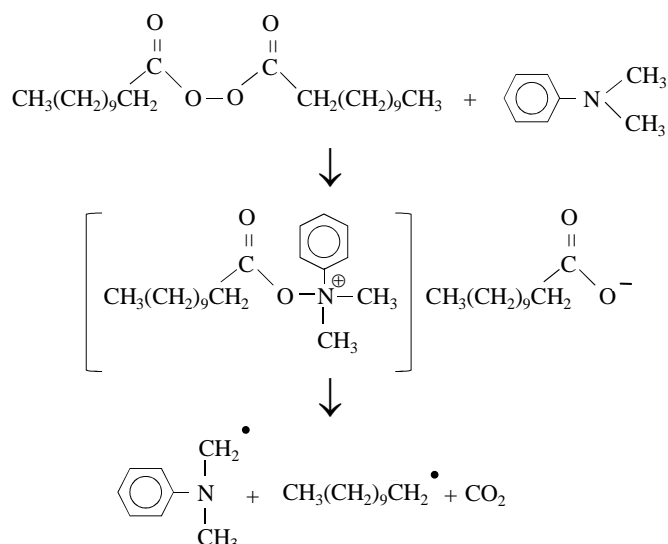


Figure 1. 9 Reaction between LPO and DMA to initiate free-radical polymerizations. Adopted from Sato et al. (1975).

generation of radicals proceeds via formation of an intermediate anilinium salt followed by a homolytic $N^{\oplus} - O$ bond cleavage into a N-methylanilinomethyl radical and a undecyl radical (see Fig. 1.9).

In this work, dispersion polymerization of MMA at low temperature has been investigated using a redox pair. The following model system was tested in order to find the best reaction conditions for producing highly monodisperse polymer particles: methyl methacrylate (MMA) as monomer, hexane as solvent, methacryloxypropyl-terminated polydimethyl siloxane (PDMS) as stabilizer, and lauroyl peroxide/N,N-dimethylaniline as redox system. Particle morphology was investigated using scanning electron microscopy (SEM) and polymer molecular weight distribution was also analyzed using gel permeation chromatography (GPC). Conversion was determined by standard gravimetric method.

Macroscopic dispersion polymerizations were carried out using small vials as reactors to assess the feasibility of dispersion polymerization of MMA in hexane and optimizing the reaction conditions. Dispersion polymerization experiments were also carried out in the confined reaction space of a monomer droplet which is suspended in the aqueous medium of water and polyvinyl alcohol (PVA). This is the first research work that deals with the production of highly uniform poly(methyl methacrylate) (PMMA) particles at low temperatures via dispersion polymerization in a nonpolar hydrocarbon solvent.

Chapter 2: Macroscopic dispersion polymerization of methyl methacrylate at low temperature

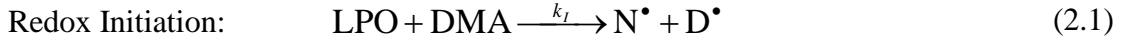
In chapter 1, various polymerization techniques that are commonly used in industrial/commercial polymerization processes were discussed. In this chapter, the macroscopic dispersion polymerization of methyl methacrylate at low temperature in a nonpolar solvent (n-hexane) using LPO/DMA redox system has been studied.

First, a preliminary study using conventional batch reactors was conducted to assess the feasibility of dispersion polymerization of methyl methacrylate. Then, the main dispersion polymerization experiments were carried out to find the reaction conditions to produce highly monodisperse micron-sized poly(methyl methacrylate) particles. The partition coefficients of the redox initiation system were also measured to study the locus of the polymerization process. The effect of recipe on monomer conversion, polymer average molecular weights, and polymer morphology were studied throughout standard gravimetric method, gel permeation chromatography (GPC), and scanning electron microscopy (SEM). Finally, the stability of the polymer particles and the occurrence of phase inversion during dispersion polymerization were investigated. The theory of dispersion polymerization and materials and methods that were used in this research work are presented in the following sections of this chapter, and then the results are discussed.

2.1 Theory of free radical dispersion polymerization using a redox pair of initiators

A free radical dispersion polymerization involves initiation, propagation, chain transfer, and termination reactions in two phases (i.e. solvent-rich phase and

polymer-rich phase). The following kinetic scheme can be applied to each of the coexisting phases of the dispersion polymerization initiated by LPO/DMA redox pair.



Propagation (for $n \geq 1$):



Chain Transfer to the Monomer and to the Solvent (for $n \geq 1$):



Chain Termination (for $n, m \geq 1$):



where $\text{N}^\bullet, \text{D}^\bullet$ = initiator radicals, M = monomer, R_1^\bullet = primary radical R_n^\bullet = live polymer radical with n monomer units, S = solvent, P_n = dead polymer molecule with n monomer units ($n \geq 2$). This kinetic mechanism is applicable to the initial homogeneous step of dispersion polymerization and to each phase after the system phase separation. Note that we assume that each single phase is still a homogeneous phase. Redox initiation is particularly interesting because it can be used to initiate the polymerization under mild reaction conditions. The mechanism of initiation reaction using LPO/DMA to produce primary radicals (equation 2.1) was adopted from the literature and introduced before in chapter 1 (see Fig. 1.8). These initiator radicals are able to attack to a monomer to produce primary radicals. Propagation (reactions 2-2

to 2-4) involves successive additions of monomers to primary or non-primary radicals to produce larger active polymer radicals (equation 2.4). Chain transfer reactions can also take place between live polymer radicals and monomer or solvent to produce dead polymer molecules that can not react with any other radicals (equations 2.5 and 2.6). The final step of the dispersion polymerization is termination reaction. Termination always involves the reaction of two active radicals, but this can go in one or two ways. The first is the simple formation of a bond between two radicals that is called combination (equation 2.7). The second termination mechanism is called disproportionation, where a portion is transferred and two dead polymer molecules are formed (equation 2.8). Although for MMA, the termination by disproportionation is dominant, termination by combination is still present and it affects the polymer molecular weight distribution.

In dispersion polymerization, the number of particles and polymer particle size distribution are dependent on the particle nucleation and growth. In the absence of an effective stabilizer, particle aggregation or agglomeration takes place. Renucleation (formation of new polymer particles in addition to the existing particles) results in an increase of the number of particles and a decrease of the average particle size. Therefore, in order to obtain monodisperse particles, renucleation should be prevented. In dispersion polymerization of methyl methacrylate in alkanes, the particle formation is normally completed in a relatively short time (Barret et al. 1969). Therefore, as mentioned before in chapter 1, the actual particle formation mechanism is open to variety of interpretations. There are two proposed mechanisms for the nucleation of the polymer particles during dispersion polymerization process: the self-nucleation and the aggregate nucleation. The mechanism of self-nucleation

is based on the idea that each propagating oligomer chain moves freely in the disperse medium until it reaches a critical molecular weight, when it collapses upon itself and is separated in the form of condensed phase to nucleate a particle. The self-nucleation theory predicts that the propagating oligomer chains do not interact with each other in the reaction medium (Fitch et al. 1971). The idea of aggregate nucleation is based on the association of growing oligomer chains in the system. In this theory, the concentration of oligomer chains and their molecular weight both influence the increase of the degree of association. The aggregates that formed are initially unstable and the oligomer chains associate only reversibly. When reaching a certain critical size, the aggregates become stabilized and gradually change to polymer particles. In dispersion polymerization in nonaqueous media, both of these mechanisms are complementary (Juba et al. 1979). In both of these theories, when the polymer particle is produced, the stabilizer prevents the polymer particles coagulation and makes them stable in the dispersion medium.

As it was mentioned before in chapter 1, at the beginning of the dispersion polymerization, there is a homogeneous system of monomer, solvent, stabilizer, and initiator. As soon as the polymer is produced, the precipitation of polymer particles is induced. In fact, the point where the polymer starts precipitating in the solution is known as phase separation point. One of the phases that is produced after phase separation is called the solvent-rich phase and the other one is called the polymer-rich phase. Thus, another important characteristic of the dispersion polymerization is its heterogeneity, and it is necessary to consider the equilibrium between different phases that are formed during the dispersion polymerization process. A ternary phase

diagram can be used to understand this phenomenon. Figure 2.1 shows a schematic ternary phase diagram for the dispersion polymerization process.

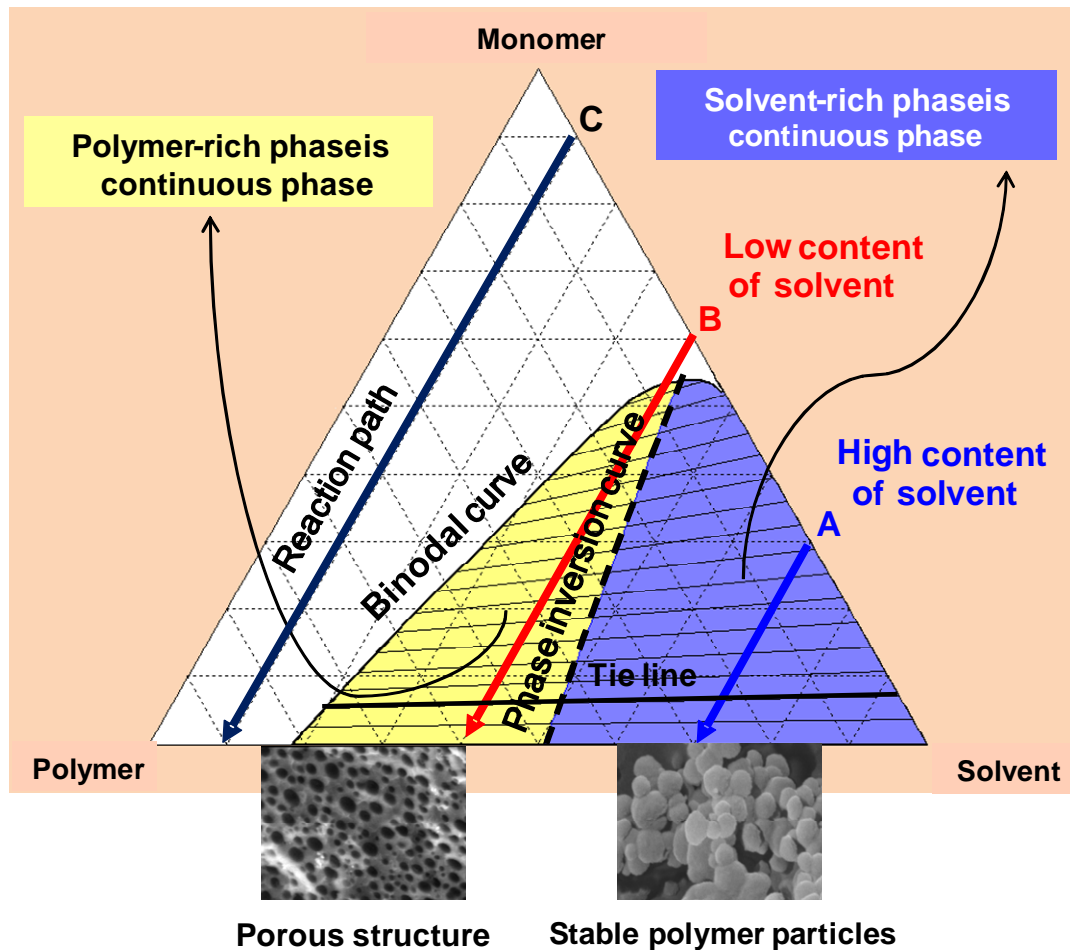


Figure 2. 1 Schematic representation of a ternary phase diagram for dispersion polymerization. Binodal curve, tie lines, reaction path, and phase inversion curve have been shown (adopted from Dr. Luciani et al. with her permission).

Ternary phase diagrams are constructed based on different methods such as visual examination or light scattering (Aggarwal et al. 1996). As it was mentioned before in chapter 1, the region outside the binodal curve, is homogeneous (single phase) and the region inside it is heterogeneous. At equilibrium, the chemical

potential of each component in the solvent-rich phase is equal to that in the polymer-rich phase and the binodal points can be determined. Tie lines can be constructed by connecting the composition of mutually stable binodal points. The composition of the phases can be determined using the ternary phase diagram. Three arbitrary reaction paths (arrows parallel to the monomer/polymer axis) are also shown in Fig. 2.1.

According to Jung et al. research work different morphological structures can be produced according to the region in which the phase separation occurs (Jung et al. 2010). At relatively high solvent contents, monomer accumulates preferentially in the polymer rich-phase and under special conditions stable polymer particles can be produced (point A in Fig. 2.1), when the solvent to monomer ratio decreases, the polymerization exhibits an initial homogeneous stage, followed by a heterogeneous stage (after the reaction path intersects the binodal curve). At special reaction conditions when the reaction starts, the solvent rich-phase is the continuous phase, but after the polymer is produced and precipitates, the polymer-rich phase becomes the continuous phase. This phenomenon is called phase inversion and the product will be a porous polymeric structure (point B in Fig. 2.1). If the solvent to monomer ratio is very low, the reaction proceeds in a single phase from the beginning to the end of the polymerization. Therefore, polymer's final morphology should be similar to those which are obtained by simple bulk polymerization of the monomer (point C in Fig. 2.1). In the following sections, the materials and methods that were used for macroscopic dispersion polymerization (section 2.2) and the experimental results obtained (section 2.3) are presented and discussed.

2.2 Materials and Methods

The dispersion polymerization of methyl methacrylate in n-hexane was carried out using 20 ml vials (VWR TraceClean) as reactors. The effects of stabilizer molecular weight and concentration, initiator concentration, and agitation on polymer particles morphology were examined. The results of this study were analyzed to carry out new set of experiments in order to find the best recipe to produce uniform monodisperse poly methyl methacrylate (PMMA) particles.

Methyl methacrylate (MMA) was used as monomer (Sigma-Aldrich). This monomer was purified by molecular sieves. For this purpose, the monomer passed through a column of F-200 activated alumina beads of 4.8 mm diameter and 340 m³/g surface area (Delta Adsorbents). Lauroyl peroxide (LPO) and redistilled N,N-dimethylaniline (DMA) as redox system of initiators (Atochem and Sigma-Aldrich) were used as received. N-hexane (Fisher) was used as solvent without any further purification. For the preliminary experiments, methacryloxypropyl-terminated polydimethylsiloxane (PDMS) of molecular weight between 4,000-6,000 g/mol was used as steric stabilizer, but for the main set of experiments, methacryloxypropyl-terminated polydimethylsiloxane (PDMS) of molecular weight between 20,000-30,000 g/mol was used as steric stabilizer. The stabilizer was purchased from Gelest Company. The high molecular weight stabilizer was chosen for main set of experiments because it can provide a good stabilization of MMA dispersions in comparison to low molecular weight PDMS (Klein et al. 2003). The properties of the chemicals used in this work are summarized in Table 2.1.

Table 2. 1 Properties of monomer, redox system, solvent, and stabilizer

Property	MMA	LPO	DMA	n-hexane	PDMS
Melting Point (°C)	-48	53-57	75	-95	<-60
Boiling Point (°C) at 760 mmHg	100	467.3	76-78	69	>205
Molecular Weight (g/mol)	100.12	398.62	121.18	86.18	4000-6000/20000-30000
Density (g/cm ³)	0.94	0.91	0.956	0.668	0.96

Several dispersion polymerizations were carried out at 30°C up to relatively high monomer conversions ($x \sim 0.8-0.9$). Initial solvent/monomer ratio, stabilizer molecular weight and concentration, stabilizer/monomer ratio, and initiator concentration were varied one at a time in order to explore the recipe able to produce the reasonable results. A typical example of the recipe used in these experiments is 48 wt. % MMA, 7 wt. % LPO, 4 wt. % DMA, 39 wt. % n-hexane, and 2 wt. % PDMS. The exact recipes used in each experiment are indicated in section 2.3.

The procedure used to carry out the macroscopic dispersion polymerizations are as follows: 1) A monomer-rich solution is prepared by mixing the required amounts of LPO (solid) and MMA (liquid) at room temperature for about 15 minutes, until complete dissolution of LPO; 2) A solvent-rich solution is made by mixing the required amounts of n-hexane (liquid) and PDMS (liquid) at room temperature for about 5 minutes; 3) Solutions (1) and (2) are mixed together in a 20-ml glass vial, and finally the corresponding DMA aliquot is added to the mixture; 4) The vial is quickly sealed with a fluoropolymer resin/siliconseptum cap, stirred, and purged with nitrogen for several minutes; 5) The sealed vial is immersed in a water bath at 30°C. Since the content of each vial is very small, the reaction temperature is reached in less

than one minute, and the polymerization can be considered essentially isothermal; 6) Vials are removed from the water-bath at different times, and the polymerization is stopped by the addition of a small amount of hydroquinone and methanol.

In order to investigate the effect of the initial solvent/monomer ratio on the size of polymer particles at early stages of the polymerization, several dispersion polymerizations were also carried out at low monomer conversions ($x \sim 0.1-0.2$). These reactions were carried out using the same procedure indicated before, but the vials were removed from the 30°C-bath a few minutes after the mixtures turned visually turbid (i.e, the system cloud points).

In all of the experiments, samples were analyzed to determine the monomer conversion, polymer molecular weight distribution (MWD), and particle morphology.

2.2.1 Determination of conversion

For all of the experiments, monomer conversion was determined by a standard gravimetric technique. It consists of precipitating the polymer with methanol, filtering, and drying the sample under vacuum at room temperature until obtaining a constant weight. In the case that the produced polymer mass was tough and it was impossible to remove it from the vial, the polymer sample was first dissolved in acetone, and then precipitated with methanol.

2.2.2 Characterization of polymer particle morphology

The morphology of polymer particles was examined by scanning electron microscopy (SEM) (Hitachi SU-70 and AMRAY) (see Figure 2.2). Dried polymer samples were spread on carbon tape attached to a small metal disk and were coated

with a thin layer of carbon using a coater instrument (Balzers Union, MED %) under argon atmosphere. Micrographs were taken for each sample at magnification that was appropriate for investigation of morphology and particle size of the samples. The size of the micro- and nano- beads was measured using the scale on the micrographs. The micrographs were analyzed to investigate the effect of different parameters such as monomer/solvent ratio, initiator concentration, etc. on average particle size and morphology of polymer samples in order to find the optimized recipe for producing uniform stable polymer particles.

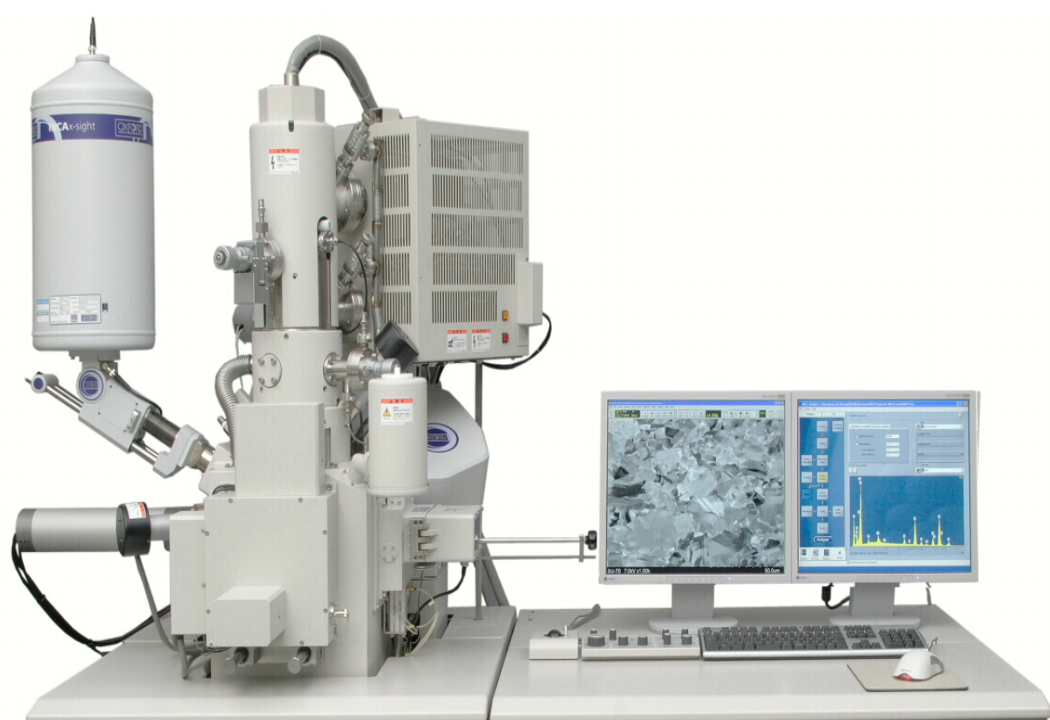


Figure 2. 2 Scanning electron microscopy (SEM) (Hitachi SU-70 and AMRAY) adopted from nano center, University of Maryland.

2.2.3 Polymer molecular weight distribution

Gel permeation chromatography (GPC) has been used to determine polymer molecular weight distributions. Isolated PMMA samples were analyzed at room temperature by GPC, using a Refractive Index (RI) detector, tetrahydrofuran (THF) as mobile phase, and poly(methyl methacrylate) (PMMA) standards for calibration. PMMA samples of polydispersities below 1.09 and weight-average molecular weights of 625500, 138500, 60150, 30530, 10290, and 3810 g/mol (Polymer Laboratories) were used as standards. Figure 2.3 shows a schematic diagram of gel permeation chromatography using a RI detector. This technique makes use of

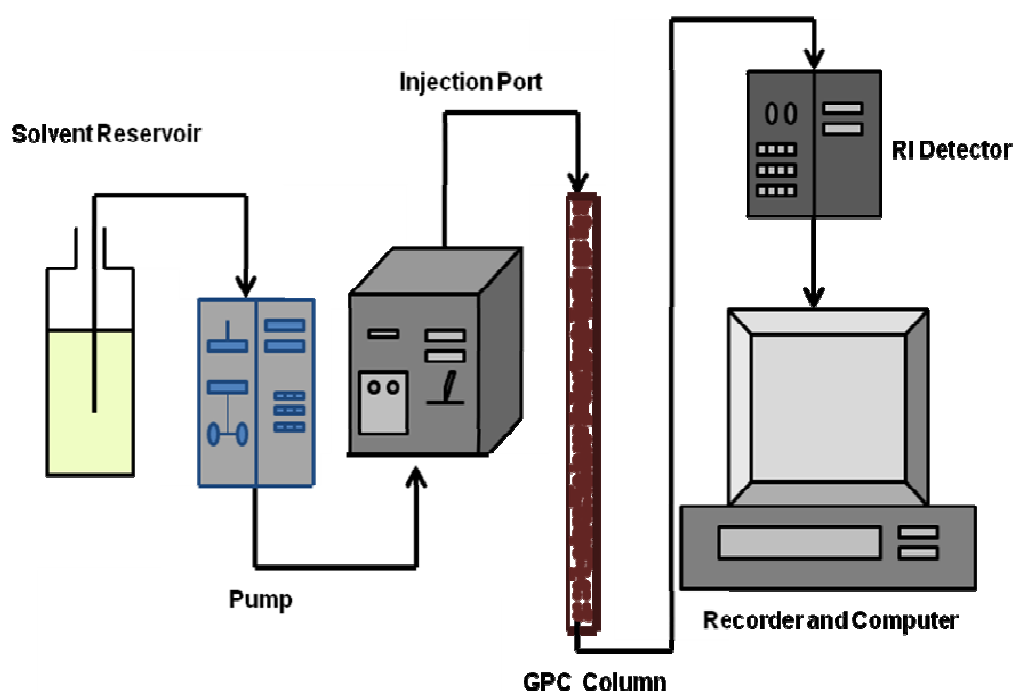


Figure 2. 3 Schematic diagram of Gel-Permeation Chromatography.

columns packed with a crosslinked polymer that is swollen by solvent. The solvent passes through the columns at a constant rate and carries a small amount of polymer

solution with unknown molecular weight. The column beads have small pores and the polymer solution contains different molecular sizes. The separation takes place in the columns due to the size of the polymer molecules in the sample since smaller molecules diffuse in to the pores and larger molecules cannot fit into the small pores and are washed out of the columns faster. The RI detector which is placed at the outlet of the columns, measures the difference in the refractive index between pure solvent and the polymer solution. A recorder is connected to the detector which plots the molecular weight distribution.

2.2.4 Determination of partition coefficients of redox pair

In order to analyze the dispersion polymerization kinetics quantitatively, it is necessary to determine the distribution of species (e.g., initiator and monomer) between phases. Unfortunately, measuring the actual concentration of an initiator or a system of initiators during a heterogeneous polymerization is very difficult since the initial concentration of initiator is very low and also it is consumed as the reaction proceeds. Additionally, a complete separation of the “stabilized” disperse phase from the continuous phase is almost impossible. Determining the initiator partition between phases through “unreactive” blends that emulate the polymerization is a typical approach to overcome these difficulties.

The partition coefficients of LPO and DMA, defined as the ratio between their concentrations in the polymer-rich phase and that in the solvent-rich phase, were measured at room temperature in this study. The measurement were carried out using unreactive blends that contained known amounts of PMMA, MMA, n-hexane, and either LPO or DMA. LPO and DMA were not added together in order to avoid the

initiation reaction. To extend these results to a real dispersion polymerization process, the underlying assumption that interaction between LPO and DMA is negligible needs to be made. Blends were agitated for 48 hours, and the upper (solvent-rich) phase was carefully extracted with a syringe to determine its volume. For the blends containing LPO, an iodometric titration was carried out to determine the number of moles of LPO in the solvent-rich phase (Bertin et al. 2004, Wagner et al. 1947, Sneeringer et al. 1971). The extracted solvent-rich phase was diluted in 10 ml of n-hexane and 10 ml of glacial acetic acid. The mixture was purged with nitrogen for several minutes, and 0.5 g of sodium iodide was added to produce a dark-brown solution that was titrated with a 0.2 M sodium thiosulfate. At the titration end point, mixture turned transparent. This technique was tested with MMA/n-hexane/LPO mixtures of known compositions, and the error in determining the LPO concentration was found to be less than 2%. The partition coefficient of LPO (K_{LPO}) was calculated as follows:

$$K_{LPO} = \frac{(n_{LPO}^0 - n_{LPO,1})}{(V^0 - V_1)} \frac{V_1}{n_{LPO,1}}$$

where n_{LPO}^0 and V^0 are the total number of moles of LPO and the total volume of the initial blends, respectively; while $n_{LPO,1}$ and V_1 are the number of moles of LPO in the solvent-rich phase and the volume of the solvent-rich phase, respectively.

For the blends containing DMA, the titration of the extracted solvent-rich phase was carried out using perchloric acid as titrant and a solution of crystal violet/chlorobenzene (0.1 wt.%) as indicator (Fritz et al. 1950, Gupta et al. 1992). The titrant consisted of a 0.5 M solution of perchloric acid in glacial acetic acid. The extracted solvent-rich phase was first diluted in 10 ml of n-hexane, and then, 1 ml of

indicator was added to the mixture to produce a violet solution. At the titration point, the mixture turned green, and the number of moles of DMA in the solvent-rich phase could be determined. The partition coefficient of DMA (K_{DMA}) was calculated using the following equation:

$$K_{DMA} = \frac{(n_{DMA}^0 - n_{DMA,1})}{(V^0 - V_1)} \frac{V_1}{n_{DMA,1}}$$

where n_{DMA}^0 and $n_{DMA,1}$ are the total number of moles of DMA added to the initial mixture and the corresponding value in the solvent-rich phase, respectively. The results of the experiments and analysis of the macroscopic dispersion polymerization of methyl methacrylate in n-hexane at low temperature are presented in the following section. Also, thermodynamics and kinetics of the polymerization reactions are discussed.

2.3 Results and Discussion

In this section, a summary of the preliminary experimental results regarding macroscopic dispersion polymerization of MMA at 30°C in n-hexane is discussed (Part A). Then, the results of main set of experiments are presented. Measurement of partition coefficients of LPO and DMA (Part B-1), low conversion experiments (Part B-2), high conversion experiments (Part B-3), and the study of stability of polymer particles and phase inversion phenomenon (Part B-4) are also explained.

A. Preliminary Experiments

Several preliminary experiments were carried at 70°C using LPO as a thermal initiator in n-hexane in order to investigate the basic characteristics of the dispersion polymerization technique. The results of these experiments showed that high molecular weight PDMS (20000-30000 g/mol) as stabilizer can provide a better stabilization for particles in comparison to low molecular weight PDMS (4000-6000 g/mol) (Klein et al. 2003). Then, a preliminary study was done to assess the feasibility of dispersion polymerization of MMA in n-hexane using a redox system (LPO/DMA) to initiate the polymerization at 30°C. In this study, the high molecular weight PDMS was used as stabilizer according to the preliminary experimental results. Moreover, the initial concentrations of MMA, LPO, DMA, and the ratio between LPO and DMA were determined from a relatively wide set of bulk polymerization experiments because they promoted fast, but controllable reactions. Free radical bulk polymerization involves the conversion of monomer into polymer without the aid of a solvent, and usually the polymer which is formed is soluble in the monomer and the bulk polymerization proceeds homogeneously. The results of those bulk polymerizations are not presented here since the focus of this research is to investigate the dispersion polymerization process. In the preliminary set of experiments, different recipes were examined as indicated in Table 2.2 and the effects of initial concentration of initiator and stabilizer, and solvent/monomer ratio on the monomer conversion and morphology of the polymer particles were investigated. Table 2.2 also shows the polymerization times and monomer conversions for these preliminary experiments. Initial mixture containing methyl methacrylate, n-hexane, PDMS, and redox initiators is a transparent solution.

Table 2. 2 Reaction conditions for dispersion polymerizations of MMA in *n*-hexane at 30°C

Exp.	Initial Masses						Time	Conversion
	MMA (g)	<i>n</i> -hexane (g)	LPO (g)	DMA (g)	PDMS (g)	Solvent/MMA ratio	(h)	(-)
A1	2.4	2.0	0.169	0.085	0.078	0.83	4	0.121
A2	2.4	2.0	0.169	0.085	0.156	0.83	4	0.151
A3	2.4	2.0	0.254	0.127	0.078	0.83	3	0.602
A4	2.4	2.0	0.254	0.127	0.156	0.83	3.5	0.711
A5	2.4	2.8	0.169	0.085	0.078	1.17	4.5	0.133
A6	2.4	2.8	0.254	0.127	0.078	1.17	3	0.354
A7	2.4	2.8	0.254	0.127	0.156	1.17	4	0.524
A8	2.4	3.8	0.254	0.127	0.078	1.58	5.5	0.307
A9	2.4	3.8	0.254	0.127	0.156	1.58	5.5	0.312
A10	2.4	9.5	0.254	0.127	0.078	3.96	8	0.103
A11	2.4	9.5	0.254	0.127	0.156	3.96	9	0.152

Since *n*-hexane is a non solvent for PMMA, polymer chains precipitate and the reaction mixture becomes turbid as the reaction proceeds.

As expected, by keeping the solvent/monomer ratio constant, the conversion increases when the initiator concentrations increase (see Table 2.2). For example, at solvent/monomer ratio of 0.83 (using 0.078 g PDMS as stabilizer), if the mass of LPO and DMA increase from 0.169 and 0.085 g to 0.254 and 0.127 g respectively, the conversion increases from 0.121 to 0.602 (compare experiments A1 and A3). High initiator concentrations result in an increase in the amount of radicals available to initiate the polymerization, and hence a faster polymerization. Also, it can be seen that stabilizer concentration does not affect the monomer conversion significantly. In

fact, if stabilizer does not participate in the reaction actively, its concentration should not affect the conversion (compare experiments A1 and A2, experiments A3 and A4, experiments A8 and A9, and experiments A10 and A11). Moreover, according to the Table 2.2, by increasing the solvent/monomer ratio the conversion decreases significantly and the polymerization becomes very slow (compare 8-9 hours for experiments A10-A11 to 3-3.5 hours for experiments A3-A4). The reason is the dilution effect produced by the high amount of n-hexane in the recipe. Variations in the monomer to n-hexane ratio can have a significant effect on the nucleation process. Increasing the monomer concentration increases the propagation rate of the oligomeric chains. Consequently, more oligomeric chains precipitate faster. Experiments A3 and A4 show high conversions at reasonable reaction times in comparison to the other experiments.

Figure 2.4 shows the SEM images corresponding to the experiments A1-A11. One of the most important aims of this study is to produce monodisperse polymer particles, and it is obvious from Figure 2.4 that the recipe of Exp. A3 can provide better results in comparison to the other recipes since the polymer particles are stable and uniform. Furthermore, Table 2.2 shows that in this case the conversion is relatively high (0.602) even at shorter reaction times. The size of the polymer particles is approximately 2 μm for Exp. A3 (see Fig. 2.4-c).

Since Exp. A3 produced uniform and stable polymer particles, it was used as a base experiment to test the method of sample preparation for SEM. The effect of two different techniques of sample preparation on polymer morphology was studied for Exp. A3. In the first method the polymer sample was washed by excess amount of hexane before drying and no methanol was added to it, but in the second method, the

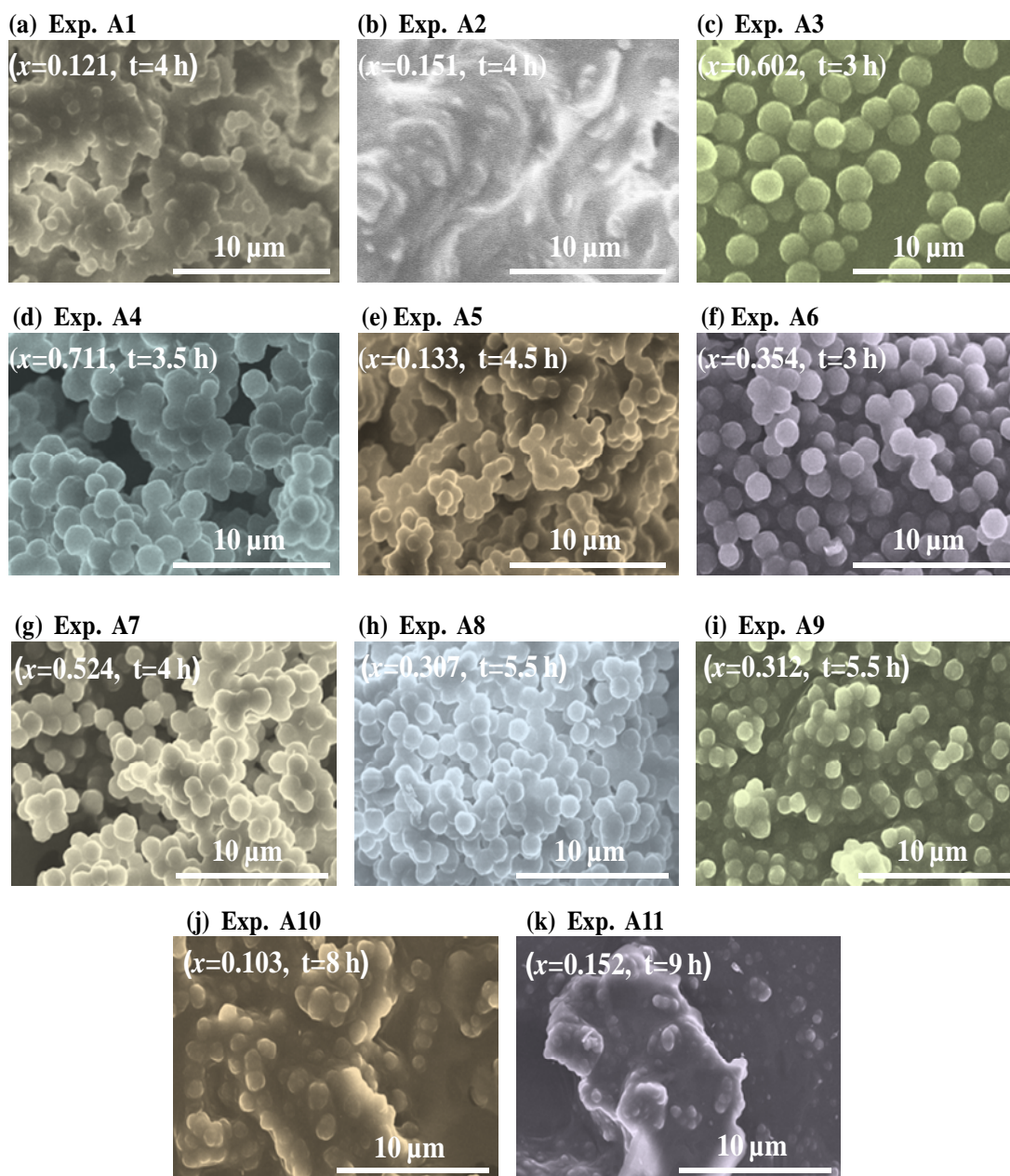


Figure 2. 4 PMMA particles obtained by dispersion polymerization of MMA in *n*-hexane at 30 °C.

methanol was added to the polymer sample and then it was dried. Figure 2.5 compares the resulting SEM images when applying these two proposed methods of sample preparation (*i.e.*, direct evaporation or initial precipitation with methanol). At

relatively high monomer conversions, both methods provide similar results (see Figs. 2.5e and 2.5f). However, some agglomeration of particles is promoted when using methanol as precipitating agent for samples exhibiting lower monomer conversions (see Figs. 2.5c and 2.5d).

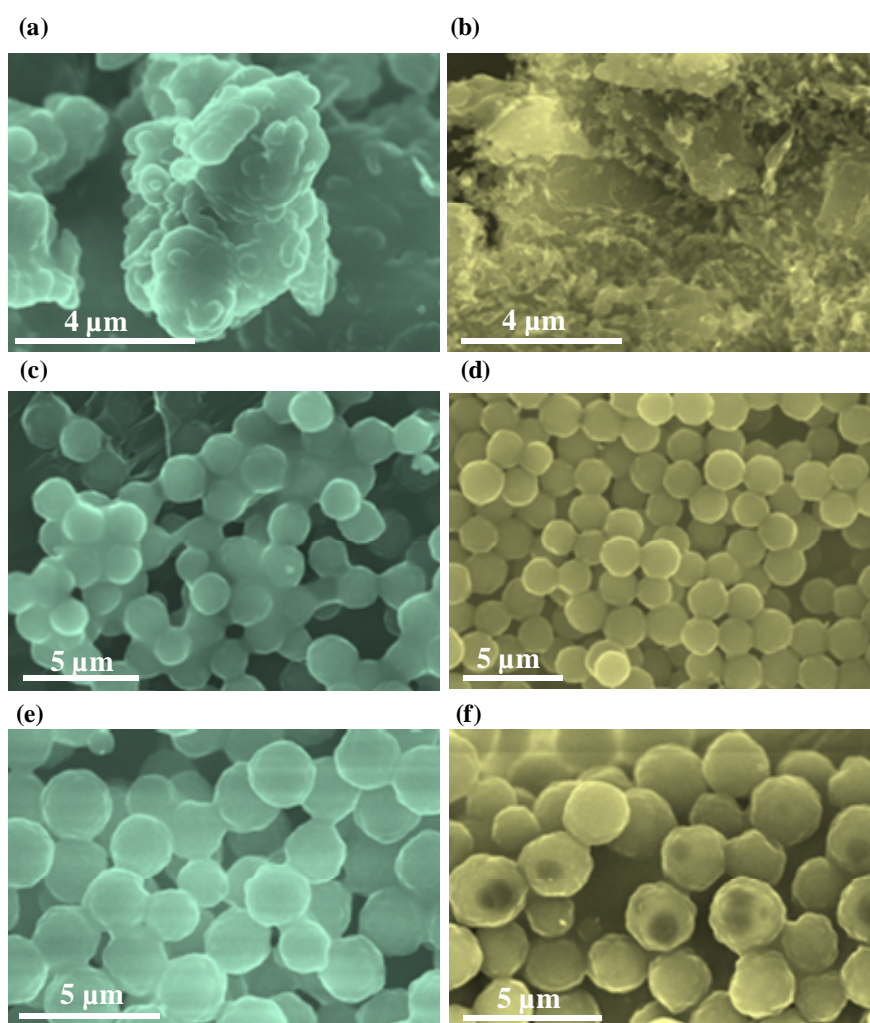


Figure 2. 5 Comparison of SEM micrographs using 2 different preparation techniques for Exp. A3. (a, c, and e) show the polymer particles obtained by precipitation with methanol; (b, d, and f) show the polymer particles obtained by direct evaporation of solvents. For (a and b) $t=1.5$ h; For (c and d) $t=3.0$ h; and for (e and f) $t=5$ h.

Recall that Exp. A3 was impressive in terms of polymerization rate and particle morphology, so its recipe was used as a base to explore in detail the characteristics of this reaction. Since the amounts of LPO and DMA used in Exp. A3 were very high (compared to the concentration used in high temperature experiments), the possibility of using lower amounts of LPO and DMA was tested. Therefore, two reactions were investigated using 10 and 25% of the initial amounts used in Exp. A3 as indicated in Table 2.3.

Table 2. 3 Reaction conditions for dispersion polymerizations of MMA in *n*-hexane at 30°C

Exp.	Initial Masses						Time (h)	Conversion (-)
	MMA (g)	<i>n</i> -hexane (g)	LPO (g)	DMA (g)	PDMS (g)	Solvent/MMA ratio		
A3	2.4	2.0	0.254	0.127	0.078	0.83	3	0.602
A12	2.4	2.0	0.025	0.013	0.078	0.83	10	0.030
A13	2.4	2.0	0.064	0.032	0.078	0.83	10	0.083

As it can be seen in Table 2.3, the conversions of Exps. A12 and A13 after 10 hours of polymerization are significantly lower than the conversion of Exp. A3 after just 3 hours of polymerization. It means that by decreasing the concentration of initiator pairs (LPO and DMA), the polymerization is too slow for any commercial applications. Figure 2.6 shows the SEM pictures of Exps. A12 and A13. It is obvious that opposite to the result of Exp. A3 which produced stable and monodisperse polymer particles, in these two cases the phase separation did not take place even after 10 hours of polymerization. These results are not surprising since as it was mentioned before by decreasing the initiator pair concentration the amount of

available radicals to initiate the polymerization decreases, and hence the reaction rate is very slow.

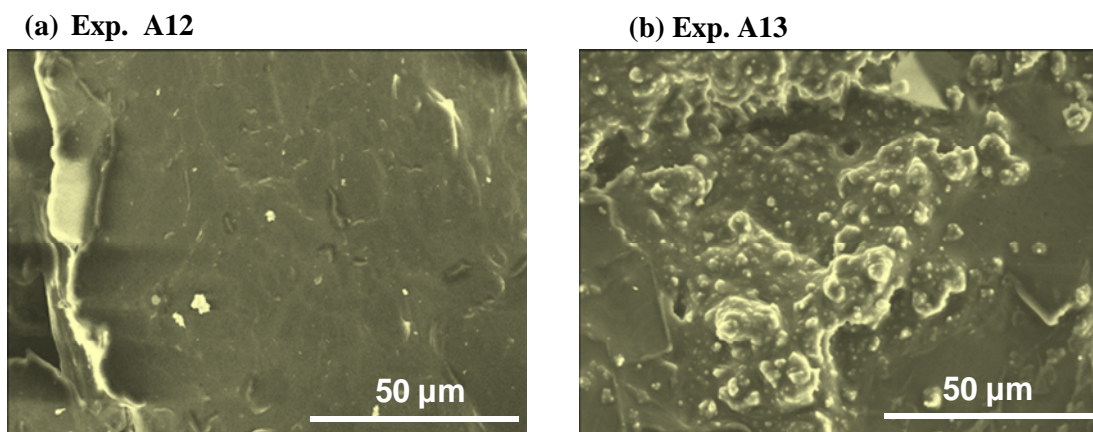


Figure 2. 6 PMMA obtained by dispersion polymerization of MMA in *n*-hexane at 30 °C after 10 hours.

Since the main objective of this research work was to investigate the dispersion polymerization of MMA under “mild” reaction conditions, no agitation was applied in the experiments listed in Table 2.2. Thus, Brownian motion of polymer particles in the medium was considered to be the main factor to induce the agglomeration of polymer particles. However, the effect of agitation on polymer particles morphology was also tested using the recipe of Exp. A3 as a base for three different agitation speeds (i.e., 200 rpm, 500 rpm, and 1000 rpm for Exps. A14, A15, and A16 respectively) (see Table 2.4).

According to Table 2.4, the monomer conversions in Exps. A3 and A14 to A16 are comparable after 5 hours of polymerization, so the polymer particle morphologies can be also compared. Figure 2.7 shows the SEM images

corresponding to samples taken after 5 hours of polymerization using different agitation speeds for the dispersion polymerization experiments listed in Table 2.4.

Table 2. 4 Reaction conditions for dispersion polymerizations of MMA in *n*-hexane at 30°C

Exp.	Initial Masses					Agitation Speed (rpm)	Time (h)	Conversion (-)
	MMA (g)	<i>n</i> -hexane (g)	LPO (g)	DMA (g)	PDMS (g)			
A3	2.4	2.0	0.254	0.127	0.078	0	5	0.803
A14	2.4	2.0	0.254	0.127	0.078	200	5	0.762
A15	2.4	2.0	0.254	0.127	0.078	500	5	0.821
A16	2.4	2.0	0.254	0.127	0.078	1000	5	0.763

Figure 2.8 shows the particle size histograms for these samples. These figures show that by increasing the agitation speed, the particle size distribution broadened. It has been postulated that the agglomeration of the particles occurs in dispersion polymerization because of suppression of repulsive force between particles. This allows the attractive potential to dominate the repulsive particle-particle interactions. Under agitation, the agglomeration of particles increases since the probability of particles collision increases. However, agitation also induces particle break up. When the level of power input increases, the break up mechanism has more probability to take place. Thus, when the agitation speed increases, a broad range of particle sizes is produced due to the agglomeration and break up mechanisms which take place simultaneously.

A more detailed set of experiments was designed based on the preliminary experiments, to get a better understanding of the polymerization process (see section B).

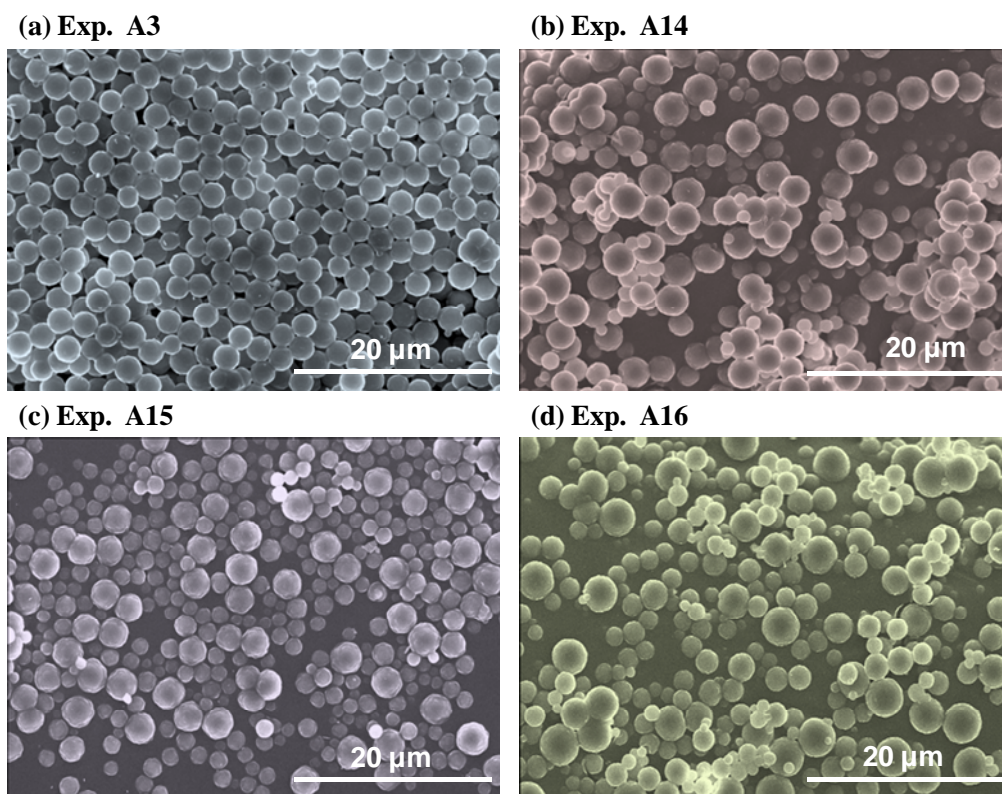


Figure 2. 7 PMMA obtained by dispersion polymerization of MMA in *n*-hexane at 30 °C after 5 hours using different agitation speeds. (a) without agitation (b) 200 rpm (c) 500 rpm (d) 1000 rpm.

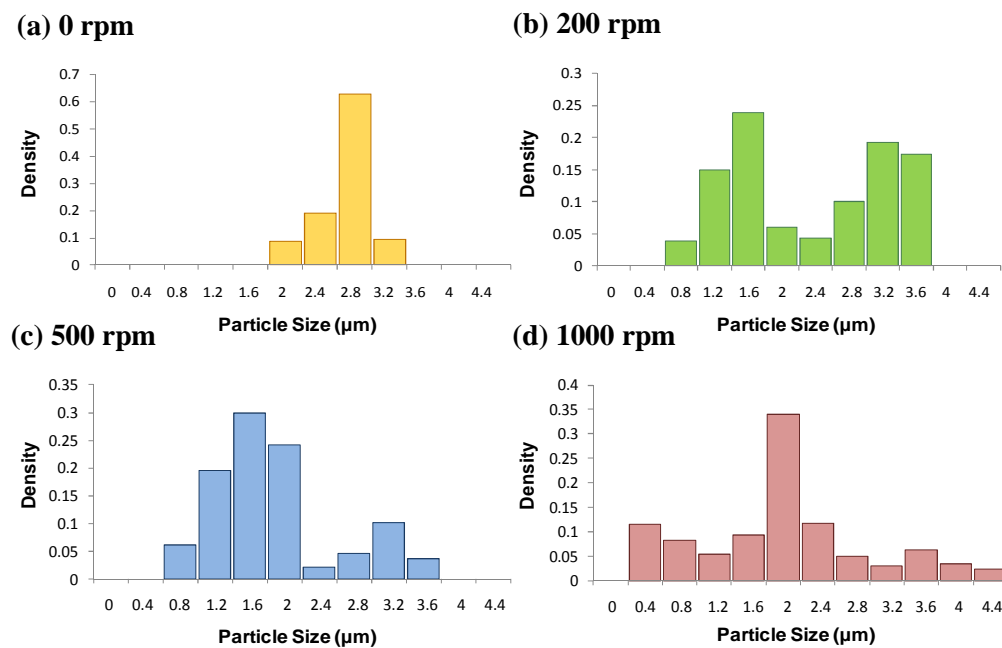


Figure 2. 8 Particle size histograms for samples in Fig. 2.7. Number-density was calculated from SEM pictures.

B. Main Experiments

B-1) Determination of LPO and DMA Partition Coefficients

Tables 2.5 and 2.6 show the results of measuring the partition coefficients of LPO and DMA at room temperature using the titration methods described before in section 2.2.4. The partition coefficient is defined as the ratio between the concentration of each of these species in the polymer-rich phase and that in the solvent-rich phase.

Table 2. 5 Determination of the LPO partition coefficients.

	Blend Composition					K_{LPO}
	MMA (g)	PMMA (g)	<i>n</i> -hexane (g)	LPO (g)	Emulated Conversion (%)	
1	5.9	0.1	9.5	0.515	1.66	41.3
2	5.9	0.1	7.6	0.463	1.66	54.0
3	5.9	0.1	5.7	0.561	1.66	52.5
4	5.9	0.2	9.5	0.491	3.27	34.1
5	5.9	0.2	7.6	0.476	3.27	7.5
6	5.9	0.2	5.7	0.504	3.27	2.6

Table 2. 6 Determination of the DMA partition coefficients.

	Blend Composition					K_{DMA}
	MMA (g)	PMMA (g)	<i>n</i> -hexane (g)	DMA (g)	Emulated Conversion (%)	
1	5.9	0.1	9.5	0.269	1.66	9.6
2	5.9	0.1	7.6	0.268	1.66	6.2
3	5.9	0.1	5.7	0.263	1.66	2.2
4	5.9	0.2	9.5	0.266	3.27	3.5
5	5.9	0.2	7.6	0.262	3.27	4.8

According to the results in Tables 2.5 and 2.6, the partition coefficients are quite higher than unity which means both LPO and DMA preferentially accumulate in the polymer-rich phase. After the phase separation point, most of the PMMA is

produced by polymerization in the monomer-swollen particles, whereas the solvent-rich phase essentially acts as a monomer reservoir. In the polymer rich phase, the amount of solvent is very low. Therefore, the polymer concentration is very high. As a result, a strong gel effect is produced, even at early stages of the dispersion polymerization and the diffusion controlled termination of the polymerization reaction occurs.

B-2) Dispersion Polymerizations (Low Conversion Experiments)

Several dispersion polymerizations at 30°C (experiments B1 to B4) were carried out at low monomer conversions ($x = 0.1\sim 0.2$) to study the effect of the initial solvent/monomer ratio on the size of the polymer particles at early stages of the polymerization. As it can be seen in Table 2.7, the polymerization recipes contain the same monomer-based concentrations of LPO, DMA, and PDMS as used for Exp. A3 (since Exp. A3 produced the best stable and monodisperse polymer particles in the preliminary set of experiments). The initial monomer/solvent ratio was varied from 0.2 to 0.9. In all these cases, the reaction was stopped immediately after the mixtures turned turbid. Table 2.8 shows the conversion, molecular weight averages, and average particle sizes of the polymers produced by experiments B1-B4.

Table 2.7 Reaction conditions for dispersion polymerizations of MMA in n-hexane at 30°C (low conversion experiments).

Exp.	Initial masses					Solvent/monomer ratio
	MMA (g)	n-hexane (g)	LPO (g)	DMA (g)	PDMS (g)	
B1	2.4	0.55	0.254	0.127	0.078	0.20
B2	2.4	1.00	0.254	0.127	0.078	0.40
B3	2.4	1.65	0.254	0.127	0.078	0.70
B4	2.4	2.20	0.254	0.127	0.078	0.90

Table 2. 8 Results of dispersion polymerizations of MMA in *n*-hexane at 30°C
(low conversion experiments).

Exp.	Results immediately after the system cloud point					
	Time (min)	Conversion (—)	\overline{M}_n (g/mol)	\overline{M}_w (g/mol)	$\overline{M}_w / \overline{M}_n$ (—)	$\overline{D}_{P,n}^{(a)}$ (μm)
B1	32	0.19	15,000	42,000	3.0	1.02
B2	23	0.16	17,000	50,000	2.9	0.73
B3	38	0.28	29,000	62,000	2.1	0.41
B4	43	0.15	31,000	85,000	2.7	0.32

^(a) Average diameter of primary particle estimated from SEM images.

Figure 2.9 shows the SEM images of the polymer particles formed at the system phase separation for the low conversion experiments presented in Tables 2.7 and 2.8.

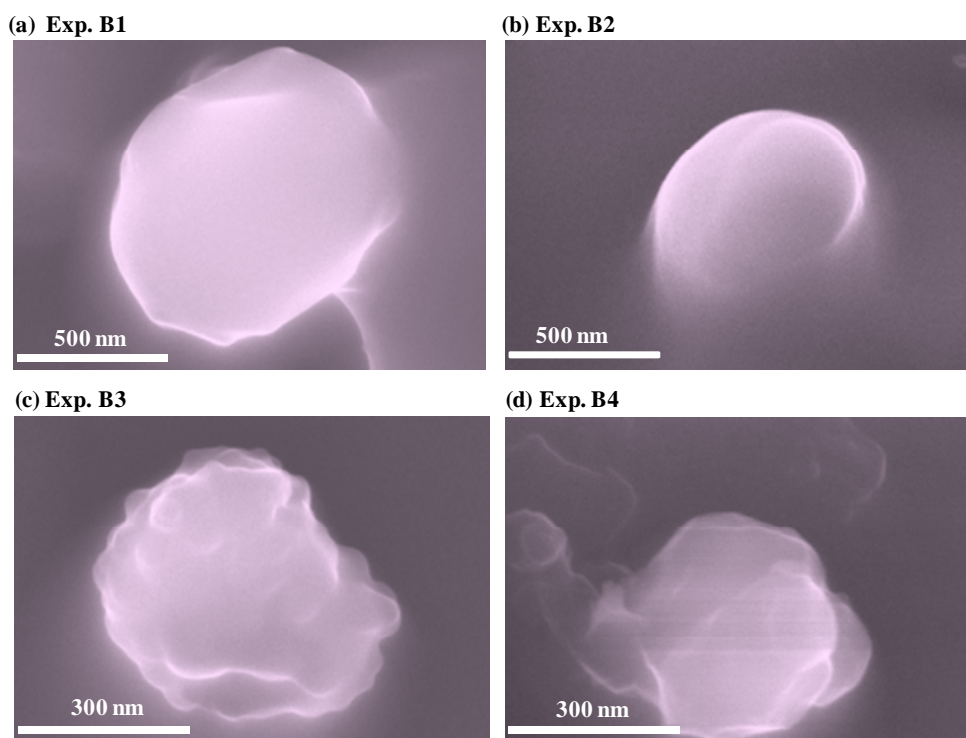


Figure 2. 9 Polymer particles obtained at early stages of dispersion polymerizations of MMA in *n*-hexane at 30°C.

Figure 2.9 shows the dramatic decrease of primary particle size (from $\sim 1\ \mu\text{m}$ to 300 nm) when the *n*-hexane/MMA ratio increases from 0.2 to 0.9. Possibly, this reduction in primary particle size is due to the reduction of the radius of gyration (R_g) of polymer chains when their solubility in the dispersion medium decreases. For a single polymer chain in a pure solvent, the scaling law between R_g and the polymer chain length (l) can be written as $R_g \propto l^\nu$, where ν accounts for the interaction between solvent and polymer ($\nu = 3/5$ for good solvents and $\nu = 1/3$ for bad solvents).

Due to the inherent instability of the primary particles, they are not completely spherical (see Fig. 2.9). It is known that primary particles are formed via agglomeration of smaller nano-domains (aggregates of coiled polymer chains). In Figs 2.9c-d, the former nano-domains of 50-80 nm can be clearly observed.

B-3) Dispersion Polymerizations (High Conversion Experiments)

As it was mentioned in section 2.2, several dispersion polymerizations were carried out at 30°C up to relatively high monomer conversions (fractional monomer conversion: $x = 0.8\sim 0.9$). The initial solvent/monomer ratio was varied in experiments B5-B10 as indicated in Table 2.9. The recipe of experiment B8 is same as Exp. A3 (that had the best result in preliminary set of experiments) and experiment B9 is a replication of Exp. B8. Table 2.10 shows the conversion, molecular weight averages, and average particle sizes of the polymers produced by experiments B5-B10.

From Table 2.10, it is obvious that after three hours of polymerization, experiments B5-B8 exhibit comparable (and relatively high) monomer conversions while experiment B10 exhibits a lower monomer conversion due to the dilution

effect. This dilution effect is produced by the significantly higher amount of n-hexane in its recipe. Tables 2.9 and 2.10 show that the monomer conversion increases as the solvent/monomer ratio decreases. This increase is related to the dilution effect produced by the solvent.

Table 2. 9 Reaction conditions for dispersion polymerizations of MMA in n-hexane at 30°C (high conversion experiments).

Exp.	Initial Masses					
	MMA (g)	n-hexane (g)	LPO (g)	DMA (g)	PDMS (g)	Solvent/MMA Ratio
B5	2.4	1.4	0.254	0.127	0.078	0.58
B6	2.4	1.4	0.254	0.127	0.062	0.58
B7	2.4	1.7	0.254	0.127	0.062	0.71
B8	2.4	2.0	0.254	0.127	0.078	0.83
B9	2.4	2.0	0.254	0.127	0.078	0.83
B10	2.4	2.7	0.254	0.127	0.078	1.12

Table 2. 10 Results of dispersion polymerizations of MMA in n-hexane at 30°C (high conversion experiments).

Exp.	Results after 3 h of polymerization				
	Conversion (—)	\overline{M}_n (g/mol)	\overline{M}_w (g/mol)	$\overline{M}_w / \overline{M}_n$ (—)	$\overline{D}_{P,n}^{(b)}$ (μm)
B5	0.870	26,000	232,000	8.9	2.66
B6	0.795	25,000	231,000	9.2	2.78
B7	0.830 ^(a)	29,000	239,000	8.2	2.35
B8	0.756	38,000	311,000	8.2	1.87
B9	0.754	37,000	254,000	6.8	1.91
B10	0.350	42,000	255,000	6.1	1.68

(a) Sample taken after 4 h of reaction; ^(b) Average diameter of particles estimated from SEM images.

It should be noticed that there is an important phenomenon that may take place during the polymerization process which is called autoacceleration, gel effect, or *Tromsdorff* effect. As conversion increases with time during the polymerization

process, the viscosity of the reaction mixture increases. At high polymer concentrations, there is an acceleration in the rate of molecular weight increase of the polymer chains that have not been terminated that is called gel effect. The reason of this behaviour is that as the polymer formed and the viscosity of the medium increases, rate of propagation which depends on diffusion of small monomer molecules and addition of them to the growing polymer chain is barely affected. On the other hand, termination involves the much slower diffusion of larger macromolecular species which try to get together. Therefore, this increase in viscosity can result in a large decrease in the rate of termination (Rosen, 1993).

Figure 2.10 shows the evolution of the monomer conversion for experiment B8 and B9 which were carried out using the recipe of Exp. A3.

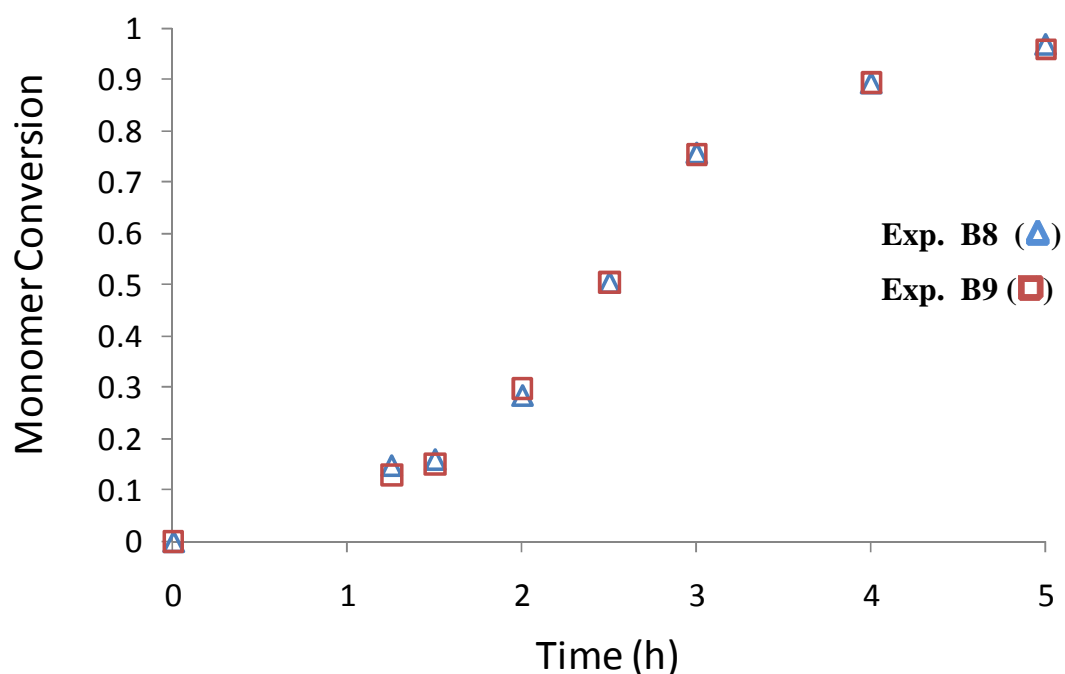


Figure 2. 10 Evolution of the monomer conversion for experiments B8 and B9.

Figure 2.10 shows that the polymerization is relatively fast using the recipe of Exp. B8. The S-shaped curves shown in Fig. 2.10 indicate that a severe gel effect is affecting Exp. B8 and its replication (Exp. B9) after about 2 hours of polymerization. This gel effect is observed since in dispersion polymerizations, the reaction can take place at three different loci: in the diluents, at the surface of the particles, and in the interior of the particles. At early stages of the polymerization, when the conversion is low, the volume of the polymer-rich phase is very low, and even though the amount of LPO and DMA contained in the solvent-rich phase is also low, the high volume of the solvent-rich phase produces enough polymers and controls the global evolution of the monomer conversion. However, at higher conversions when the volume of solvent-rich phase decreases due to the migration of the polymer produced in the solvent-rich phase toward the polymer-rich phase, polymerization reaction occurs mostly in the interior of the particle (polymer-rich phase) and this leads to a reduction of macro-radical mobility and hence a decrease in termination reaction rate in comparison to propagation reaction rate. As a result, an autoacceleration of the polymerization rate is induced at moderate monomer conversions, when the volume of the polymer-rich phase is high enough.

Tables 2.8 and 2.10 also show the average polymer molecular weights for the high and low conversion experiments. The following points can be extracted from Tables 2.9 and 2.10: (i) stabilizer does not affect significantly the molecular weights of polymers produced via dispersion polymerization (compare the results of Exps. B5 and B6); (ii) the polymer weight-average molecular weight (\overline{M}_w) shows a significant increase as the solvent/monomer ratio increases. As a result, polymers with very broad molecular weight distributions are obtained. The reason is that low molecular

weight chains produced in the solvent-rich phase (where diffusion limitations are almost negligible) coexist with high molecular weight chains produced in the polymer-rich phase (where a strong gel effect is present even at early stages of the polymerization). Low conversion experiments validate this statement. At the system phase separation point, most of the polymer has been produced in the solvent-rich phase. Table 2.8 shows that molecular weights and polydispersities of those polymer chains are quite low compared to those obtained at higher monomer conversions (where the effect of the polymer-rich phase becomes significant). Figures 2.11a-b shows the evolution of polymer average molecular weights for Exp. B8.

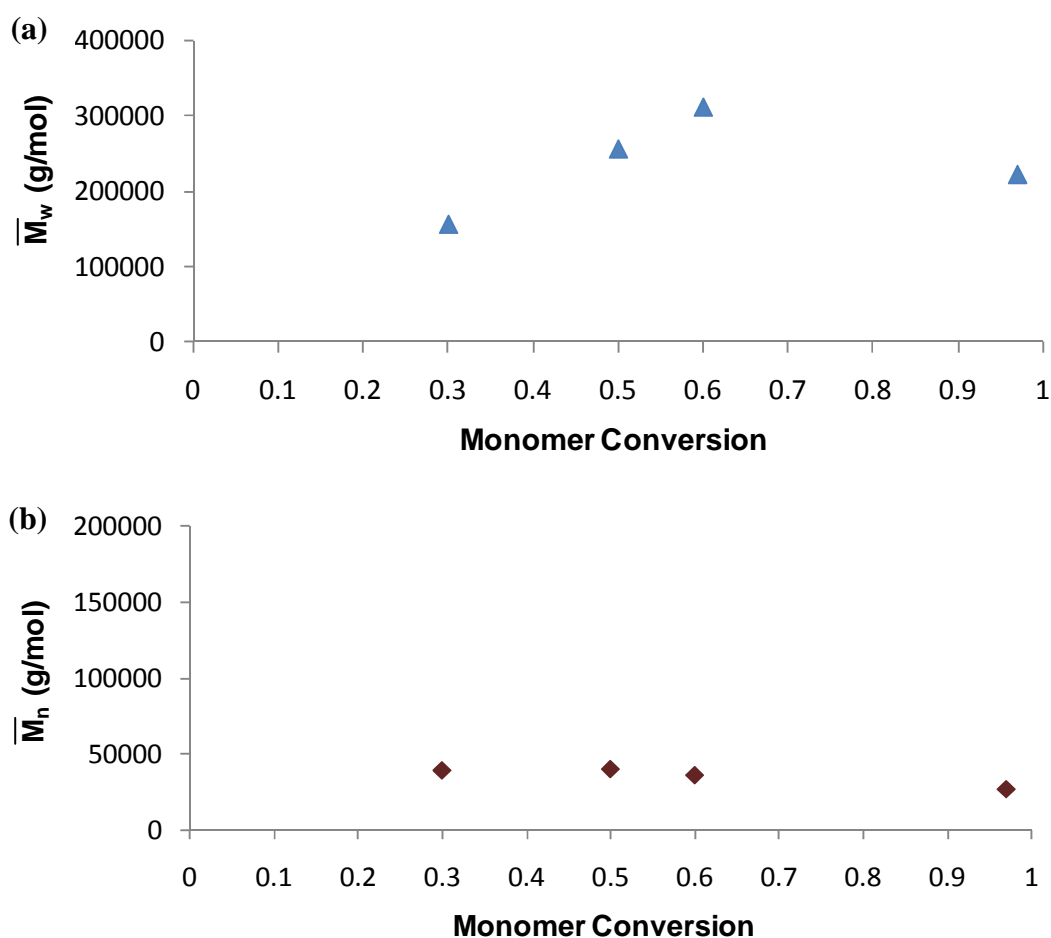


Figure 2. 11 Evolution of the polymer molecular weight with the monomer conversion for Exp. B8. (a) Weight-average molecular weight; (b) number-average molecular weight.

Figure 2.11 shows that while the number-average molecular weight remains essentially constant along the polymerization (Fig. 2.11b), the weight-average molecular weight seems to reach a maximum at monomer conversion close to 60% (Fig. 2.11a). The polymer that is produced in solvent-rich phase exhibits lower molecular weights than the polymer which is produced in polymer-rich phase because: (a) gel effect is negligible in solvent-rich phase, (b) chain transfer reactions to solvent increases. According to the results of partition coefficient experiments, polymer-rich phase is the main loci of polymerization. The consumption of monomer in polymer-rich phase is faster than the decrease in the radical total concentration in that phase. For this reason, the average molecular weights of the polymer produced in polymer-rich phase decrease while the average molecular weights of polymer produced in solvent-rich phase remains essentially constant throughout the polymerization process.

The measurable average molecular weight is the result of combining the polymer produced in both phases. At low conversions, it is controlled by the polymer produced in the solvent-rich phase while at higher conversions the polymer produced in polymer-rich phase is the controller factor. For this reason, the evolution of polymer weight average molecular weight in Fig. 2.11-a shows a maximum at intermediate conversions (~ 0.6).

Figures 2.12a-d also shows the evolution of the molecular weight distributions (MWDs) of Exp. B8. In agreement with our previous explanation, MWD at low conversions exhibits a noticeable shoulder at high molar masses due to the coexistence of short polymer chains produced in solvent-rich phase and long polymer chains produced in polymer-rich phase (Fig. 2.12a). At higher monomer conversions,

however, the mass of polymer produced in the polymer-rich phase is very high, and the molecular weight distributions become broad but unimodal (Figs. 2.12b-d).

According to Table 2.10, polymers with polydispersities higher than 6 are produced. Again, the coexistence of shorter chains produced in the solvent-rich phase with long polymer chains produced in the polymer particles can explain this result. The bimodality distribution of molecular weight is a characteristic of precipitation polymerization and is the consequence of polymerization that takes place both in continuous phase and inside the polymer particles. This behavior is not seen in bulk polymerization since there is just one locus for polymerization.

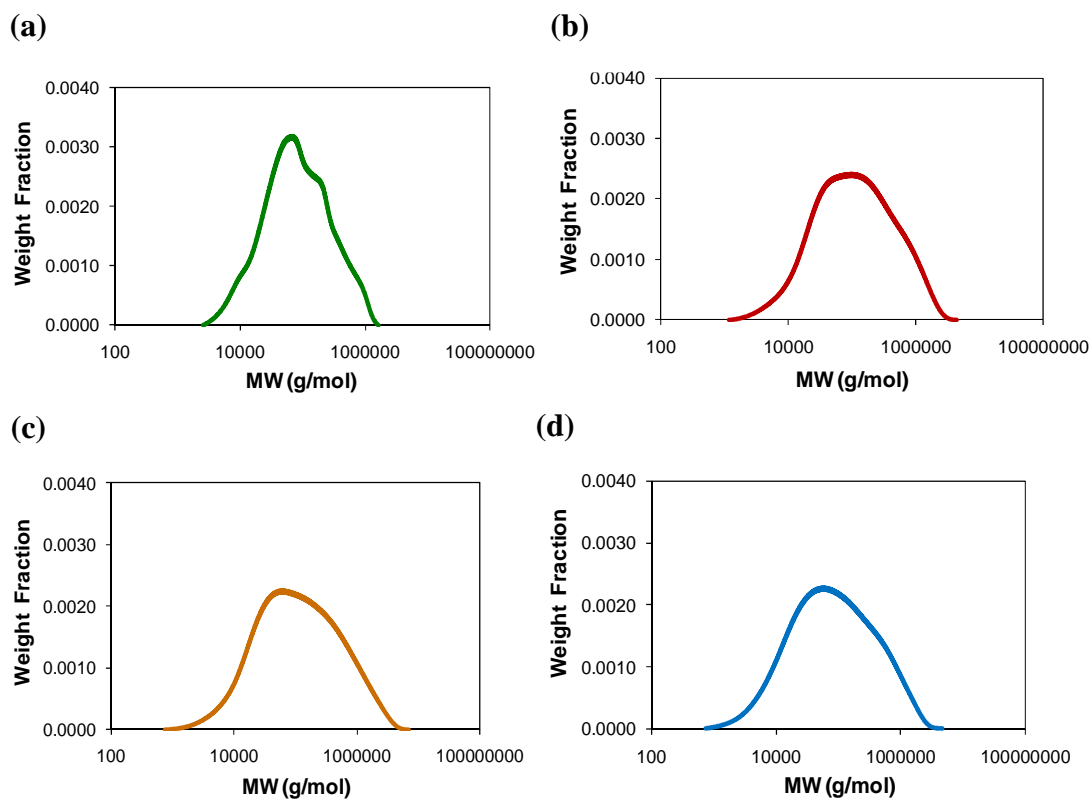


Figure 2. 12 Molecular weight distributions (MWDs) for Exp. B8 at different conversions where x shows conversion. (a) $x = 0.3$; (b) $x = 0.5$; (c) $x = 0.6$; (d) $x = 0.97$.

Figure 2.13 shows the SEM images corresponding to samples taken after 3 hours of polymerization using different ratios of monomer to solvent for the dispersion polymerization experiments listed in Table 2.9. Since the monomer conversions in Exps. B5-B8 are comparable after 3 hours of polymerization, the polymer particle morphologies can be also compared. Recall that except for Exp. B10, the monomer conversions are very high for all these samples. Stable and well-defined spherical particles of 2-4 μm can be observed. Interestingly, Exp. B8 (and Exp. B9 which is the replicate of Exp. B8) exhibits a very narrow particle size distribution. Under the investigated conditions (according to Table 2.9), the initial concentration of PDMS that was chosen from a very narrow range ($\sim 1\text{-}2$ wt. %) does not significantly affect the final particle size (compare Figs. 2.13a and 2.13b).

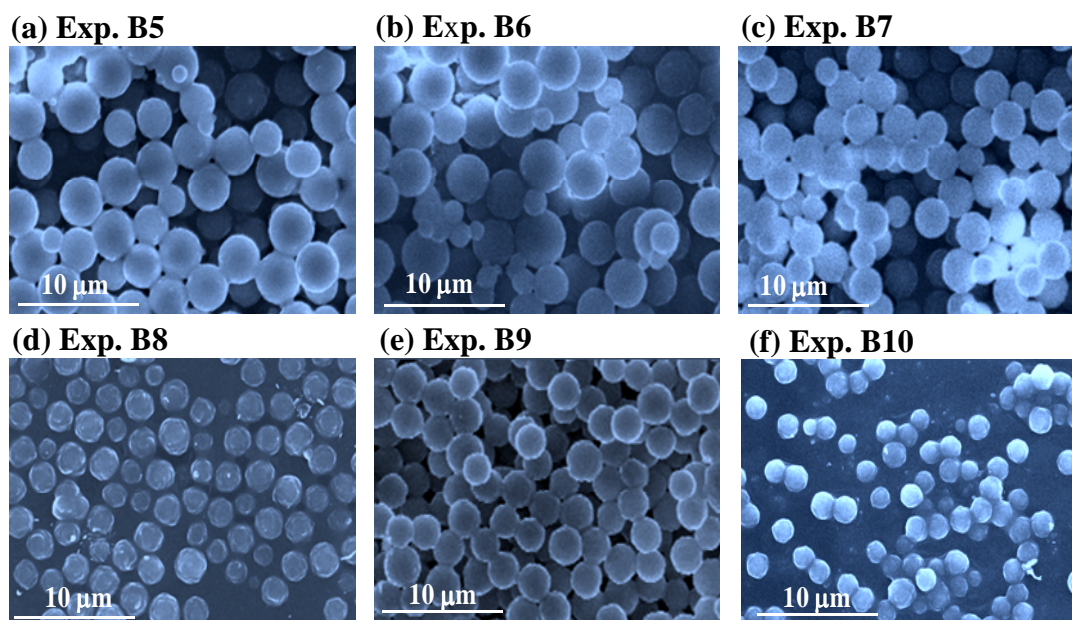


Figure 2. 13 PMMA particles obtained by dispersion polymerization of MMA in *n*-hexane at 30 °C. Samples were taken after 3 h of polymerization.

It is interesting that an increase in the *n*-hexane/monomer ratio (~0.5 to 1.2) produces a considerable reduction of the particle size (compare Figs 2.13a-b with Figs. 2.13c-e). This is due to the fact that primary particles generated in a solvent-enriched medium are smaller than those generated in a monomer-enriched medium, as will be noted in the low conversion experiments. It is important to consider that the initial medium solvency is crucial in determining the final particle size since particle formation is restricted to the early stages of the dispersion polymerization. The ultimate particle size and particle size distribution also depend on the agglomeration that takes place during and after the particle formation stage. Table 2.10 shows that the average particle size decreased with higher hexane (solvent) to monomer concentration ratio. With hexane to monomer ratio of 0.58 the sizes of the particles obtained were in the range of 1.6-4 μm ; while the particle sizes were in the range of 0.8-2.8 μm , 1.2-2.4 μm , and 1.2-2 μm for hexane to monomer ratios of 0.72, 0.83, and 1.12, respectively. Since hexane is not a good solvent for PMMA, higher initial ratio of MMA to hexane leads to increase in the medium solvency for the polymer. Higher solubility of the medium results in higher molecular weight polymeric chains that precipitate out in the nucleation stage, together with more agglomeration of particles associates with higher monomer to hexane ratio, this adds up to an increase in the particle size.

Figure 2.14 shows the number-density histograms for Exps. B5-B10 that were calculated from SEM pictures. Even though just a reduced number of polymer particles was considered to find the number-density, the graphs show the broadness of the particle size distribution qualitatively. It can be seen that Exps. B8-B10 exhibit a relatively narrow particle size distribution (Fig. 2.14).

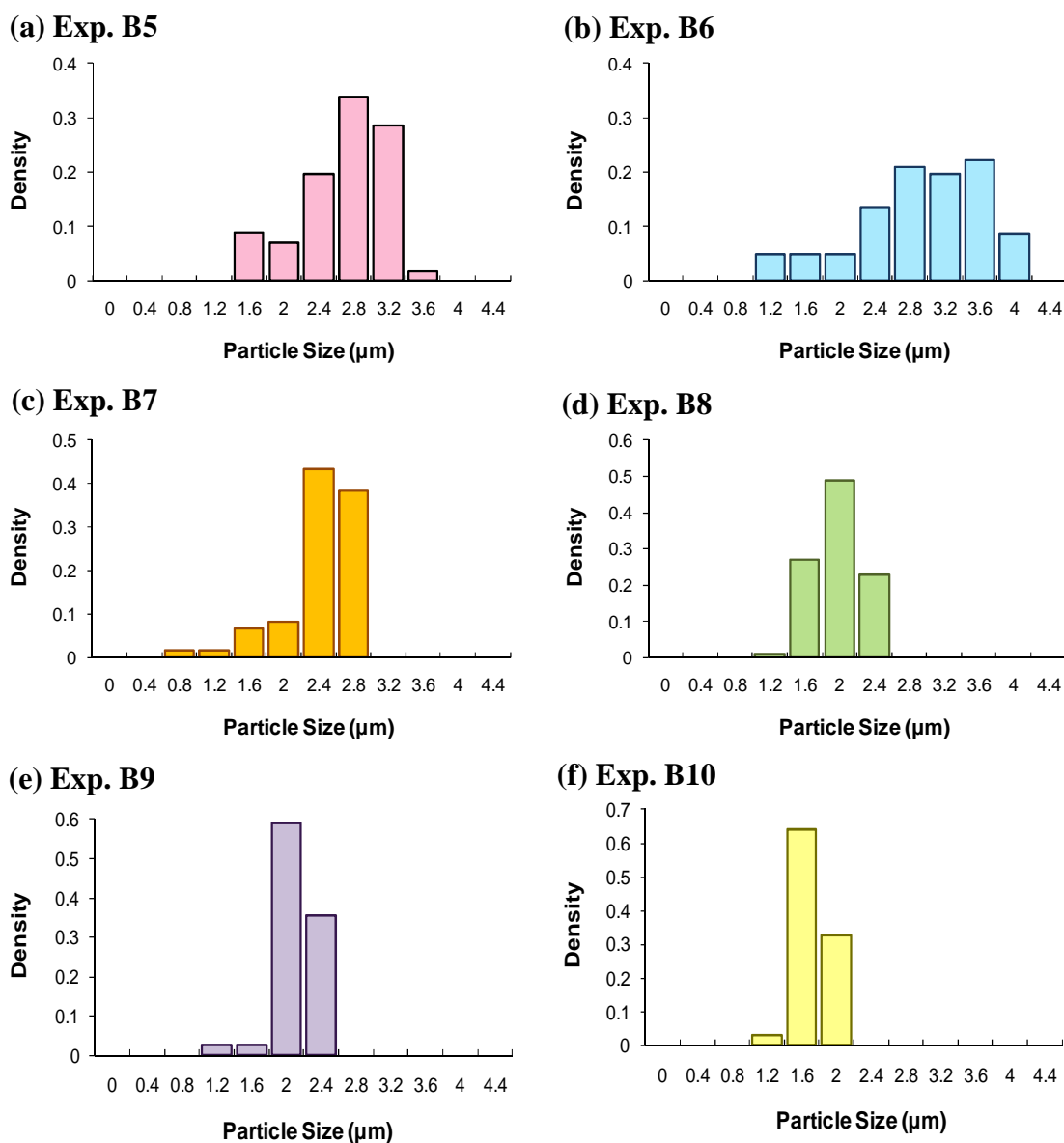


Figure 2. 14 Particle size histograms for samples in Fig. 3.10. Number-density was calculated from SEM pictures.

Figure 2.15 and 2.16 show the development of the PMMA particles as reaction proceeded obtained for Exp. B8 and Exp. B6, respectively. In both of these experiments, stable polymer particles were developed after 2.5 hours of polymerization (*i.e.*, no significant agglomeration of particles is observed).

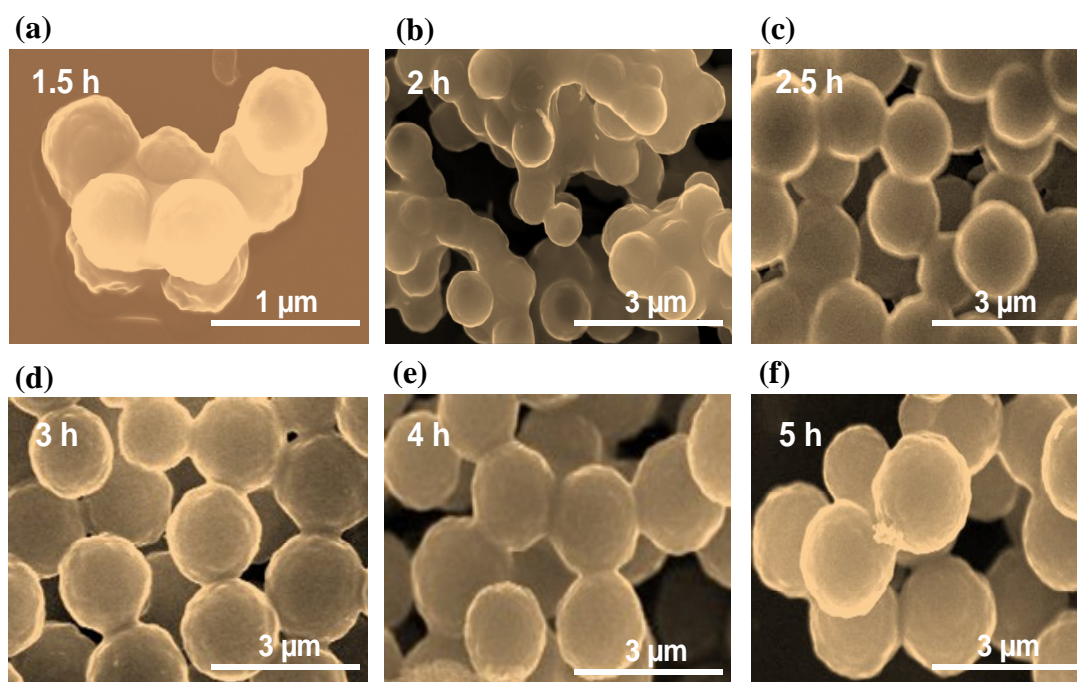


Figure 2. 15 Evolution of the poly(methyl methacrylate) (PMMA) morphology with time for Exp. B8. Reaction times were as follows: (a) $t=1.5$ h; (b) $t=2.0$ h; (c) $t=2.5$ h; (d) $t=3.0$ h; (e) $t=4.0$ h; and (f) $t=5.0$ h.

Figure 2.15 shows that unstable primary polymer particles are nucleated at the beginning of the dispersion polymerization process. These primary particles agglomerate and further polymerization takes place while the stabilization starts. After almost 2 hours of polymerization, the stabilizer is capable of preventing the agglomeration of the polymer particles so highly monodisperse polymer particles are produced (see Fig. 2.15c-e). The polymer particles grow as the polymerization proceeds and polymer particles with the average size of $2.5\ \mu\text{m}$ are produced after 5 hours of polymerization (see Fig. 2.15f).

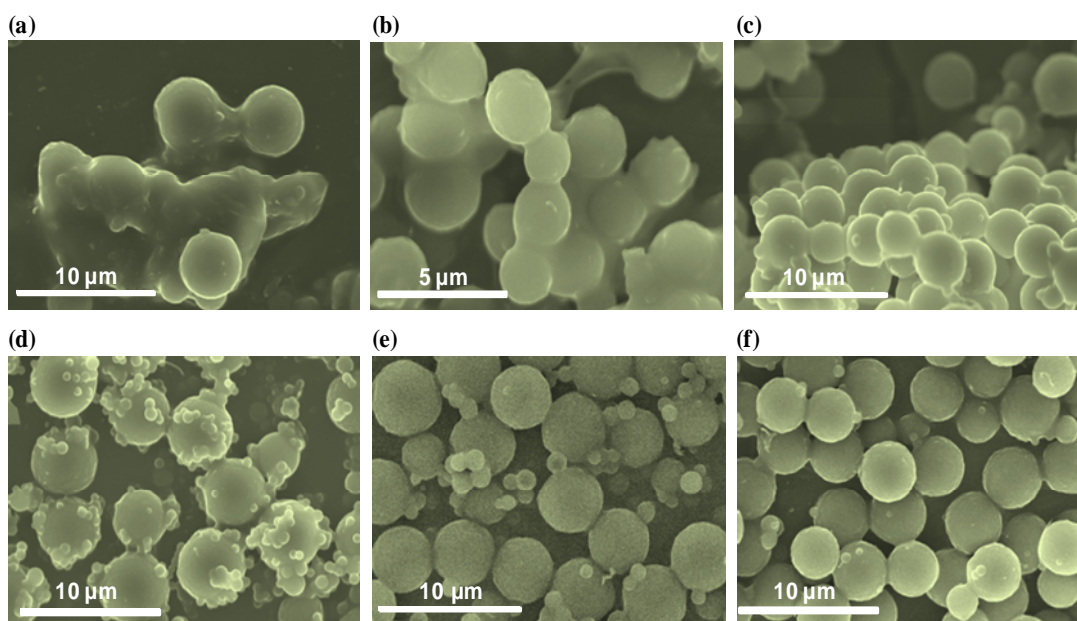


Figure 2. 16 Evolution of particle morphology for Exp. B6. Reaction times were as follows: (a) $t=1.5$ h; (b) $t=2.0$ h; (c) $t=2.5$ h; (d) $t=2.75$ h; (e) $t=3.0$ h; and (f) $t=3.5$ h.

Interestingly, in Exp. B6, stable micron-sized polymer particles of about 3-4 μm coexist with unstable nano-sized polymer particles of about 300-500 nm during the first 3 hours of polymerization (see Figs. 2.16c-e). After 3.5 hours, however, almost all of the smaller particles have disappeared via agglomeration with the larger ones, and a quite uniform particle size distribution is observed (see Fig. 2.16f). The uniformity of particle sizes produced by the investigated dispersion polymerization can also be explained in terms of the partition coefficients of LPO and DMA. Since LPO and DMA exhibit a significant preference for the polymer-rich phase, homogeneous nucleation of primary particles takes place, essentially, at the system phase separation point. Due to the limited initiation in the solvent-rich phase, most of the polymer is produced in the polymer-rich phase. For that reason, particles nucleated at the phase separation point can grow uniformly throughout the

polymerization. In case of Exp. B6 (Fig. 2.16), it seems that the lower amount of solvent in the recipe generates a favorable environment for the polymer chains to remain in the solvent-rich phase before precipitating, and a non-instantaneous nucleation is induced.

As indicated before, Exp. B8 was duplicated (Exp. B9 is its replication) using the best recipe (Exp. A3) of preliminary experiments in order to produce stable and monodisperse PMMA particles. The results of experiments showed that conversion, polymer molecular weights, and particle morphology were reasonably reproduced (see Table 2.10 and Figs. 2.10 and 2.13). This is a remarkable result for a redox-initiated polymerization, since this type of polymerization is usually very sensitive to inhibitors such as oxygen during the preparation of the reaction mixture.

B-4) Study of the stability of the polymer particles and phase inversion phenomenon

Among many morphological phenomena that occur during polymerization processes, the study and prediction of phase inversion phenomenon is very important. Phase inversion is the process by which an initially continuous phase domain becomes the dispersed phase domain and vice versa. The morphology of the system needs to be established before and after the phase inversion process; therefore, study of this phenomenon and its effects on polymer particles stability is valuable. Thus, in order to produce a desirable polymer product, it is necessary to have a better understanding of this phenomenon. For example, during the dispersion polymerization process of MMA in n-hexane, when the polymerization starts, there is

a homogeneous solution of monomer, solvent, initiator and stabilizer, but when the polymerization proceeds and PMMA particles are produced, phase separation occurs and two phases are formed that are solvent-rich phase and polymer-rich phase. Usually the solvent-rich phase is the continuous phase during the polymerization, but if the phase inversion phenomenon takes place the polymer-rich phase can replace the solvent-rich phase as the continuous phase. This can affect the desirable polymer particles morphology, so it is important to study the conditions that may induce the phase inversion process.

Producing stable and uniform polymer particles is crucial for some special applications, so several experiments were carried out according to Table 2.11 in order to investigate the conditions that promote the phase inversion.

Table 2. 11 Reaction conditions for dispersion polymerizations of MMA in *n*-hexane at 30°C

Exp.	Initial Masses					
	MMA (g)	<i>n</i> -hexane (g)	LPO (g)	DMA (g)	PDMS (g)	Solvent/MMA ratio
B11	2.4	2.0	0.254	0.127	0.078	0.83
B12	2.4	2.0	0.254	0.127	0.83
B13	2.4	1.2	0.254	0.127	0.078	0.5
B14	2.4	1.2	0.254	0.127	0.5
B15	2.4	0.5	0.254	0.127	0.078	0.21
B16	2.4	0.5	0.254	0.127	0.21

Figure 2.17 and 2.18 show the evolutions of the particle morphologies for Exp. B11 and B12. The recipe of these experiments is same, but in experiment B12 no stabilizer was used in order to test the effect of stabilizer on stability and morphology of the polymer particles. As it is expected, in Exp. B11 (replication of

Exp. A3), stable polymer particles were developed after 2.5 hours of polymerization (see Fig. 2.17 d-e) and no appreciable agglomeration of particles was observed. The average particle size in this case is about 2 μm .

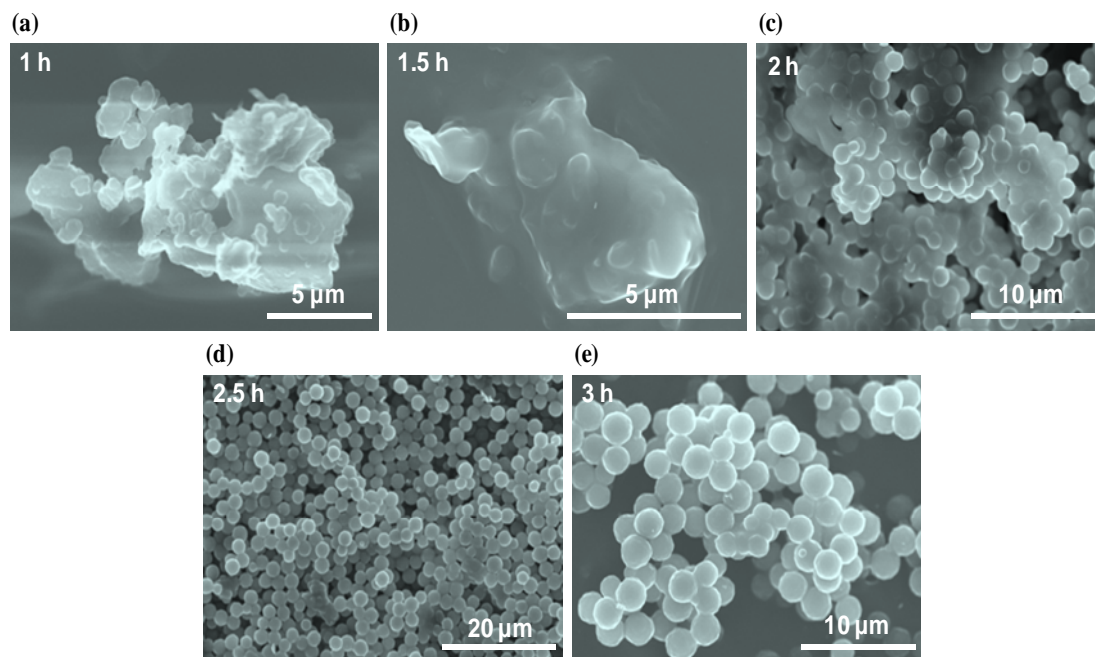


Figure 2. 17 Evolution of the poly(methyl methacrylate) (PMMA) morphology with time for Exp. B11. Reaction times are as follows: (a) $t=1$ h; (b) $t=1.5$ h; (c) $t=2$ h; (d) $t=2.5$ h; and (e) $t=3$ h. The solvent/monomer ratio is 0.83 and PDMS (stabilizer) concentration is 0.078 g.

Figures 2.17 and 2.18 show that the rate of polymerization for Exp. B12 is higher than Exp. B11 and in this case instead of 2.5 hours, just after 1 hour of polymerization, stable polymer particles are produced even though no stabilizer was used. The average polymer particle size in Exp. B12 is 4.5 μm . These polymer particles are larger than the polymer particles which were produced in Exp. B11, and it seems that the size polydispersion of these particles is also higher. After 1.5 hours of polymerization, the polymer particles start to agglomerate (see Fig. 2.18-c) and at

the end of polymerization a mass of agglomerated particles is produced (see Fig. 2.18-d and e).

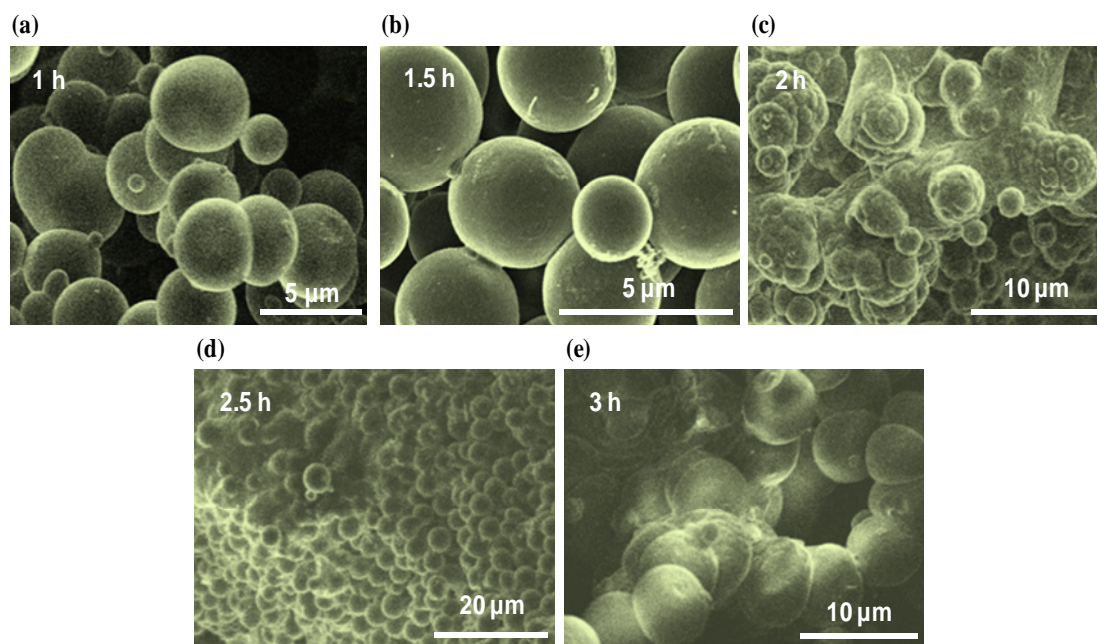


Figure 2. 18 Evolution of the PMMA morphology with time for Exp. B12. Reaction times are as follows: (a) $t=1$ h; (b) $t=1.5$ h; (c) $t=2$ h; (d) $t=2.5$ h; and (e) $t=3$ h. The solvent/monomer ratio is 0.83 and PDMS (stabilizer) concentration is zero.

It should be noted that even without using stabilizer, the polymer particles hold their spherical shape even after severe agglomeration.

Moreover, the significance of experiment B12 is very important: to produce stable polymer particles larger than $2\text{ }\mu\text{m}$, the recipe of Exp. B11 can be used without any stabilizer, but the polymerization should be stopped before 1.5 hours. Longer polymerization times will cause the particle agglomeration. Furthermore, it seems that in these cases using the solvent/monomer ratio of 0.83 there is no evidence of phase inversion, even after 3 hours of polymerization.

According to Table 2.11, the solvent/monomer ratio was decreased in Exps. B13 and B14 (in comparison to Exps. B11 and B12) to study the effect of this parameter on polymer morphology. The only difference of Exp. B13 and B14 is the absence of any stabilizer in Exp. B14. Figures 2.19 and 2.20 show the corresponding evolutions of the particle morphologies during 3 hours of polymerization.

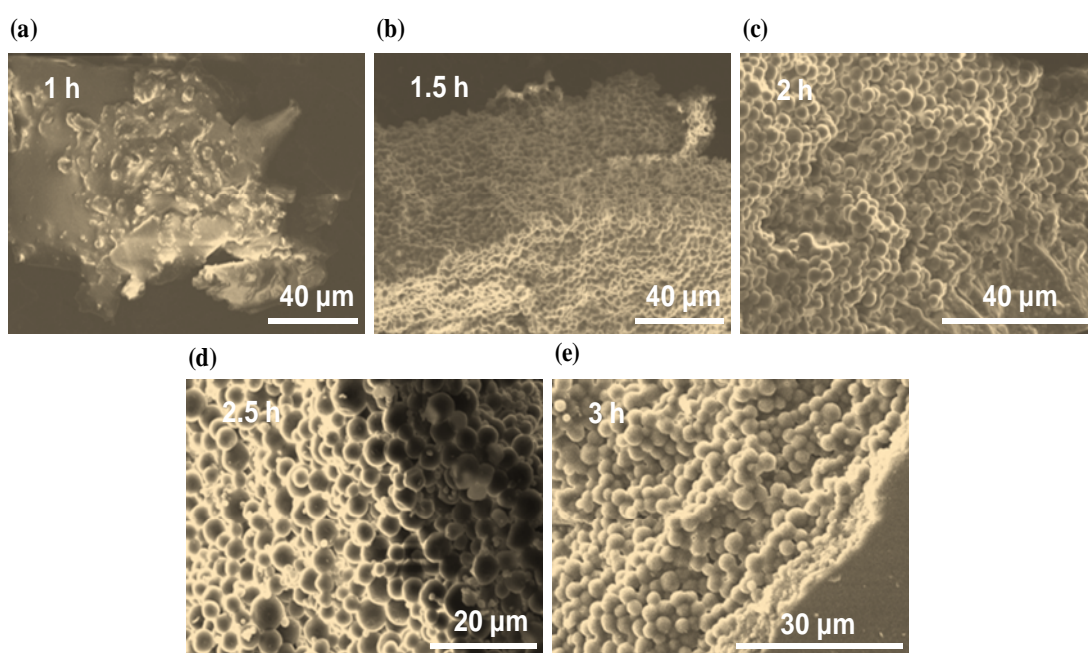


Figure 2. 19 Evolution of the poly(methyl methacrylate) (PMMA) morphology with time for Exp. B13. Reaction times are as follows: (a) $t=1$ h; (b) $t=1.5$ h; (c) $t=2$ h; (d) $t=2.5$ h; and (e) $t=3$ h. The solvent/monomer ratio is 0.5 and PDMS (stabilizer) concentration is 0.078 g.

Figure 2.19 shows that when the solvent/monomer ratio decreases from 0.83 to 0.5 (see Figs. 2.17 and 2.19 and compare Exps. B11 and B13) a mass of agglomerated spherical particles with average size of $4.5\text{ }\mu\text{m}$ is produced (Exp. B13) instead of stable and monodisperse spherical polymer particles with average size of $2\text{ }\mu\text{m}$ which were produced in Exp. B11. It is interesting that in this case it is not

possible to produce separate polymer particles during the polymerization process, but the agglomerated polymer particles are still spherical and their shape does not change. Also, it seems that no phase inversion has taken place even after 3 hours of polymerization.

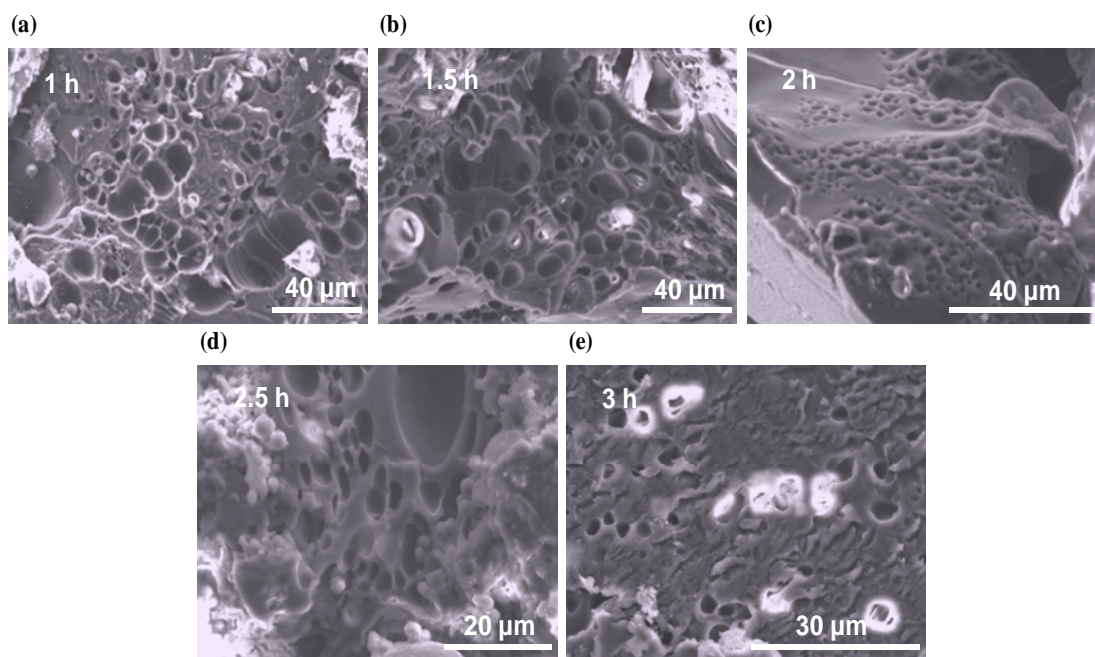


Figure 2. 20 Evolution of the poly(methyl methacrylate) (PMMA) morphology with time for Exp. B14. Reaction times are as follows: (a) $t=1$ h; (b) $t=1.5$ h; (c) $t=2$ h; (d) $t=2.5$ h; and (e) $t=3$ h. The solvent/monomer ratio is 0.5 and PDMS (stabilizer) concentration is zero.

Fig. 2.20 shows that if the solvent/monomer ratio decreases from 0.83 (Exp. B11) to 0.5 without using any stabilizer (Exp. B14) phase inversion takes place very fast since it can be observed that after 1 hour of polymerization there is enough evidence of phase inversion phenomenon (see Fig. 2.20-a). In this case, after starting the polymerization since there is no stabilizer, the primary particles are agglomerated very fast. Then, most of the polymerization takes place inside polymer-rich phase and

the viscosity of the polymerization medium increases gradually. In a short time interval, the solvent that is not a good solvent for the polymer is trapped in the polymer-rich phase generating spherical droplets. The polymerization proceeds outside these droplets and a mass of porous polymer is produced. After the solvent is removed via evaporation, spherical hollows are left behind (see Fig. 2.20).

Figures 2.21 and 2.22 show the evolutions of the particle morphologies for Exps. B15 and B16 during the first 3 hours of polymerization. Exp. B16 has the same recipe as Exp. B15, but no stabilizer was added. In these two experiments, the solvent/monomer ratio is 0.21 which is almost 25% of the solvent/monomer ratio in Exp. B11 that produced highly stable and monodisperse polymer particles. As expected, since the solvent/monomer ratio in Exps. B15 and B16 is very low, after starting the polymerization the polymer particles agglomerate very fast and just after 1 hour of polymerization the system phase inversion can be observed (see Figs. 2.21 and 2.22). It is clear that when the ratio of solvent/monomer decreases to 0.21 it is impossible to produce stable particles with or without using stabilizer and the only product of the experiment will be a membrane-like hollow polymer structure. This structure is developed shortly after starting the polymerization, when the solvent is trapped in the polymer-rich phase and phase inversion takes place. It is interesting that even when the phase inversion takes place and solvent droplets are trapped inside the polymer-rich phase during the polymerization, since the concentration of solvent is very high at the interface of the solvent droplet in comparison to that in the polymer-rich phase, the polymer particles that are formed at this interface do not agglomerate easily and so they still can be observed in the SEM images (see Fig. 2.21-d).

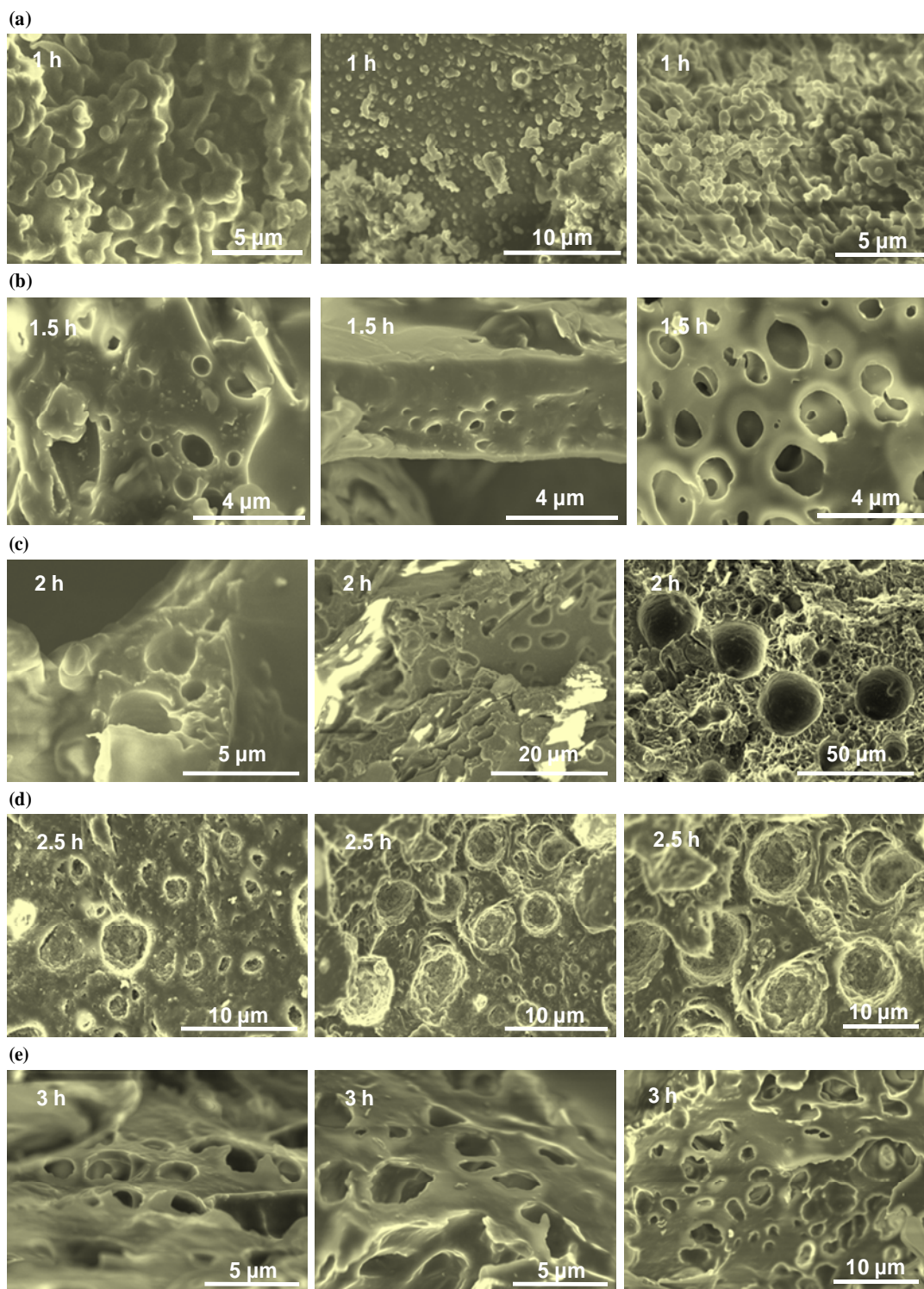


Figure 2. 21 Evolution of the poly(methyl methacrylate) (PMMA) morphology with time for Exp. B15. Reaction times are as follows: (a) $t=1$ h; (b) $t=1.5$ h; (c) $t=2$ h; (d) $t=2.5$ h; and (e) $t=3$ h. The solvent/monomer ratio is 0.21 and PDMS (stabilizer) concentration is 0.078 g.

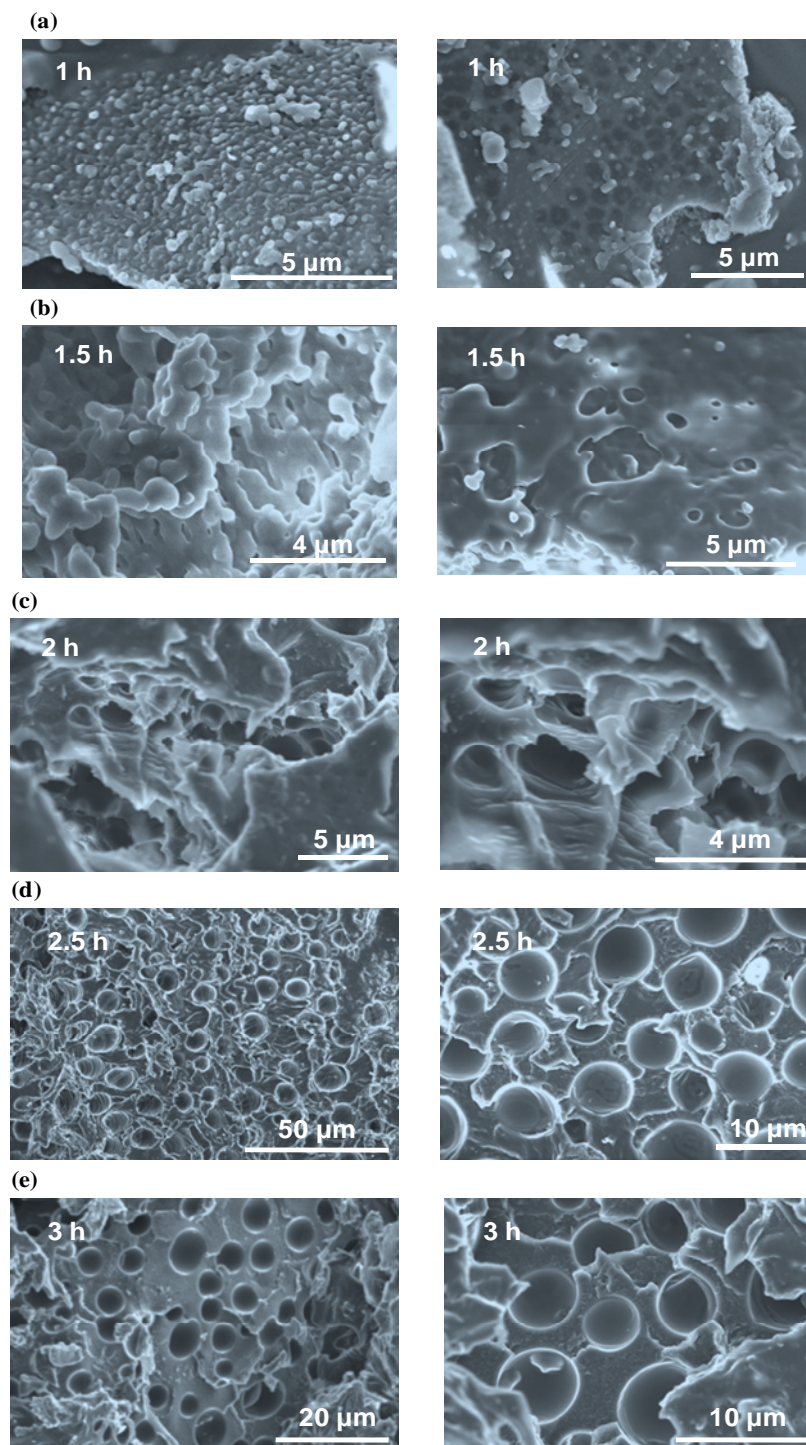


Figure2. 22 Evolution of the poly(methyl methacrylate) (PMMA) morphology with time for Exp. B16. Reaction times are as follows: (a) $t=1$ h; (b) $t=1.5$ h; (c) $t=2$ h; (d) $t=2.5$ h; and (e) $t=3$ h. The solvent/monomer ratio is 0.21 and PDMS (stabilizer) concentration is zero.

Again it should be noticed that if the purpose of the dispersion polymerization according to its application is to produce stable and uniform polymer particle without any agglomeration, setting the ratio of solvent to monomer to 0.21 is not a good choice.

In chapter 3, the knowledge of the macroscopic dispersion polymerization experiments that were studied in this chapter will be used to carry out a new set of experiments to study the dispersion polymerization in suspended monomer micro-droplets (as a confined space for polymerization reaction) in an aqueous medium.

Chapter 3: Micro dispersive suspension polymerization of methyl methacrylate at low temperature

In chapter 2, macroscopic dispersion polymerization of MMA in n-hexane at low temperature was studied carefully. In this chapter, the micro dispersive suspension polymerization (MDSP) of methyl methacrylate at low temperature in n-hexane using LPO/DMA redox system has been studied. The knowledge of macroscopic dispersion polymerization of MMA is used to design the experiments in order to investigate the feasibility of producing PMMA particles using this new technique and the morphology of the polymer particles that can be produced is studied.

First, the materials and methods that were used in MDSP experiments are presented in the following sections of this chapter, and then the results are discussed.

3.1 Materials and Methods

- Micro dispersive suspension polymerization

Jung et al. (2008) produced micron size hollow polymer particles with special morphology through a micro dispersive suspension polymerization (MDSP) at 70°C. In this type of polymerization, each monomer droplet (oil-phase) which is suspended in the medium (aqueous phase), serves as a micro reactor for regular dispersion polymerization.

In this work, several micro dispersive suspension polymerization experiments were designed and carried out at 30°C in an agitated system using 100 and 500 ml jacketed batch reactors. These experiments were designed in order to assess the

feasibility of reproducing same polymer structures as Jung et al. (2008) produced at 70°C but in this case, using a redox system of initiators (LPO/DMA) at low temperature.

Poly(vinyl alcohol) (PVA) (87-89% hydrolyzed) was purchased from Sigma-Aldrich Company and used as water-soluble stabilizer. Its molecular weight was in the range of 85000-124000 g/mol. Deionized water was used as the suspension medium and the monomer (MMA), redox pair (LPO/DMA), non-solvent (n-hexane) and oil-soluble stabilizer (PDMS) were used as the oil-phase (their properties and providers have been mentioned before in chapter 2 section 2.2). In these set of experiments the high molecular weight of PDMS (20000-30000 g/mol) was used.

The experimental apparatus for the MDSP of MMA with agitation is shown schematically in Figure 3.1. It consists of a 100 or 500 ml glass-jacketed batch reactor, a heating bath, a thermometer, a 6-bladed-impeller, stir-pak impeller speed controller (Cole-Palmer stir-pak mixer model 4554-10), a nitrogen inlet, and a condenser. The content of the reactor was heated by circulating water in the jacket of the reactor.

The procedure that was used in this set of experiments is as follows. First, an aqueous solution was prepared by mixing the required amounts of deionized water and polyvinyl alcohol (PVA) at room temperature for about 18 hours, until complete dissolution of PVA. This solution was purged with nitrogen for several minutes. Then, a monomer-rich solution and a solvent-rich solution were prepared using the same procedure used before for preparing the regular dispersion polymerization of MMA (see section 2.2). Each of these two solutions was purged by nitrogen

separately. Then, the solutions were mixed together to make the oil-solution and purged with nitrogen again.

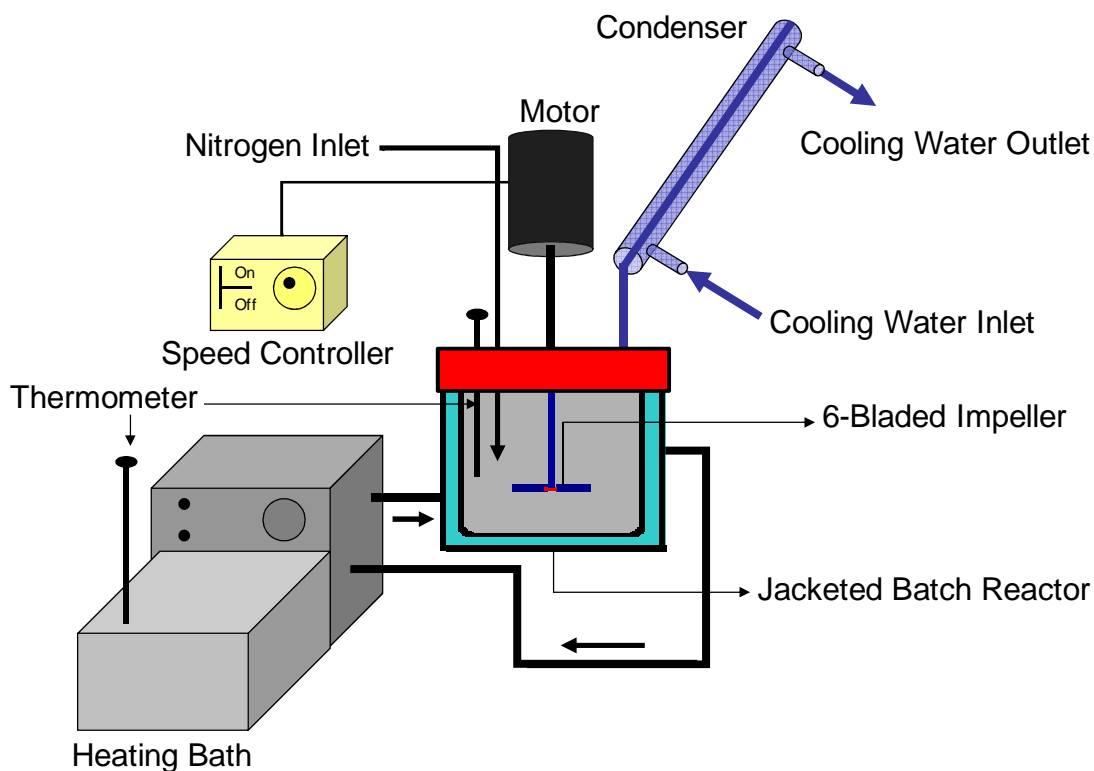


Figure 3. 1 Schematic diagram of the apparatus used for MDSP experiments.

After turning on the heating bath and adjusting it at 30°C, first the aqueous solution and then the oil-solution was poured in the reactor while a light flow of nitrogen was blowing to remove oxygen. Finally, the corresponding amount of DMA was added to the mixture in the reactor and then the door of the reactor was sealed. Then, the agitation was set at 500 rpm. At the end of the polymerization process (at a predetermined time), hydroquinone was added to the mixture in order to stop the polymerization and the polymer removed from the reactor. Polymer samples were analyzed to find the conversion and morphology.

- **Determination of PMMA/MMA/n-hexane cloud points**

There are different methods to construct ternary phase diagrams such as titration method. In this technique, transparent polymer/solvent solutions of known compositions are prepared, and the non-solvent is slowly added into the solutions until they turn turbid as polymer starts to precipitate. The onset turbidity (cloud point) of the samples is most widely detected by visual examination. Titration method is not working very well when the concentration of polymer is relatively high because the high viscosity of the polymer/solvent solution prohibits the uniform mixing of the added non-solvent and generates the appearance of local turbidity. Therefore, in this work, cloud points for the PMMA/MMA/n-hexane system were determined by conducting *in situ* dispersion polymerization experiments of MMA in the presence of n-hexane at 30°C using LPO/DMA as redox pair of initiators to overcome the drawbacks of the titration method (Jung et al. 2010). Such limitations are avoided based on the fact that polymer chains are produced homogeneously in monomer/non-solvent solution and they precipitate thereafter. In what follows, a description of the proposed technique is provided. First, a LPO/MMA solution was prepared at room temperature and loaded into five 20-ml glass vials. The initial concentration of LPO was 0.32 (mol/l-MMA) in each vial. Different amounts of n-hexane were added into the mixtures in different vials in order to provide different weight ratios of MMA to (MMA + n-hexane) (0.3, 0.5, 0.7, 0.75, and 0.8) in different vials. The solution in each vial was purged with nitrogen gas for 1 minute and then the vials were sealed and DMA was added to each vial using a syringe. The concentration of DMA was 0.52 (mol/l-MMA). Finally the vials were immersed in a clear water bath at 30°C to start the polymerization. The vials were taken from the bath as soon as their contents

turned visually turbid. Then, a mixture of hydroquinone (inhibitor) and methanol was added to stop the reaction. The amount of PMMA at the cloud point was determined using the same gravimetric method that was explained before in chapter 2. This method consists of precipitating the polymer with methanol, filtering, and drying under vacuum until constant weight. Since the vials were sealed, it was assumed that the mass of n-hexane remained constant during the polymerization experiments. These experiments were carried out twice in order to be sure that the cloud points were measured precisely. The results of all of the experiments are discussed in the following section.

3.2 Results and Discussion

As it was mentioned before in chapter 2, the recipe of Exp. A3 and its replications (Exps. B8, B9, and B11) produced the best results in the set of investigated macroscopic dispersion polymerization experiments. It is also interesting to study if it is possible to carry out the same procedure of dispersion polymerization at room temperature but in suspended monomer micro-droplets instead of using conventional batch reactors. In order to do that, an experimental set up was designed. 100-ml and 500-ml batch reactors were operated at 30°C and the reaction mixture was mechanically agitated (~500 rpm) under nitrogen atmosphere to carry out Exps. C1-C4. Table 3.1 shows the recipes of Exps. C1-C4. The initial mixture (oil-phase) containing monomer, solvent, redox initiator, and dispersion stabilizer was suspended in an aqueous medium of deionized water in the form of micro-droplets. These droplets were produced by simple mechanical agitation, and were stabilized by addition of poly(vinyl alcohol) (PVA). The volume ratio of the oil phase to aqueous

phase was 0.48 for Exps. C1-C4. The conversions were 17%, 12%, 13%, and 23% after 7 hours of polymerization for experiments C1 to C4 respectively. SEM images of these experiments (not presented here), showed that just the recipe of Exp. C4 can be used to produce stable polymer particles, but the conversion in all of these experiments is very low.

Table 3. 1 Reaction conditions for micro dispersive suspension polymerization of MMA at 30°C

Exp.	Aqueous Phase (weight fraction)		Oil Phase (weight fraction)				
	Deionized water	PVA	MMA	LPO	DMA	PDMS	n-hexane
C1	0.985	0.015	0.724	0.082	0.041	0.025	0.128
C2	0.985	0.015	0.667	0.076	0.038	0.023	0.196
C3	0.985	0.015	0.642	0.072	0.036	0.022	0.228
C4	0.985	0.015	0.557	0.063	0.032	0.019	0.329

Figure 3.2 shows the morphology of the polymer particles produced in experiment C4. As it can be seen in Fig. 3.2 polymer microspheres of about 10-30 μm with unique internal structures were produced. Each polymer particle acted as a micro-reactor, where smaller nano-sized polymer particles precipitate as in regular dispersion polymerization. In other words, the reactor has been replaced by suspended monomer micro-droplets.

Experiment C4 was repeated four times in order to check the reproducibility of the polymer particles, but unfortunately the results showed that the polymer particles morphology is difficult to reproduce and just a few polymer particles are observed even after 7 hours of polymerization. Moreover, the conversion was still low and in some replications of experiment C4, the same morphology was observed in SEM images even though it seemed that these particles are easily broken since they were not stabilized well. Thus, a new set of experiments were designed to overcome

Table 3. 2 Reaction conditions for micro dispersive suspension polymerization of MMA at 30°C

Exp.	Aqueous Phase (weight fraction)		Oil Phase (weight fraction)				
	Deionized water	PVA	MMA	LPO	DMA	PDMS	n-hexane
C5	0.971	0.029	0.618	0.070	0.035	0.021	0.256
C6	0.971	0.029	0.578	0.130	0.033	0.020	0.239
C7	0.971	0.029	0.597	0.067	0.067	0.021	0.248

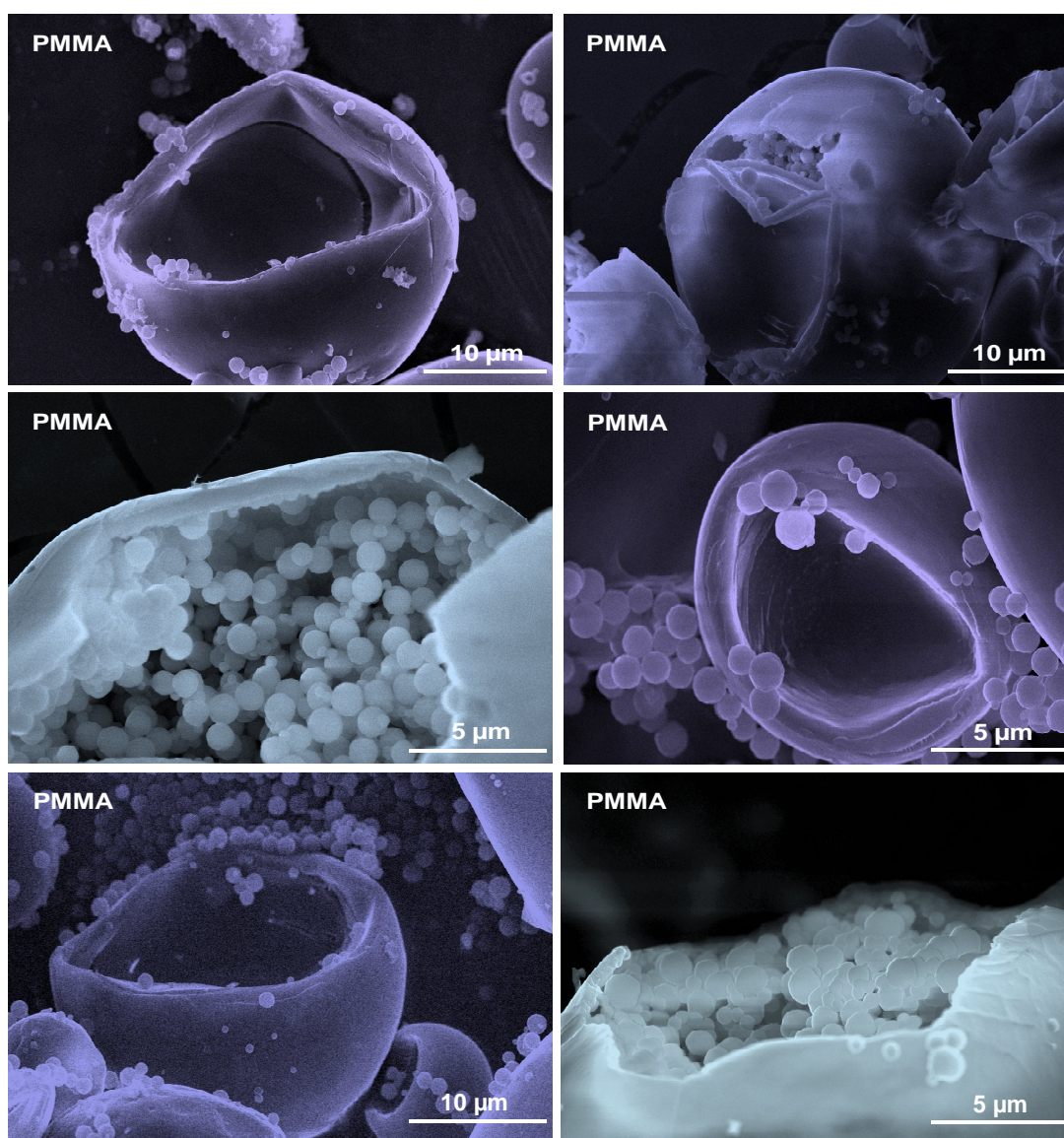


Figure 3. 2 Morphology of the poly(methyl methacrylate) (PMMA) particles obtained by micro dispersive suspension of MMA in water at 30°C for Exp. C4. Time of the reaction is 7 hours and conversion is 0.23.

these issues. According to Table 3.2, the PVA concentration was increased to provide a better stabilization, and the concentrations of LPO and DMA also increased to enhance the reaction rate. The volume ratio of the oil phase to aqueous phase was 0.48 for Exps. C5-C7.

The conversions were 19%, 46%, and 91% after 5 hours of polymerization for experiments C5 to C7 respectively. SEM images of these experiments showed that just the recipe of Exp. C7 can be used to produce stable polymer particles, and also it should be noted that the conversion in this experiment is very high. Figure 3.3 shows the morphology of the polymer particles produced in experiment C7. Again polymer particles (similar to Exp. C4) with special internal morphology can be observed. The size of these microspheres is about 30-60 μm and they contain smaller polymer particles.

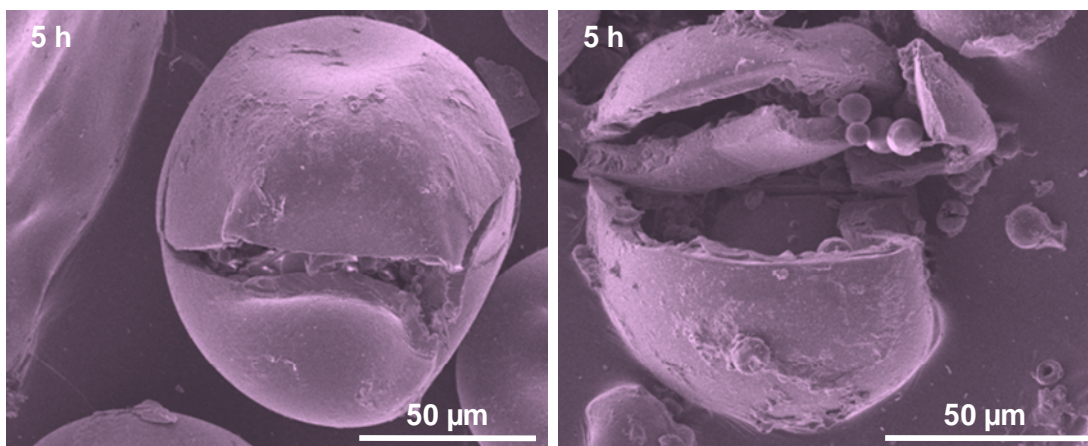


Figure 3. 3 Morphology of the poly(methyl methacrylate) (PMMA) particles obtained by micro dispersive suspension of MMA in water at 30°C for Exp. C7. Time of the reaction is 5 hours and conversion is 0.91.

According to the ternary phase diagram of the system (see Fig. 3.4) (All the thermodynamic discussion and calculation part of this work was adopted from Dr. Luciani theoretical work (Emdadi et al. 2011)), the weight ratio of the MMA to (MMA + n-hexane) is 0.7 in Exp. C7. The experimental data (black dots) (from cloud point measurements) and theoretical data (solid curve) (from Dr. Luciani simulation calculations) that have been shown in Figure 3.4, are in good agreement which is a good proof of the reliability of simulation results (the difference is because of the experimental errors). Experiment C7 was repeated (Exp. C8 is its replication) to study the morphology evolution of the polymer particles during the polymerization,

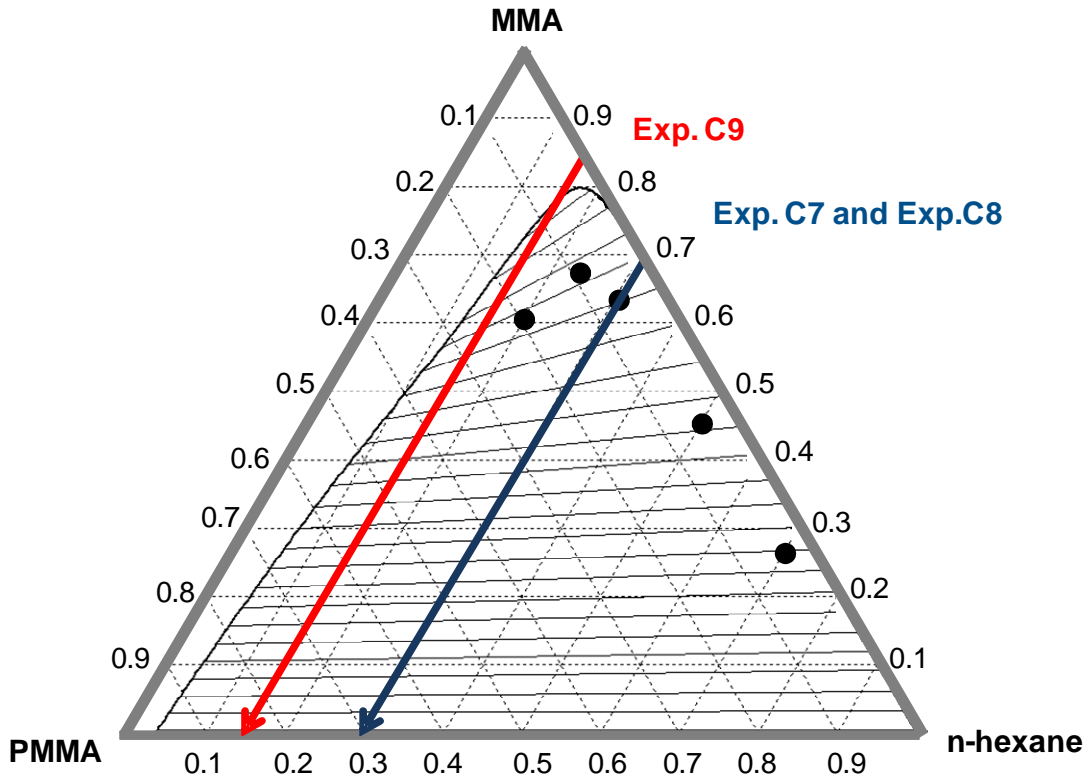


Figure 3. 4 Ternary phase diagram for dispersion polymerization of MMA in n-hexane calculated at 30°C. The solid curve shows the simulation results (adopted from Dr. Luciani simulation (Emdadi et al. 2011)) and the black dots show the experimental results (from cloud point measurements). Binodal curve, tie lines, and reaction path for Exp. C7, Exp. C8, and Exp. C9 have been shown.

and also another recipe was examined based on the ternary phase diagram in order to check the possibility of producing different morphology by changing the ratio of MMA to hexane in the recipe. The weight ratio of the MMA to (MMA + n-hexane) increased to 0.85 in Exp. C9 (see Table 3. 3). Figures 3.5 and 3.6 show the evolutions of the particle morphologies for Exps. C8 and C9 during 5 hours of polymerization respectively.

Table 3. 3 Reaction conditions for micro dispersive suspension polymerization of MMA at 30°C

Exp.	Aqueous Phase (weight fraction)		Oil Phase (weight fraction)				
	Deionized water	PVA	MMA	LPO	DMA	PDMS	n-hexane
C8	0.971	0.029	0.597	0.067	0.067	0.021	0.248
C9	0.971	0.029	0.694	0.078	0.078	0.024	0.125

According to Fig. 3.5, after 1 hour of polymerization single hollow polymer particles with the diameter of 20-100 μm are produced (see Fig. 3.5-a). When the polymerization proceeds, the smaller micron-sized polymer particles that are formed inside each polymer particle precipitate and finally polymer particles with a special internal morphology are produced (see Fig. 3.5-b to 3.5-e). SEM images show that the smaller particles inside each particle are stable and do not coagulate.

This result, shows that by using the recipe of Exp. C7 (or Exp. C8 as its replication) when the weight ratio of monomer to (monomer + solvent) is 0.7, the dispersion polymerization process that takes place inside each suspended monomer droplet is similar to the dispersion polymerization process that took place before in conventional dispersion polymerization of MMA at 30°C (recall Exp. A3) and produced stable polymer particles.

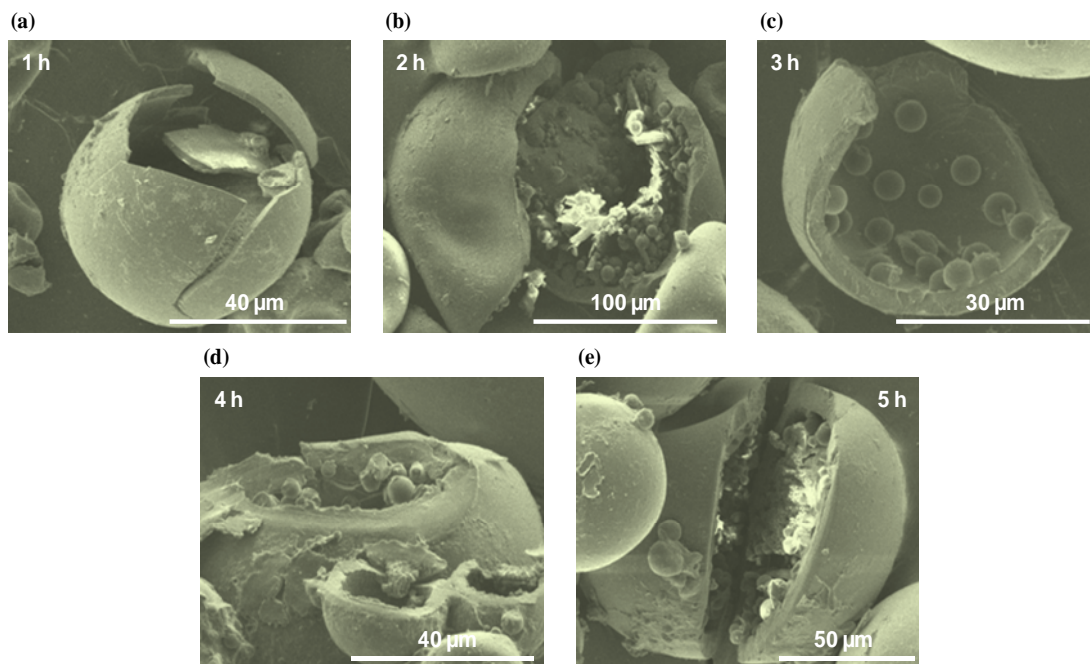


Figure 3. 5 Evolution of the PMMA morphology with time for Exp. C8. Reaction times are as follows: (a) $t=1$ h, $x=0.228$; (b) $t=2$ h, $x=0.385$; (c) $t=3$ h, $x=0.625$; (d) $t=4$ h, $x=0.826$; and (e) $t=5$ h, $x=0.908$ where t is time of the polymerization reaction and x is the conversion.

According to the ternary phase diagram of the MMA/PMMA/n-hexane system (Fig. 3.4) and our previous discussion about ternary phase diagram (chapter 2 section 2.1), it is expected that when the weight ratio of monomer to (monomer + solvent) increases, during the dispersion polymerization process, the system phase inversion may take place. The solvent trapped in the polymer-rich phase, may then produce a porous structure.

Fig. 3.6 shows that when the weight ratio of MMA to (MMA + n-hexane) is increased to 0.85 an interesting internal structure evolution is observed. When the polymerization starts, a core-shell structure is formed (see Fig. 3.6-a). Then dispersion polymerization inside each particle proceeds, and smaller polymer particles precipitate. Since the amount of MMA is very high in comparison to the n-

hexane, these polymer particles agglomerate (see Figs. 3.6-b and 3.6-c). Finally, the system phase inversion occurs and a porous structure of polymer is developed inside each polymer particle (see Figs. 3.6-d and 3.6-e).

Again it can be seen that the knowledge of conventional dispersion polymerization of MMA at 30°C and the ternary phase diagram of the polymerization system was very useful in designing a micro-dispersive suspension polymerization process in order to control the polymerization conditions to produce polymer particles with different internal morphologies that are suitable for special applications.

A new set of experiments were designed to check the morphology of the polymer particles that may be produced when the weight ratio of the MMA to (MMA + n-hexane) is changed in the range of 0.3 to 0.7. Table 3.4 shows the recipes of the experiments C10-C15.

Table 3. 4 Reaction conditions for micro dispersive suspension polymerization of MMA at 30°C

Exp.	Aqueous Phase (weight fraction)		Oil Phase (weight fraction)				
	Deionized water	PVA	MMA	LPO	DMA	PDMS	n-hexane
C10	0.971	0.029	0.275	0.031	0.031	0.010	0.653
C11	0.971	0.029	0.358	0.040	0.040	0.013	0.549
C12	0.971	0.029	0.439	0.049	0.049	0.015	0.448
C13	0.971	0.029	0.518	0.058	0.058	0.018	0.348
C14	0.971	0.029	0.553	0.062	0.062	0.019	0.304
C15	0.971	0.029	0.567	0.064	0.064	0.020	0.285

The conversions were 11%, 13%, 21%, 32%, 84%, and 93% after 5 hours of polymerization for experiments C10 to C15 respectively. The SEM images of experiments C10 and C11 (that are not presented here) showed that it is impossible to produce stable polymer particles using the recipes of these two experiments when

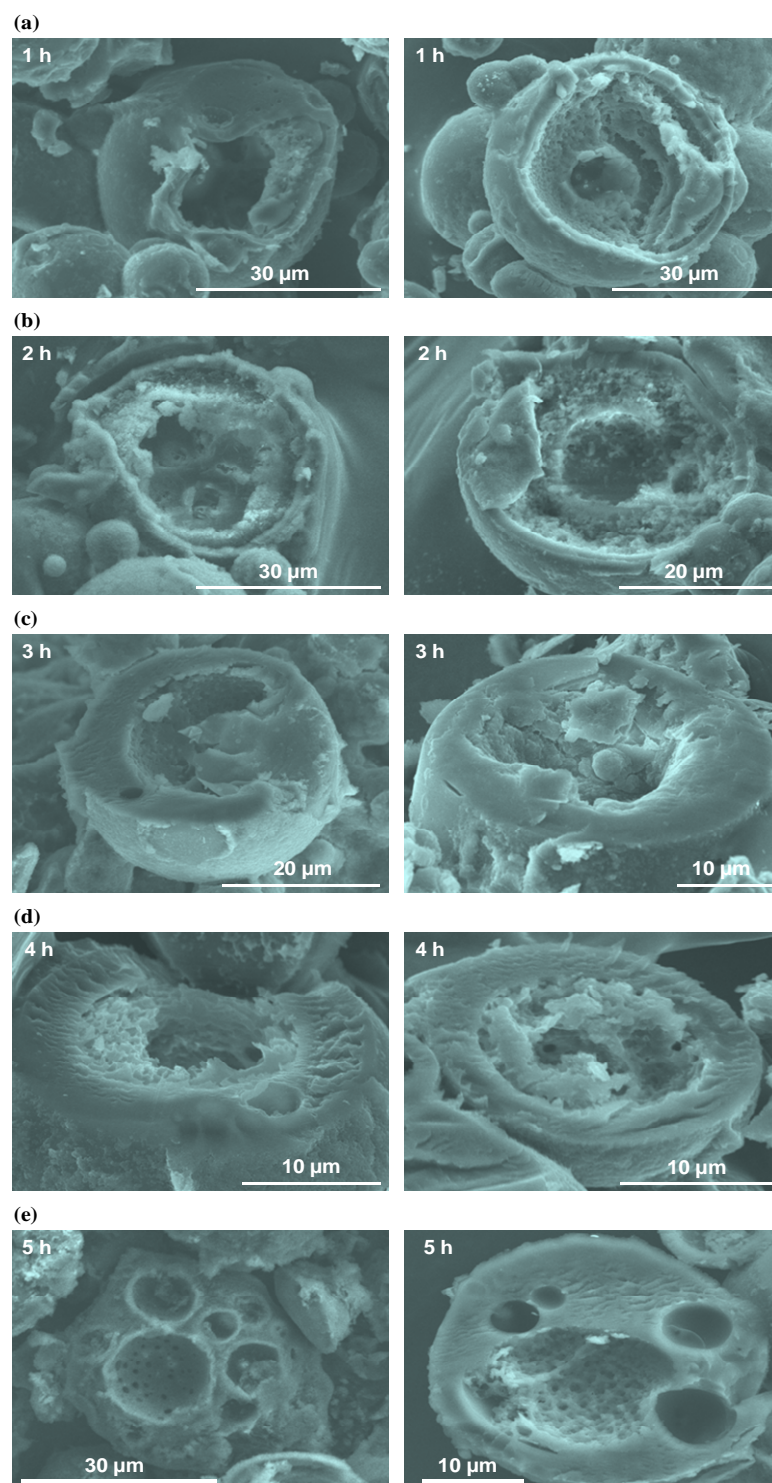


Figure 3. 6 Evolution of the PMMA morphology with time for Exp. C9. Reaction times are as follows: (a) $t=1$ h, $x=0.509$; (b) $t=2$ h, $x=0.919$; (c) $t=3$ h, $x=0.954$; (d) $t=4$ h, $x=0.979$; and (e) $t=5$ h, $x=0.996$ where t is time of the reaction and x is the conversion.

the weight ratio of MMA to (MMA + n-hexane) is 0.3 (for Exp. C10) and 0.4 (for Exp. C11). Figure 3.7 shows the morphology of the PMMA particles produced in experiments C12-C15. The weight ratio of MMA to (MMA + n-hexane) is 0.5, 0.6, 0.65, and 0.67 for experiments C12 to C15 respectively. It can be seen that in this range, micron-sized hollow PMMA polymer particles with thin wall thickness that contain smaller polymer particles inside them are produced and when the weight ratio of MMA to (MMA + n-hexane) increases from 0.5 to 0.67, more small particles are produced inside each hollow PMMA particle. As it is obvious in Fig. 3.7, these polymer particles show a significant degree of shrinkage. These experiments were replicated and same results were obtained. The reason could be the method of drying of the polymer particles. In other words, since the wall thickness of the PMMA

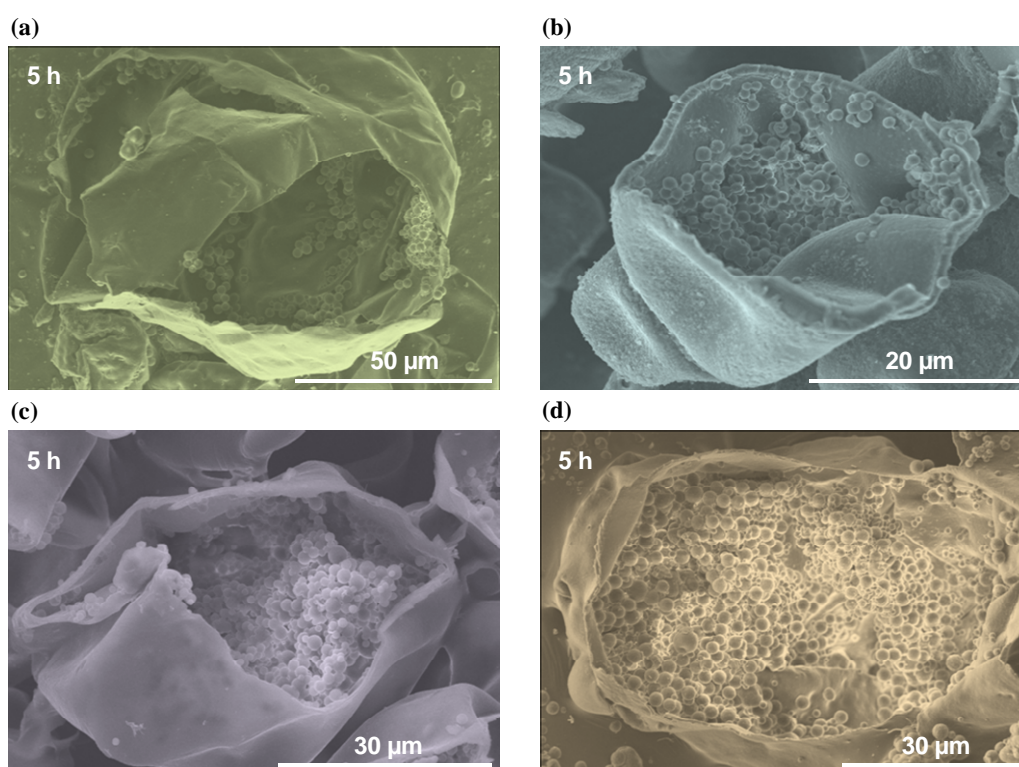


Figure 3.7. Morphology of the poly(methyl methacrylate) (PMMA) particles obtained by micro dispersive suspension polymerization of MMA at 30°C after 5 hours. (a) Exp. C12, $x=0.21$; (b) Exp. C13, $x=0.32$; (c) Exp. C14, $x=0.84$; and (d) Exp. C15, $x=0.93$ where x is the conversion.

particles is so thin if the solvent evaporation from the polymer particles during the drying process takes place too fast, particles shrink. Since in all of the previous experiments polymer samples were dried under the hood for 1 day and then in the vacuum oven for 1 day, a new experiment designed in order to test the effect of the method of drying on the polymer particles shrinkage. In fact, Exp. C15 repeated and the PMMA particles that were obtained after 5 hours of polymerization dried using different combinations of drying under the hood and drying under the vacuum oven. These combinations included drying the polymer sample 2 days under the hood and then 3 days in the vacuum oven, 3 days under the hood and then 2 days in the vacuum oven, and 4 days under the hood and then 1 day in the vacuum oven. Figure 3.8 shows the morphology of the polymer particles that were obtained using these three different methods of drying. Conversion was 92% for this experiment. Unfortunately, as it can be seen in Fig. 3.8 the polymer particles shrink using all of these different drying methods. It means that even by increasing the drying time of polymer particles under the hood before putting them in the vacuum oven, it is impossible to avoid the shrinkage phenomenon of polymer samples when a combination of these two instruments (hood and vacuum oven) is used. Thus, a new experiment was carried out to investigate the reason of this shrinkage further. Four new different methods of drying were used to check the effect of new drying methods on polymer particles shrinkage. These methods included of drying the polymer just in the vacuum oven for 10 days, drying the polymer in an ice-bath at room temperature for 4 days and then drying it under the hood for 6 days, drying the polymer just under the hood for 10 days, and drying the polymer under low pressure using the liquid nitrogen. Experiment C15 was repeated and the particles dried using these techniques.

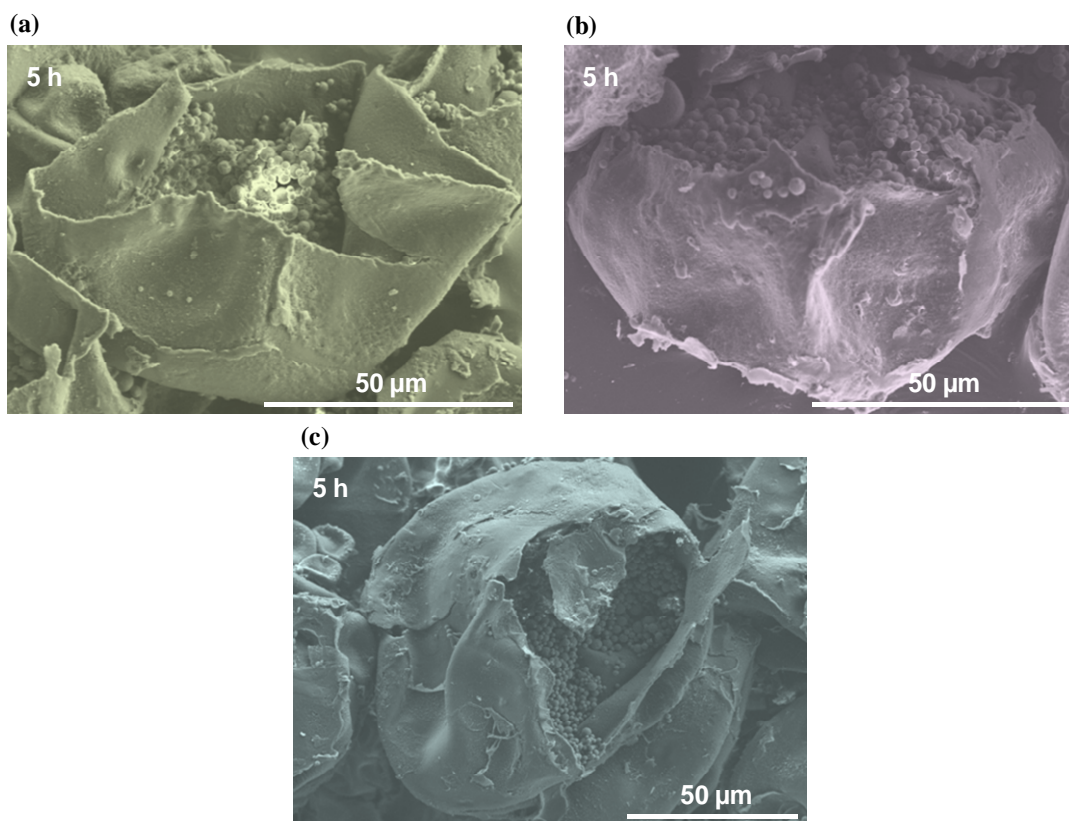


Figure 3.8. Morphology of the poly(methyl methacrylate) (PMMA) particles obtained for Exp. C15 using different methods of drying. Conversion was 0.92 after 5 hours of polymerization. (a) particles dried under the hood for 2 days and then in the vacuum oven for 3 days; (b) particles dried under the hood for 3 days and then in the vacuum oven for 2 days; (c) particles dried under the hood for 4 days and then in the vacuum oven for 1 day.

Figure 3.9 shows the morphology of the PMMA particles that were obtained using these different methods of drying. The conversion was 95% after 5 hours of polymerization for this experiment. SEM images of this experiment show that stable polymer particles without any shrinkage are only observed when the polymer particles are dried under low pressure using liquid nitrogen (see Fig. 3.9-d). In all the other cases, if the polymer sample is dried under the hood or in the vacuum oven or even in the ice-bath at room temperature, the shrinkage of the PMMA particles is observed (see Fig. 3.9-a to 3.9-c). When the polymer sample is dried just in vacuum

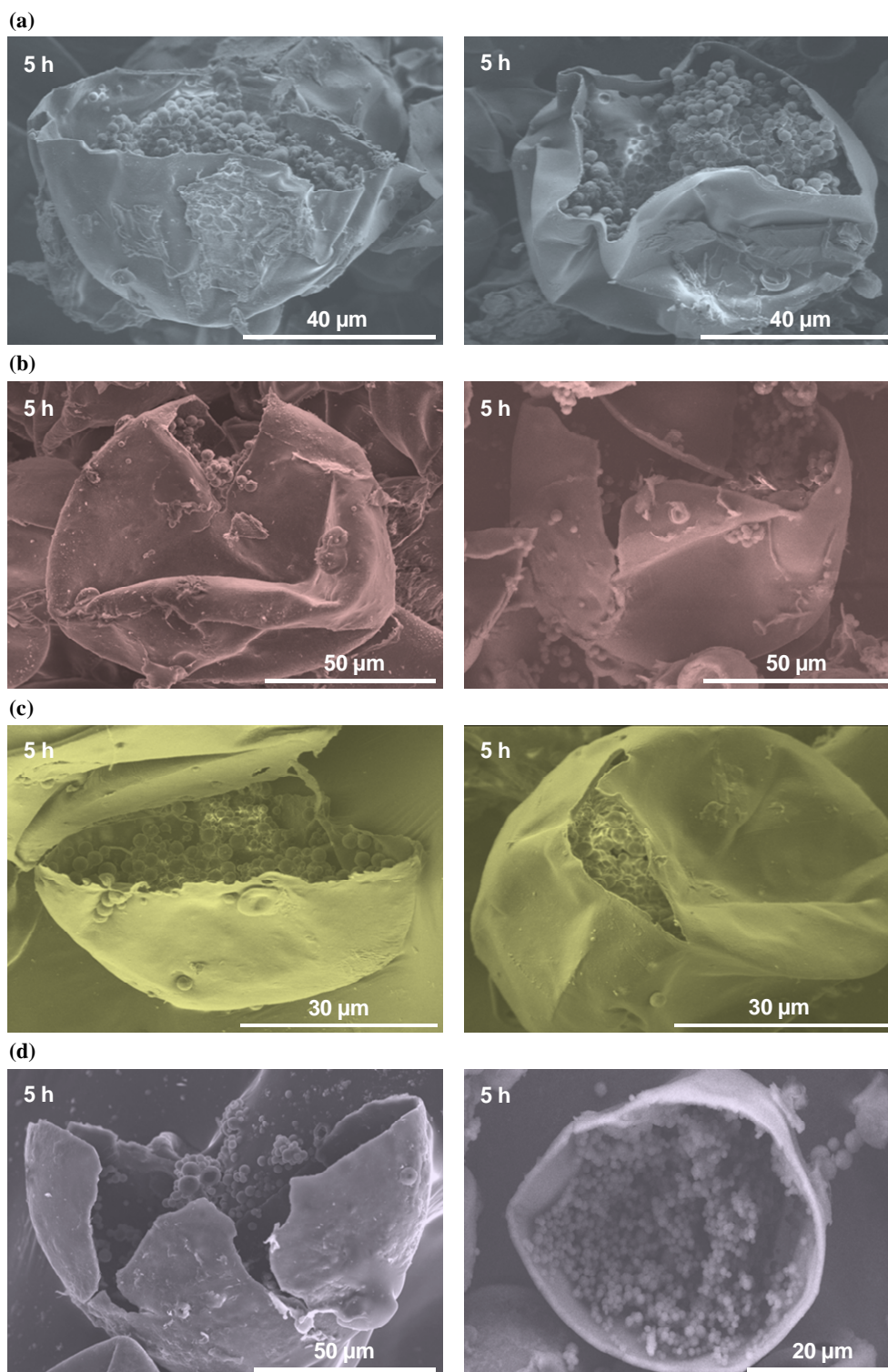


Figure 3.9. Morphology of the poly(methyl methacrylate) (PMMA) particles obtained for Exp. C15 using different methods of drying. Conversion was 0.95 after 5 hours of polymerization. (a) particles just dried in the vacuum oven for 10 days; (b) particles dried in the ice-bath at room temperature for 4 days and then under the hood for 6 days; (c) particles just dried under the hood for 10 days; (d) particles were dried under low pressure using the liquid nitrogen.

oven, the particles shrink very much in comparison to the other cases because the rate of solvent evaporation from the polymer particles is high in the vacuum oven. It seems that when the weight ratio of MMA to (MMA + n-hexane) is less than 0.7 and more than 0.4, since the amount of solvent (n-hexane) in the recipe is relatively high and the wall thickness of the resulted polymer particles is too thin, the method of drying the polymer particles has a strong effect on particles morphology. In other words, drying the polymer particles under the hood or in the vacuum oven is not efficient to provide stable polymer particles without any shrinkage.

Drying the particles under a low pressure using the liquid nitrogen is the only useful method in order to do not let the particles to shrink. The reason of this is the ability of this method to reduce enough the rate of evaporation of the solvent from the polymer particles and do not let them shrink.

Chapter 4: Conclusion and future work considerations

The purpose of this study was to investigate the feasibility of dispersion polymerization of methyl methacrylate (MMA) in n-hexane as a nonpolar hydrocarbon solvent at low temperature using a redox pair of initiators in conventional batch reactors and in micron-sized suspended monomer droplets. Lauroyl peroxide (LPO) and N,N-dimethylaniline (DMA) were used as a redox pair of initiators in order to initiate the polymerization reaction at low temperature. Methacryloxypropyl-terminated polydimethylsiloxane (PDMS) of high molecular weight (20000-30000 g/mol) was used as the oil-soluble steric stabilizer. Molecular weight distributions of the resulting polymers for the conventional dispersion polymerization experiments, were investigated through the use of gel permeation chromatography (GPC) and conversion of the polymer samples was determined using a standard gravimetric method. The effects of initiator concentration, stabilizer concentration, and monomer/solvent ratio on the average particle size and polymer morphology were studied by the use of the micrographs obtained from scanning electron microscopy (SEM). Experiments were carried out up to low and high conversions in order to study the complete evolution of the polymer morphology during the dispersion polymerization. Partition coefficients of LPO and DMA also measured to provide a better understanding of the polymerization locus and kinetics of the process. Moreover, the stability of the polymer particles and the probability of the phase inversion phenomenon and its conditions during the polymerization were investigated. The results showed that the redox pair of LPO and DMA is a suitable system to initiate the dispersion polymerization of MMA in n-hexane at low temperature and to obtain high conversion in reasonably short reaction times.

Polymer particle size of a few microns can be readily obtained in a small scale without any mechanical agitation. The proposed polymerization technique explores, for the first time, the production of highly uniform and stable micron-sized poly(methyl methacrylate) (PMMA) particles in a nonpolar hydrocarbon solvent under mild reaction conditions. Moreover, experimental results suggest that the preference of LPO and DMA to accumulate in the polymer-rich phase can explain both the uniformity of particle sizes and the broad molecular weight distributions (MWDs).

On the basis of this research work, more sophisticated experimental and theoretical research can be made to analyze in detail the partition of all the species (including low molecular weight species but also polymer chains) in different phases.

The knowledge that obtained from the conventional dispersion polymerization of MMA at low temperature in this research work was then used to design and carry out a new set of experiments in suspended monomer droplets. Poly(vinyl alcohol) (PVA) was used to stabilize the monomer droplets in an aqueous medium. In this case, each monomer droplet acts as a micro-reactor where dispersion polymerization takes place. The SEM images showed that according to the recipe that is used for the oil-phase (the ratio of monomer to solvent is very important), polymer particles with different internal morphologies can be produced. The knowledge of the conventional dispersion polymerization which takes place inside each monomer droplet is vital to control the agglomeration of precipitating particles that can drive to an internal system phase inversion. Future work can be focused on improving the experimental technique and optimizing the recipe to generate a comprehensive protocol for the production of polymer particles with complex internal structures. It should be noticed

that this research work was the first attempt in producing stable polymer particles at low temperature using the LPO/DMA as a redox pair of initiators in dispersion polymerization and before that there was no knowledge of this special polymerization system. In fact many factors such as monomer concentration, solvent concentration, initiator concentration, stabilizer concentration, time of reaction, and temperature and also the interaction of these factors may affect the polymerization process and the uniformity and stability of the resulted polymer particles, but when this project was started we did not have any idea about the level of each of these factors that can provide the best result. Now with the aid of the experimental results of this research work we are able to design new sets of experiments based on the levels that we have found experimentally in order to find the best levels of these factors for optimizing the polymerization process. There are many statistical designs of experiments such as full factorial design, fractional factorial design, central composite design, and etc. that can be used for this purpose (Montgomery and Runger, 2007). It is interesting to note that for full factorial design if there are k factors that affect the process and each of these factors has 2 levels, it is necessary to run 2^k experiments to test the effect of each of these factors and their interactions on the process response variable. For example for the dispersion polymerization process that we considered in this research work if we assume that we have 6 factors that may affect the stability of the polymer particles (as a response variable) each of them with 2 levels, then it is necessary to carry out 64 experiments in order to find the best levels of each of these factors that may provide the best results.

Nomenclature

D^\bullet	initiator radical
I	initiator
k	phase ($k=1$: non-solvent-rich phase, $k=2$: polymer-rich phase)
K_{DMA}	partition coefficient of DMA
K_{LPO}	partition coefficient of LPO
l	polymer chain length
M	monomer
M_n	dead polymer chain with n monomer units ($n \geq 2$)
\overline{M}_n	number-average molecular weight
\overline{M}_w	weight-average molecular weight
n_{DMA}^0	total number of moles of DMA added to the initial mixture
$n_{DMA,1}$	number of moles of DMA in the solvent-rich phase
n_i	number of moles of species i
N^\bullet	initiator radical
n_{LPO}^0	total number of moles of LPO
$n_{LPO,1}$	number of moles of LPO in the solvent-rich phase
P	polymer
P_n	dead polymer molecule with n monomer units ($n \geq 2$)
P_n^\bullet	live polymer radical with n monomer units
r	molar volume ratio of non-solvent to polymer
R	gas constant
R^\bullet	initiator radical
R_1^\bullet	primary radical
R_g	radius of gyration of polymer chains
R_n^\bullet	live polymer radical with n monomer units
s	molar volume ratio of non-solvent to monomer
S	solvent/non-solvent
T	absolute temperature

V^0	total volume of the initial blend
V_1	volume of the solvent-rich phase
X	monomer, chain transfer agent, solvent, polymer, impurity, and etc.
ΔG_m	Gibbs free energy of mixing
ϕ_i	volume fraction of species i
$\chi_{i,j}$	interaction parameter between species i and j
μ_i	chemical potential of species i in the mixture
$\Delta\mu_{i,k}$	chemical potential for each species i referred to the standard state
ν	interaction parameter between solvent and polymer ($\nu = 3/5$ for good solvents and $\nu = 1/3$ for bad solvents)

References

- Aggarwal, A.; Saxena, R.; Wang, B.; Caneba, G. T. *J Appl Polym Sci*, 62, 2039 (1996).
- Almog, Y.; Reich, S.; Levy, M. *Brit. Polym. J.*, 14, 131 (1982).
- Antl, L.; Goodwin, J.W.; Hill, R.D.; Ottewill, R.H.; Owens, S.M.; Papworth, S. *Colloid Surf.*, 17, 67 (1986).
- Arshady, R.; Ledwith, A. *Reactive Polymers*, 1, 159 (1983).
- Bahar, T.; Tuncel, A. *Polymer Engineering and Science*, 39, 1849 (2004).
- Bai, F.; Yang, X.; Li, R.; Huang, B.; Huang, W. *Polymer*, 47, 5775 (2006).
- Bamnolker, H.; Margel, S. *J Polym Sci Part A: Polym Chem*, 34, 1857 (1996).
- Barret, K. E. J. *Dispersion Polymerization in Organic Media*; New York, 1987.
- Barret, K. E.; Thomas, H. R. *J. Polym. Sci. Part A.*, 7, 2650 (1969).
- Bergbreiter, D. E. *Angewandte Chemie-International Edition*, 38, 2870 (1999).
- Bertin, D.; Coutand, F.; Duc, M.; Galindo, C.; Gigmes, D.; Marque, S.; Tordo, P.; Vuillemin, B. *e-polymers*, 10, 1 (2004).
- Boh, B.; Knez, E.; Staresinic, M. *Journal of Microencapsulation*, 22, 715 (2005).
- Bourgeat-Lami, E.; Guyot, A. *Colloid Polym Sci*, 275, 716 (1997).
- Chang, Z.; Liu, G.; Fang, F.; Tian, Y.; Zhang, Z. *Chem. Eng. Sci*, 101, 195 (2004).
- Chen, J.; Zeng, Z.; Yang, J.; Chen, Y. *J. Polym. Sci. Part A*, 46, 1329 (2008).
- Chen, Y.; Yang, H. W. *Journal of Polymer Science: Part A: Polymer Chemistry*, 30, 2765 (1992).
- Corner, T. *Colloid Surf*, 3, 119 (1981).
- Croucher, M. D.; Winnik, M. A., *Future Directions in Polymer Colloids*, NATO ASI Series E # 138, 213 (1987).

- Dai, Q.; Wu, D.; Zhang, Z.; Ye, Qiang. *Polymer*, 44, 37 (2003).
- Dawkins, J.V.; Taylor, G. *Polymer*, 20, 599 (1979).
- Delgado, M.; Spanka, C.; Kerwin, L. D.; Wentworth, P.; Janda, K. *Biomacromolecules*, 3, 262 (2002).
- Dinsmore, A. D.; Hsu, M. F.; Nikolaides, M. G.; Marquez, M.; Bausch, A. R.; Weitz, D. A. *Science*, 298, 1006 (2002).
- Emdadi, L.; Luciani, C. V.; Lee, S. Y.; Baick, I. H.; Choi, K. Y. *Polymer Engineering & Science*, DOI: 10.1002/Pen.21971 (2011).
- Emmerich, O.; Hugenberg, N.; Schmidt, M.; Sheiko, S. S.; Baumann, B.; Weis, J.; Ebenhoch, J. *Advanced Materials*, 11, 1299 (1999).
- Fitch, R. M.; Tsai, C.H. *Polymer Colloids*, Plenum Press, New York, 1971.
- Frank, R. S.; Downey, J. S.; Stover, H. D. H. *J Polym Sci Part A: Polym Chem*, 36, 2223 (1998).
- Fritz, J. S. *Anal. Chem*, 22, 1028 (1950).
- Fu, G. D.; Shang, Z. H.; Hong, L.; Kang, E. T.; Neoh, K. G. *Macromolecules*, 38, 7867 (2005).
- Gross, J. R., US Patent 5403870, 4/4/1995.
- Gupta, S. K.; Nanoti, S. M.; Rawat, B. S. *J. Chem. Eng. Data*, 37, 162 (1992).
- Guven, G.; Tuncel, A.; Piskain, E. *Colloid Polym. Sci*, 282, 708 (2004).
- Hattori, M.; Sudol, E. D.; El-Aasser, M. S. *J Appl Polym Sci*, 50, 7, (1993).
- Ho, C.; Chen, S.; Amiridis, M. D.; Van Zee, J. W. *Journal of Polymer Science: Part A: Polymer Chemistry*, 35, 2907 (1997).
- Horak, D.; Krystufek, M.; Spevacek, J. *Journal of Polymer Science: Part A: Polymer Chemistry*, 38, 653 (2000).
- Im, S. H.; Jeong, U. Y.; Xia, Y. N. *Nature Materials*, 4, 671 (2005).

- Itou, N.; Masukawa, T.; Ozaki, I.; Hattori, M.; Kasai, K. *Colloids and Surfaces a-Physicochemical and Engineering Aspects*, 153, 311 (1999).
- Jacobelli, H.; Bartholin, M.; Guyot, A. *J Appl Polym Sci*, 23, 927 (1979).
- Jeong, J. M.; Chung, Y. C.; Hwang, J. H. *J. Biotechnol*, 94, 255 (2002).
- Jiang, B. B.; Gao, C. Y.; Shen, J. C. *Colloid and Polymer Science*, 284, 513 (2006).
- Jiang, S.; Sudol, E. D.; Dimonie, V. L.; El-Aasser, M. S. *J Polym Sci Part A: Polym Chem*, 45, 2105 (2007).
- Johnson, L. M.; Fairbanks, B. D.; Anseth, K. S.; Bowman, C. N. *Biomacromolecules*, 10, 3114 (2009).
- Juba, M. R. *ACS Symposium Series*, Washington, D. C., 104, 267 (1979).
- Jung, Y.; Luciani, C.V.; Han, J.J.; Choi, K.Y. *Journal of Applied Polymer Science*, 116, 3648 (2010).
- Kargupta, K.; Rai, P.; Kumar, A. *J. Appl. Polym. Sci.*, 49, 1309 (1993).
- Kiatkamjornwong, S.; Kongsupapsiri, C. *Polymer International*, 49, 1395 (2000).
- Kim, B. S.; Kim, J. W.; Suh, K. D. *Journal of Applied Polymer Science*, 76, 38 (2000).
- Kim, J. W.; Chang, I. S.; Kang, H. K. *Polymer Science & Technology*, 13, 422 (2002).
- Kim, J. W.; Joe, Y. G.; Suh, K. D. *Colloid and Polymer Science*, 277, 252 (1999).
- Kim, J. W.; Ko, J. Y.; Jun, J. B.; Chang, I. S.; Kang, H. H.; Suh, K. D. *Colloid and Polymer Science*, 281, 157 (2003).
- Kim, O. H.; Lee, K.; Kim, K.; Lee, B. H.; Choe, S. *Polymer*, 47, 1953 (2006).
- Klein, S. M.; Manoharan, V. N.; Pine, D. J.; Lange, F. F. *Colloid Polym Sci*, 282,

7 (2003).

- Kulin, L. I.; Flodin, P.; Ellingsen, T.; Ugelstad, J. *J Chromatogr*, 514, 1 (1990).
- Langer, R. *Nature*, 392, 5 (1998).
- Lee, K. C.; Her, J. H.; Kim, K. J. *International Journal of Polymer Analysis and Characterization*, 14, 600 (2009).
- Lee, K. C.; Lee, S. E.; Song, B. K. *Macromolecular Research*, 10, 140 (2002).
- Li, G. L.; Yang, X. Y.; Wang, B.; Wang, J. Y.; Yang, X. L. *Polymer*, 49, 3436 (2008).
- Li, W. H.; Stover, H. D. H. *J Polym Sci Part A: Polym Chem*. 37, 2899 (1998).
- Lok, K. P.; Ober, C. K. *Can J Chem*, 63, 209 (1985).
- Lopez de Arbina, L.; Barandiaran, M. J.; Gugliotta, L.; Asua, J. M. *J. Polym. Sci. Part A: Polym. Chem*, 24, 1683 (1994).
- Lovelace, A. M.; Vanderhoff, J. W.; Micale, F. J.; El-Asser, M. S.; Kornfeld, D. M. U. S. Patent 4247434, 1/27/1981.
- Lu, Y. Y.; El-Aasser, M. S.; Vanderhoff, J. W. *J. Polym. Sci., Polym. Phys.*, 26, 1187 (1988).
- Montgomery, D. C.; Runger, G. C. Applied Statistics and Probability for Engineers. *John Wiley & Sons, Inc, Fourth Edition*, 538-617 (2007).
- Moore, J. C. *J Polym Sci: Part A*, 2, 835 (1969).
- Mu, G. H.; Shen, H. G.; Qiu, J. X.; Gu, M. Y. *Applied Surface Science*, 253, 2278 (2006).
- Nakashima, T.; Ono, T. *Colloid Polym Sci*, 286, 1587 (2008).
- Nomura, M.; Harada, M.; Eguchi, W.; Nagata, S. *J. Appl. Polym. Sci.*, 16, 835 (1972).

- Ober, C. K.; Hair, M. L., *J. Polym. Sci, Part A*, 25, 1395 (**1986**).
- Ober, C. K.; Lok, K. P. *Macromolecules*, 20, 2689 (**1987**).
- Odian, G. Principles of Polymerization, Wiley-Interscience, New York, **1981**.
- Okaya, T.; Kikuchi, K.; Suzuki, A.; Ikeda, N. *Polymer International*, 54 (1), 143 (**2004**).
- Okubo, M.; Konishi, Y.; Inohara, T.; Minami, H. *Journal of Applied Polymer Science*, 86, 1087 (**2002**).
- Okubo, M.; Minami, H.; Komura, T. *Journal of Applied Polymer Science*, 88, 428 (**2003**).
- Okubo, M.; Minami, H.; Yamamoto, Y. *Colloid and Polymer Science*, 279, 77 (**2001**).
- Paine, A. J.; Deslandes, Y.; Gerroir, P.; Henrissat, B. *J Colloid Interface Sci*, 138, 157 (**1990 (a)**).
- Paine, A. J.; Luymes, W.; McNulty, J. *Macromolecules*, 23, 3104 (**1990 (b)**).
- Paine, A. J.; McNulty, J. *Polym. Sci., Polym. Chem*, 28, 2569 (**1990 (c)**).
- Pathmamanoharan, C.; Slob, C.; Lekkerker, H. N. W. *Colloid Polym. Sci*, 267, 448 (**1989**).
- Pelton, R. H.; Osterroth, A.; Brook, M. A. *J Colloid Interface Sci*, 137, 120 (**1990**).
- Pelton, R. H.; Osterroth, A.; Brook, M. A. *J Colloid Interface Sci*, 147, 523 (**1991**).
- Qiang, Ye.; Weidong, H.; Xuwu, G.; Haiting, J.; Huarong, L.; Zhicheng, Z. *Journal of applied Polymer Science*. 86, 2567 (**2002**).
- Qiu, K.; Shui, L.; Feng, X. *Chinese J. Polym. Sci*, 2, 64 (**1984**).

- Rosen, S. L., *Fundamental Principles of Polymeric Materials*, John Wiley, New York, **1993**.
- Ruiters, M.; Herman, J. Protection of biologically active molecules using amphiphiles, WO2006/043809 A1 (**2006**).
- Sato, T.; Kita, S.; Otsu, T. *Makromol. Chem*, 176, 561 (**1975**).
- Schork, F. J.; Luo, Y.; Smulders, W.; Russum, J. P.; Butte, A.; Fontenot, K. *Adv Polym Sci*, 175, 129 (**2005**).
- Seo, H. J.; Ahn, J. H.; Lee, K. C. *Polymer (Korea)*, 22, 861 (**1998**).
- Shen, S.; Sudol, E. D.; El-Aasser, M. S. *Journal of Polymer Science: Part A: Polymer Chemistry*, 32, 1087 (**1994**).
- Sneeringer, P. V.; Stenberg, V. I. *Anal. Letters*, 4, 485 (**1971**).
- Soane, D. S.; Houston, M. R. US Patent 6617364, **9/9/2003**.
- Song, Z.; Poehlein, G. W. *Journal of Macromolecular Science, Part A*, 25, 1587 (**1988**).
- Sowa, T.; Watanabe, T.; Seguchi, T.; Okamoto, J. *J Polym Sci Polym Chem*, 17, 67 (**1979**).
- Srinivasan, S.A.; Hedrick, J.L.; McKean, D.R.; Miller, R.D.; Hilbom, J.G. *Polymer*, 39, 1497 (**1998**).
- Stejskal, J.; Kratochvil, P.; Konak, C. *Polymer*, 32, 2435 (**1991**).
- Sudol, E. D. In *polymeric Dispersions: Principles and Applications*; Asua, J. M., Ed; NATO ASI series E 335, Kluwer Academic Publishers: Dordrecht, The Netherlands, **1997**; p 141.
- Tseng, C. M.; Lu, Y. Y.; El-Aasser, M. S.; Vanderhoff, J. W. *J. Polym. Sci., Part A*, 24, 2995 (**1986**).

- Turovskii, N. A.; Opeida, I. A.; Kushch, O. V. *Russian J. Organic Chem*, 39, 642 (2003).
- Ugelstad, J.; Mork, P. C.; Berge, A.; Ellingsen, T.; Khan, A. A. *In emulsion polymerization*. I. Piirma, Ed., Academic Press, New York, 383, **1982**.
- Urban D, Takamura K (eds). *Polymer dispersions and their industrial applications*. Wiley-VCH, Weinheim, **2002**.
- Uyama, H.; Kobayashi, S. *Polymer International*, 34, 339 (1994).
- Vanderhoff, J.W.; Bradford, E.B. *Polymer Colloid I*; Plenum Press: New York, **1971**.
- Wagner, C. D.; Smith, R. H.; Peters, E. D. *Anal. Chem*, 19, 976 (1947).
- Wang, D.; Dimonie, V. L.; Sudol, E. D.; El-Aasser, M. S. *J Appl Polym Sci*, 84, 2721 (2001).
- Williamson, B.; Lukas, R.; Winnik, M. A.; Croucher, M. D. *J. Colloid Int. Sci.*, 119, 559 (1987).
- Winnik, M. A.; Lukas, R. Chen, W. F.; Furlong P.; Croucher M. D. *Makromol Chem-M Symp*, 10, 483 (1987).
- Wu, H. S.; Sun, F.; Dimonie, V. L.; Klein, A., US Patent 5834526, **11 /10/1998**.
- Xu, X. L.; Asher, S. A. *Journal of the American Chemical Society*, 126, 7940 (2004).
- Xu, Z. *Journal of Dispersion Science and Technology*, 21, 869 (2000).
- Yang, S.; Shim, S. E.; Jin, M.; Chang, Y. H.; Choe, S. *Colloid Polym Sci*, 283, 41 (2004).
- Yang, W.; Yang, D.; Hu, J.; Wang, C.; Fu, S. *J Polym Sci Part A: Polym Chem*, 39, 555 (2001).
- Yasuda, M.; Seki, H.; Yokoyama, H.; Ogino, H.; Ishimi, K.; Ishikawa, H.

- Macromolecules*, 34, 3261 (**2001**).
- Ye, Q.; Ge, X.; Liu, H.; Jia, H.; He, W.; Zhang, Z. *J. Macromol. Sci. Pure Appl. Chem. Part A*, 39, 545 (**2002 (a)**).
 - Ye, Q.; Zhang, Z.; Ge, X.; Ni, Y.; Wang, M. *Colloid Polym. Sci.*, 280, 1091 (**2002 (b)**).
 - Yuan, H. G.; Kalfas, G.; Ray, W. H. *J. Macromol. Sci., Rev. Macromol. Chem. Phys. C31* (2 & 3), 215 (**1991**).
 - Zhang, W.; Tao, M.; Hu, Z.; Zhang, Z. *Colloids Surf. A*, 305, 58 (**2007**).